PERFORMANCE OF MULTI-HOP AD-HOC NETWORKS IN WIRELESS ENVIRONMENTS

BY

MOHAMMAD M. ABDELLATIF

A Thesis Presented to the

DEANSHIP OF GRADUATE STUDIES

KING FAHD UNIVERSITY OF PETROLEUM & MINERALS

DHAHRAN, SAUDI ARABIA

In Partial Fulfillment of the
Requirements for the Degree of

MASTER OF SCIENCE

In

TELECOMMUNICATION ENGINEERING

February 2009

KING FAHD UNIVERSITY OF PETROLEUM & MINERALS
DHAHRAN 31261, SAUDI ARABIA

DEANSHIP OF GRADUATE STUDIES

This thesis, written by **MOHAMMAD M. ABDELLATIF** under the supervision of his thesis advisor and approved by his thesis committee, has been presented to and accepted by the Dean of Graduate Studies, in partial fulfillment of the requirements for the degree of **MASTER OF SCIENCE IN TELECOMMUNICATION ENGINEERING**

Thesis Committee

Dr. Salam A. Zummo
(Chairman)

Dr. Maan Kousa
(Member)

Dr. Ibrahim O. Habiballah
Department Chairman

Dr. Yahya Al-Harthi
(Member)

Dr. Salam A. Zummo
Dean of Graduate Studies (A)

24/2/09
Date

عمادة الدراسات العليا
DEANSHIP OF GRADUATE STUDIES

Dedicated to

My Beloved Parents

and

My Brothers and Sisters

ACKNOWLEDGEMENTS

In the name of Allah, the Most Gracious and the Most Merciful

All praises are due to Allah (SWT) for His kindest blessings on me and all the members of my family. I feel sincerely privileged to glorify His Name through this small accomplishment, and I ask Him to accept it as an act of worship. I ask for His blessings, mercy and forgiveness. May the peace and blessings of Allah be upon His dearest prophet, Muhammad (Peace Be upon Him).

My deep appreciation goes to my advisor Dr. Salam A. Zummo. He was always there when I needed him and he answered all my questions. I am extremely grateful to him for his prompt replies and his numerous proofreads. I am also very grateful to my thesis committee members, Dr. Maan Kousa and Dr. Yahya Al-Harthi, for their interest, cooperation and constructive advice.

I am grateful to the chairman of the Electrical Engineering Department, Dr. Ibrahim O. Habiballah, for his kind help and cooperation, and to our former chairman, Dr. Jamil M. Bakhashwain, for his timely advice and guidance. I am also thankful to

all faculty and staff members for their kind support and continuous cooperation. I would like to acknowledge the support and facilities provided by King Fahd University of Petroleum and Minerals.

I would like to thank my colleagues and friends for their concern and help, especially Motasm M. Hassan for his great support in the OFDM part.

Last but not least, I humbly offer my sincere thanks to my parents for their incessant inspiration, blessings and prayers.

Contents

List of Tables

List of Figures

THESIS ABSTRACT

Name: MOHAMMAD M. ABDELLATIF

Title: PERFORMANCE OF MULTI-HOP AD-HOC NETWORKS IN WIRELESS ENVIRONMENTS

Degree: MASTER OF SCIENCE

Major Field: TELECOMMUNICATION ENGINEERING

Date of Degree: February 2009

Multi-hop relaying is a promising technique for the next generation of wireless communications. Multi-hop networks help to combat fading by employing a distributed space diversity system. In order to enhance the diversity gain, improve the error performance of the network, and reduce the power consumption, an error control code is usually employed in wireless networks. In this thesis, we consider convolutional codes, which provide low implementation complexity and short delays. The aim is to investigate the error performance of uncoded and convolutionally coded multi-hop networks over different channel models in different network topologies. We will consider multi-hop networks with series, and parallel topologies. In addition, different forwarding techniques at the relay nodes will be considered. We will test the proposed multi-hop system with narrowband, code division multiple access (CDMA) and orthogonal frequency division multiplexing (OFDM).

Keywords*: Multi-hop, Diversity, BEP, CDMA, SGA, PEP, Coded OFDM, Convolutional Code.*

King Fahd University of Petroleum and Minerals, Dhahran.
February 2009

Abstract (Arabic)
ملخص الرسالة

الاسم: محمد محمود عبد اللطيف

عنوان الرسالة: أداء الشبكات المخصصة متعددة القفزات في الأوساط اللاسلكية

الدرجة: الماجستير في هندسة الاتصالات

التخصص الرئيسي: هندسة الإتصالات

تاريخ التخرج: فبراير - 2009م

تعتبر شبكات الترحيل متعددة القفزات تقنية واعدة للجيل القادم الاتصالات اللاسلكية. شبكات الترحيل متعددة القفزات تساعد في مكافحة تلاشى الارسال باستخدام نظام التنوع الفضائي. من أجل لتعزيز الحصول على التنوع ، وتحسين أداء الشبكة ، والحد من استهلاك الطاقة ، عادة ما يستخدم في الشبكات اللاسلكية شفرات حل الخطأ. في هذا العمل ، نحن نستخدم الشفرات الملتفة (Convolutional codes) ،فهي سهلة التركيب بالإضافة إلي قصر مدة تأخيرها. الهدف من هذا البحث هو إختبار أداء الشبكات متعددة القفزات المشفرة و الغير مشفرة خلال قنوات مختلفة مع استخدام أشكال مختلفة من الشبكات باستخدام طرق ترحيل مختلفة. بالإضافة إلى ذلك سوف نختبر النظام المقترح مع الإرسال ضيق المدى و ارسال (CDMA) و ارسال (OFDM).

درجة الماجستير في العلوم
جامعة الملك فهد للبترول والمعادن
الظهران، المملكة العربية السعودية

Chapter 1

Introduction

Next generation wireless networks are expected to provide services that need high data rates with very high bandwidth efficiency compared to previous generations. As the number of wireless terminals increases, higher system capacity is needed to provide the high data rate required by all these terminals. It is not practical to install more base stations to serve the large number of terminals, especially when these terminals are located in a pico-cell environment. In addition, the multipath fading problem arises from the reflection of the transmitted signal over many objects in the environment surrounding a transmitter and receiver. As a result, the receiver receives the superposition of multiple copies of the transmitted signal, each having traveled through a different path. The multipath fading increases the number of errors in the transmission, and therefore it requires additional re-transmissions, which decreases the net throughput of the communication network. The effects of

multipath fading can be combated by using diversity.

Diversity is based on the fact that several independent fading channels are unlikely to fade simultaneously, and so by transmitting several replica of the message over orthogonal channels (time slots, frequencies, or antennas) we can reduce the multipath fading effect. The problem with multiple antennas is that they are not practical for hand-held terminals. The obvious solution is to use these terminals to relay the data between them without the need to install new base stations. However, these terminals have limited power, and hence using them as relays will drain their power sources very quickly. In such scenarios, the data transmission has to be made error-free so that no re-transmissions are required, thus saving more power. One way to achieve this is by implementing an error control code with low implementation complexity and low power consumption in order to reduce the bit error probability (BEP).

The rest of this chapter is organized as follows. In Section 1.1, we lay the required background for wireless systems and the fading mitigation techniques. In Section 1.2, the multihop networks are presented. An up-to-date literature survey is given in Section 1.3. In Section 1.4, we list the thesis contributions. Finally, Section 1.5 gives an outline for the rest of the thesis.

1.1 Background

1.1.1 Wireless Channels

In wired communication systems, the only source of error is the thermal noise, whereas in mobile communications errors arise from different sources, such as shadowing and multipath fading. Because of this, the design of mobile radio systems is much more complex. Therefore, in order to develop an optimum design for communication systems for use over mobile channels, we must first understand the nature of these channels.

Wireless channels are different from wired channels in many aspects. For example, the interference from other transmitters affects the communication quality severely. Also, because of the constant change of the environment and the mobility of the terminals "transmitter or receiver or both" the signal is scattered over many objects in the surroundings [1].

When a signal is transmitted over a wireless channel, the received signal envelope goes through rapid random variations. There are three types of variations: a gradual decrease of the signal mean strength with the distance which is called "signal attenuation"; slow variation of the mean independent of the distance referred to as "shadowing"; and a fast variation over-riding the slow fading signal mean referred to as "small-scale fading". The path loss due to signal attenuation in dB can be calculated as $10n\log(d)$, where d is the distance between the transmitter and the

receiver, usually measured in meters, and n is the path loss exponent which depends on the environment. The measured value of the path loss exponent n is usually found between 2 and 4, where $n = 2$ indicates the case of free-space communication. In some buildings and some other indoor environments, the path loss exponent can reach values in the range of 4 to 6. On the other hand, the path loss exponent can be less than 2 in corridors or tunnels [2].

Small-scale fading is caused by constructive or destructive summation of several versions of the transmitted signal which arrive at the receiver via different paths. These different versions combine at the receiver, and, depending on their relative phase differences, they either add or subtract, which creates the random fluctuation in the amplitude of the received signal. Even when the mobile terminal is stationary, the received signal may still fade because of the movement of the objects around the receiver.

The discrete-time signal model that is widely used to describe the transmission of signals over a channel with small scale fading is given by [3]

$$y_t = \sqrt{d^{-n}}\alpha_t x_t + \eta_t, \tag{1.1}$$

where y_t is the received signal during the t^{th} sampling instant, x_t is the transmitted signal with average energy of E_s, η_t is a sample of an additive white Gaussian noise (AWGN) random process with zero mean and variance σ^2, and α_t is the fading amplitude of the channel.

When there is a line-of-sight (LOS) between the transmitter and the receiver, one of the multipath components becomes dominant, and this component is called LOS [2]. In this case, the fading envelope follows the Rice distribution. In the absence of a LOS component, the envelope of the received signal is found to follow a Rayleigh Distribution, whose probability density function (pdf) is given by

$$p(r) = \frac{r}{\sigma^2} \exp\Big(- \frac{r^2}{2\sigma^2}\Big), \tag{1.2}$$

where the variance of the signal equals $(2 - \frac{\pi}{2})\sigma^2$ [3]. Another fading distribution is the Nakagami-m distribution, which is used frequently to fit the statistics of faded signals transmitted through indoor environments. Under Nakagami fading, the pdf of the received signal envelope is given by

$$p(r) = 2\Big(\frac{m}{2\Omega}\Big)^2 \frac{1}{\Gamma(m)} r^{2m-1} \exp\Big(- \frac{mr^2}{2\Omega}\Big), \tag{1.3}$$

where $\Gamma(.)$ is the Gamma function, 2Ω is the mean signal power, and $m \geq 1/2$. By setting $m = 1$, the Nakagami distribution reduces to the Rayleigh distribution. For values of $\frac{1}{2} \leq m \leq 1$, we obtain pdf's that have larger tails than Rayleigh distributed random variables. For values of $m > 1$, the tail of the pdf decays faster than that of the Rayleigh pdf. As m increases, the severity of the fading decreases [3].

The delay between the first and the last arrival is usually referred to as the maximum delay spread and denoted by τ_M. Based on the relation between τ_M and the symbol period T_s, we can define two types of fading channels [4]:

- Flat fading channels, in which all the frequency components of the transmitted signal fade with the same value. This channel is encountered if $\tau_M \ll T_s$. The effects of such channel can be overcome by employing diversity or coding [2].

- Frequency-selective fading channels, in which the value of fading is different for different frequency components of the transmitted signal. This happens when $\tau_M \gg T_s$. In this case, equalization can be used to reduce the effect of the channel [2].

Another property of the channel is its coherence time, $\triangle t$, which is defined as the period in which the channel response is highly correlated. Two types of fading channels can be defined based on the relation between $\triangle t$ and the symbol period T_s [5]:

- Slow fading channels, in which different symbols of the transmitted signal fade with the same value. This channel is encountered when $\triangle t \gg T_s$.

- Fast fading channels, in which the value of fading is different for different symbols of the transmitted signal. This happens when $\triangle t \ll T_s$.

Many techniques have been proposed in the literature to overcome the effect of multipath fading, one of which is diversity, which is discussed next.

1.1.2 Diversity

Diversity is used to provide more than one independently faded version of the transmitted signal (diversity branches) at the receiver in order to produce a better version of the transmitted signal. Consider two independently faded versions of the transmitted signal. The probability distribution of the fading determines the probability of outage, which is defined as the probability of the signal envelope falling below a certain threshold. If the probability of signal outage i.e., $P(r_i < R_{th}) = 0.2, i = 1, 2$ then the probability that both signals will fade simultaneously is $P(r_1 < R_{th}, r_2 < R_{th}) = 0.2^2 = 0.04$.

There are many ways of combining the diversity branches. In selection diversity (SC), the best diversity branch is selected for detection. In maximal ratio combining (MRC), the signals from each diversity branch are aligned in phase, and weighted by their channel gains before adding them coherently. If the weights used in MRC is set to be the same for all the branches, then the resulting combining scheme is called equal gain combining (EGC) [3]. Different diversity branches can be provided using one of the following techniques:

- Time diversity: Because the channel characteristics change with time, another replica of the signal can be sent after a certain time interval. This time interval must be longer than the coherence time of the channel, $\triangle t$. This time separation is required in order to ensure that the channel characteristics have

changed enough.

- Frequency diversity: Another replica of the signal is transmitted over a different frequency. The frequency difference between the two versions must be more than the channel coherence bandwidth $\triangle f$ which is the bandwidth over which the channel response is high correlated.

- Space diversity: Here, multiple antennas can be used at the receiver to receive different versions of the transmitted signal where each version suffers a different fading channel.

The system which uses antenna arrays at both the transmitter and the receiver is called the multiple-input-multiple-output (MIMO) system. While MIMO systems improve the system capacity greatly [1], it is difficult to implement antenna arrays on hand-held terminals due to size, cost and hardware limitation. In order to overcome this problem, a technique known as cooperative communication was introduced [6, 7, 8, 9, 10]. This technique allows single-antenna mobile units to get some of the benefits of MIMO systems in a distributed manner. The basic idea is that single-antenna mobile units in a multi-user scenario can share their antennas in a manner that creates a virtual MIMO system. Furthermore, terminals can relay signals for other terminals without the need for base stations. Such a network is referred to as a multi-hop network, which is the main theme for this work and will be discussed in Section 1.2. Next we will discuss error control coding, which is another method

used to combat multipath fading.

1.1.3 Error Control Coding

A major concern of any communication network designer is the control of errors so that data can be reliably reproduced at the receiver. There are two conventional types of error control codes, block codes and convolutional codes [11].

In block codes, the encoder divides the information into message blocks $\mathbf{u}$ each of length k bits. The encoder transforms each of the messages composed of k bits into an n-bit codeword $\mathbf{v}$. Therefore, corresponding to the 2^k different possible messages, there are 2^k different possible codewords at the encoder output. The set of 2^k codewords of length n bits is called an (n, k) block code. The ratio $R_c = k/n$ is referred to as the code rate. Since the output codeword depends only on the corresponding k-bit information message, the encoder is memory-less and can be implemented with combinational logic circuits [11].

The other type of error control coding is the convolutional code. In this case, the encoder takes the k-bit message $\mathbf{u}$ and creates an n-bit coded vector $\mathbf{v}$. However, the coded vector depends not only on the corresponding k-bit message $\mathbf{u}$ as in block codes, but also on the previous m k-bit messages. Such an encoder is said to have a memory order of m. An (n,k) convolutional code with memory order m is called an (n, k, m) convolutional code. Since the encoder has memory, it must be implemented with sequential logic circuits. Figure 1.1 shows the diagram of a

binary (2,1,2) convolutional encoder [11].

1.1.4 Code Division Multiple Access (CDMA)

Multiple access is the ability of many users to communicate with each other while sharing a common transmission medium. Wireless multiple-access communications are facilitated if the transmitted signals are orthogonal or separable in some sense. Signals may be separated in time (time-division multiple access or TDMA), frequency (frequency-division multiple access or FDMA), or code (code-division multiple access or CDMA) [3].

CDMA is realized by using spread-spectrum modulation while transmitting signals from multiple users in the same frequency band at the same time. The data from each user is superimposed with a different pseudorandom pattern. Thus, a particular receiver can recover the transmitted data intended for it by knowing the pattern used by the corresponding transmitter. All signals use the entire allocated spectrum, but the spreading sequences or frequency-hopping patterns are different. Information theory indicates that, in an isolated cell, CDMA systems achieve the same spectral efficiency as TDMA or FDMA systems only if optimal multiuser detection is used [1]. However, even with single-user detection, CDMA is advantageous for multi-cell networks, because it eliminates the need for frequency and timeslot coordination among cells, and it allows carrier-frequency reuse in adjacent cells. In addition, frequency planning is vastly simplified in CDMA networks. Another advantage of

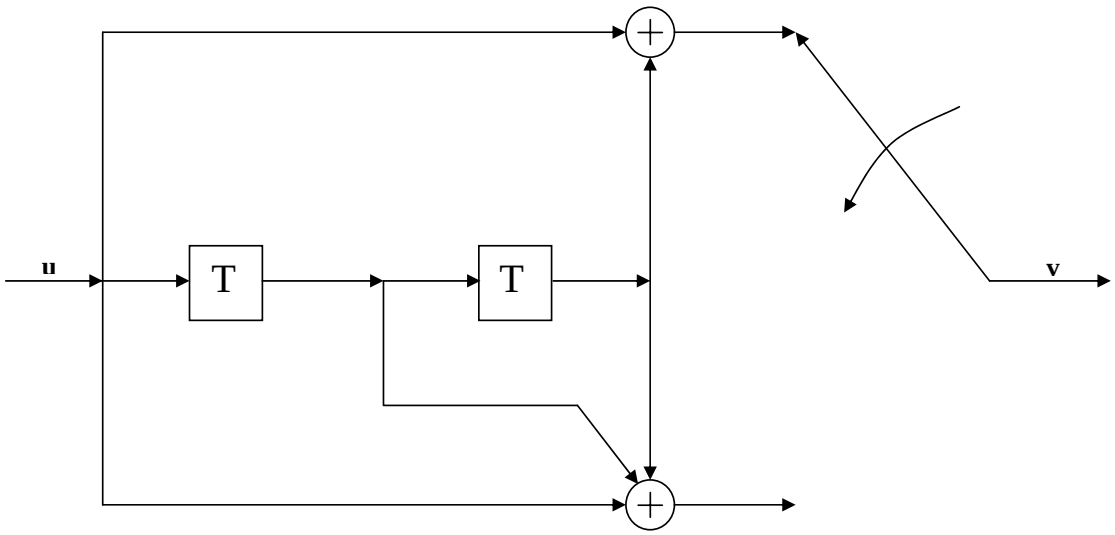

Figure 1.1: Structure of a binary (2,1,2) convolutional encoder.

CDMA networks is the strong resistance to jamming, interception, and multipath interference.

The two principal types of spread-spectrum techniques are direct-sequence spread-spectrum (DSSS) and frequency-hopping spread-spectrum (FHSS). CDMA is a specific type of DSSS when there are multiple users in the system. In this thesis, we consider only DS-CDMA. Chapter 3 discusses the application and performance of multihop relaying in CDMA networks.

1.1.5 Orthogonal Frequency-Division Multiplexing (OFDM)

OFDM systems are attractive to mitigate frequency-selective multipath fading in a wireless environment [4]. OFDM has been proposed for military applications since the 1960s by Chang and Gibby [12]. The idea behind the proposal was to trans-

mit multiple narrow-band signals in parallel by multiplexing them onto orthogonal sub-channels. These closely-spaced orthogonal sub-carriers are used to carry data in parallel. The data is divided into several parallel data streams or channels, one for each sub-carrier. Each sub-carrier is modulated with a conventional modulation scheme (such as binary phase shift keying) at a low symbol rate, reducing the effect of inter-symbol interference (ISI) resulting from the frequency selectivity of the channel. OFDM has developed into a popular scheme for wideband digital communication, whether wireless or over copper wires, used in applications such as digital television, audio broadcasting, wireless networking and broadband internet access [13].

The main advantage of OFDM over other single-carrier schemes is its ability to cope with the frequency selectivity of the channel and multipath fading without the need for complex equalization filters. Other advantages are: robustness against narrowband interference; ISI and fading caused by multipath propagation; and very high spectral efficiency resulting from the use of overlapping orthogonal subcarriers. Also, channel equalization is simplified because OFDM may be viewed as using several parallel low-rate narrowband signals rather than one high-rate wideband signal [13]. OFDM systems require additional methods to exploit diversity, since the performance of uncoded OFDM systems in time and frequency-selective fading channels is similar to the performance over narrowband fading channels. A widely used approach is to implement error control coding with OFDM. Coding, in combination

with interleaving can achieve performance results that are far better than those of uncoded OFDM systems.

We will discuss the application and performance of convolutionally coded multihop relaying in OFDM networks in Chapter 4.

1.2 Multi-hop Networks

Because the number of mobile users increases every day, high channel capacity is required in order to realize high data rate transmission for these users. One way to enhance the channel capacity is to realize a multi-hop ad-hoc network. In multi-hop networks, ordinary mobile terminals are used to relay the data from the transmitter to the receiver without the need for a base station. Other advantages for multi-hop networks include larger coverage area, flexible routing capability, low power consumption, and better quality of service in poor fading channel conditions [14].

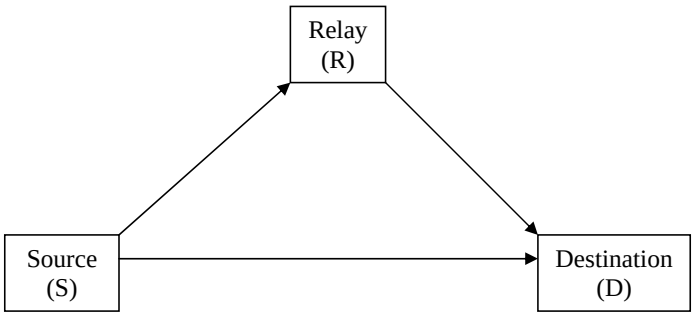

Figure 1.2: Multi-hop network with one relay.

In direct transmission between a source node (S) and a destination node (D), the discrete-time signal model is given by [3]

$$y_d = \sqrt{d_{sd}^{-n}}\alpha_{sd}x_s + \eta_d, \tag{1.4}$$

where y_d is the received signal at the destination, α_{sd} is the channel fading amplitude between the source and the destination, x_s is the transmitted signal from the source, d_{sd} is the distance between the source and the destination, n is the path loss exponent, and η_d is the AWGN component at the destination.

Relays can handle the data before forwarding it to the destination using one of the following methods:

- Amplify-and-forward (AF): Also called non-regenerative technique [15]. In AF scheme, the relay node receives the signal y_r, amplifies it, and forwards it to the destination node. The signal model is given by

  $$y_d = \sqrt{d_{rd}^{-n}}G\alpha_{rd}y_r + \eta_d, \tag{1.5}$$

  where G is the amplification coefficient, and the term α_{rd} is the fading amplitude of the channel between the relay node and the destination node. The value for the gain is usually chosen as

  $$G^2 = \frac{E_r}{E_s d_{rd}^{-n}\alpha_{rd}^2 + N_{0_r}}, \tag{1.6}$$

  where E_s is the energy of the transmitted signal from the source, E_r is the energy of the transmitted signal at the output of the relay, and N_{0_r} is the noise

average power at the relay node. The choice of this gain aims to invert the fading and the attenuation effects of the first hop while limiting the output power of the relay if the fading amplitude of the first hop is low [16].

- Decode-and-forward (DF): In this system, the relay node decodes the data, encodes it again, and forwards it to the destination node. It is sometime referred to as a regenerative technique [15]. The received signal at the destination node using DF scheme is given by

$$y_d = \sqrt{d_{rd}^{-n}}\alpha_{rd}\hat{y}_r + \eta_d, \tag{1.7}$$

  where $\hat{y}_r$ is the signal after being encoded by the relay node.

- Compress-and-forward (CF): In this case, the relay node forwards a compressed version of the received signal to the destination node. This compressed version is used as side information at the destination. This scheme achieves gains comparable to MIMO transmission [17].

In the case of more than one relay node, there are different network topologies. In this thesis, we will consider network topologies that are mathematically tractable. Among these are parallel, serial, and hybrid topologies as shown in Figure 1.3. A lot of research has been done in the area of multi-hop networks. Some researchers are trying to create reliable routing protocols to route the data within the network as in [18] and the references therein. Others have been working on scheduling algorithms

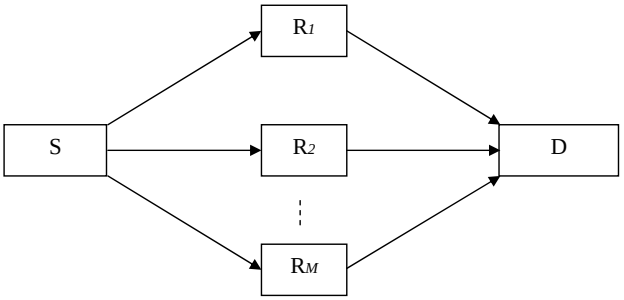

(a) Parallel topology

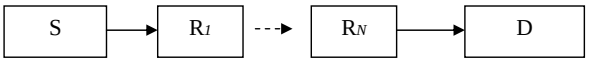

(b) Serial topology

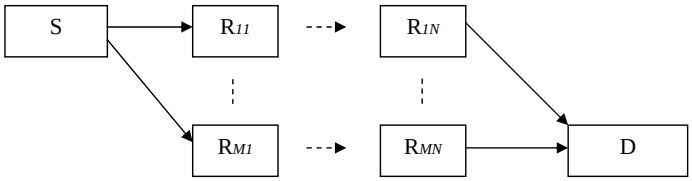

(c) Hybrid topology

Figure 1.3: Multi-hop network topologies (a) Parallel topology, (b) Serial topology, and (c) Hybrid topology.

to select the order of the transmission as in [19] and the references therein, or else to enhance the performance of the bit error probability (BEP) by implementing error correction codes as in [14] and the references therein. In this thesis, we consider both uncoded and convolutionally coded multi-hop networks employing narrowband transmission as well as wideband transmission using CDMA and OFDM techniques.

1.3 Literature Survey

In [16], Hasna *et al.* focused on two-hop wireless networks and derived the end-to-end error performance over independent Rayleigh fading channels. In particular, they presented closed-form expressions for the statistics of the harmonic mean of two independent exponential variates, which is used to characterize the error performance of the system. They also showed comparisons of outage probability, BEP and outage capacity between non-regenerative and regenerative systems. The main conclusion was that networks employing regenerative relays outperform those employing non-regenerative relays at low average SNR. However, at high average SNR, it was shown that the two systems are essentially equivalent in terms of outage probability average BEP and outage capacity.

In [20], Hasna considered an N-hop series non-regenerative relaying model. He derived an expression for the end-to-end SNR of the N-hop network and an upper bound to it. This expression was used to evaluate the average SNR, the amount of

fading, and average BEP of the system. The numerical results show that relaying enhances the system performance compared with equivalent direct transmission. In addition, relaying also reduces the severity of fading.

In [21], Hasna *et al.* studied the performance of a two-hop wireless networks with AF relays having fixed gains in terms of outage probability and average BER. They proposed a relaying scheme in which the relays select their gains based on the first hop's average SNR. It was shown that the difference in error performance between the network with fixed gains and the variable-gain relays is not large, and that the relays with fixed gains can even outperform the variable-gain relays at low SNR. In addition, it was shown that the loss in performance due to relay saturation in minimal and happens in low average SNR regimes only.

In [14], Wada *et al.* considered turbo coded multi-route multi-hop networks using parity check bits. They showed the detailed system model and the effect of the turbo code in performance improvement. The problem with turbo codes is that the destination node must know the channel state information. However, by using parity bits, the channel information of the whole route can be easily estimated by treating the channel as a binary symmetric channel. Finally it was shown by numerical examples that the proposed system does not perform well over AWGN channels but it is quite effective in fading channels.

In [22], Yang *et al.* presented a closed-form expression for the average outage duration (AOD) of multi-hop networks employing DF relays over different fading channel

models, namely, "Rayleigh, Ricean, and Nakagami". The AOD expression was used to compare between direct and relayed transmission schemes over a Rayleigh fading channel. They studied the effect of the number of hops and the number of co-channel interferers. The results showed that the gain provided by relaying increases with the number of relays used with fixed-distances separating the relays. However, when the number of hops is increased to extend the coverage area, the performance degrades with this increase.

In [23], Leib *et al.* considered the union bounding techniques for error control codes with limited interleaving over block fading Ricean channels. They showed that the traditional union bounding technique, which sums averaged pairwise error probabilities, yields very loose results especially for block fading Rayleigh channels. Additionally, the researchers presented a modified union bounding technique, which limits the conditional union bound before averaging over the fading process, and thus avoids the explosion of the union bound for low SNR. This modified bounding technique provides much tighter, and hence more useful, numerical results, but it requires L-fold numerical integration where L is the number of diversity subchannels. Examples were shown for terminated convolutional codes, but the necessity for optimization before averaging in the block fading channels can be extended to other block codes as well.

In [24]. Hunter *et al.* presented an analytical methodology for evaluating the performance of a two-user coded cooperation system. The results they obtained provide

accurate estimates for the bit error rate (BER) and block error rate (BLER) of coded cooperation. The results showed that the coded cooperation framework does achieve full diversity. However, their approach becomes inaccurate and complicated when the number of cooperating users exceeds two.

In [25], Zummo investigated the performance of coded cooperation diversity with multiple cooperating users, where the users form a cluster and cooperate their coded data to a common base station. The researcher derived the end-to-end bit error probability for users in a cluster, and showed results for different cluster sizes and SNRs. He also derived a union bound on the end-to-end bit error probability averaged over different cooperation scenarios, such as no cooperation and all cooperation scenarios considering both correlated and un-correlated Rayleigh fading channels. Numerical results showed that for a fixed inter-user channel quality, the small-sized clusters perform better than the large-sized clusters in terms of probability of error.

In [26], Balakrishnan *et al.* analyzed the performance of different error control codes used in wireless sensor networks. They evaluated the BER and the power consumption of three error control codes: namely, Binary BCH codes, Reed-Solomon (RS) codes, and convolutional codes. They considered AWGN and Rayleigh fading channel models. The results showed that in terms of code rates the binary BCH codes perform better than RS codes, but the RS performs better for lower BER. The results show that the power consumed by the binary BCH and RS codes is lower than that of the uncoded channel, for the same BER performance, whereas coded net-

works employing convolutional codes consume more power than that of the uncoded networks.

In [27], Sunay *et al.* showed how to calculate the error probabilities for various unbalanced DSCDMA systems using the standard Gaussian approximation (SGA), improved Gaussian approximation (IGA), and Fourier series based schemes (FS). They used these three approaches to calculate the error probability of a scarcely populated system, a system with a dominant interferer, a system in a fading channel, and a multimedia system with a single high processing gain user. Results showed that the SGA gives less accurate results when the number of active users in the system is low. The IGA gives more accurate results for a scarcely populated system and a system with a dominant interferer. FS give the most accurate results for all cases.

In [28], Zhao *et al.* investigated the performance of coding-spreading tradeoff in DSCDMA systems when using rate-compatible punctured turbo (RCPT) and rate-compatible punctured convolutional (RCPC) codes. Additionally, they tested the best RCPC and RCPT code rate in terms of maximizing the system spectral efficiency and minimizing the optimal power allocation where the receiver is either a matched filter (MF) or a minimum mean-square error (MMSE). The results showed that, for the MF receiver, the coding-spreading tradeoff favors a code-rate reduction. Conversely, for the MMSE receiver, when the SNR value and the system load are increased, the best code rate also increases. Another conclusion was that under

similar operating conditions, the best code rate of the RCPT codes is lower than that of the RCPC codes. Also, the best code rate for a Rayleigh fading channel is lower than that for an additive white Gaussian noise channel.

In [29], Hoshyar *et al.* showed that OFDM is in the category of correlated block fading systems (CBFS). They presented the performance analysis of CBFS, and computed an upper bound for the pairwise error probability. Simulation results showed that the performance of the system is limited by the code structure and channel profile. The maximum achievable diversity is determined by the channel profile, which is achieved by good enough codes. It is expected also that by using diversity increasing methods such as antenna diversity, turbo code brings about more considerable gain to the system.

In [30], Dai *et al.* proposed an OFDM-based selective relaying scheme, where the relay selection at each hop is performed on a per-subcarrier basis and joint selection is adopted at the last two hops. The outage analysis done by Dai *et al.* showed that full spatial diversity gain can be achieved with this proposed selective OFDMA relaying. In contrast, no diversity gain can be obtained if the entire OFDM block chooses the same relay with the highest combined SNR. It is also demonstrated that, with coding among the subcarriers, superior performance can be achieved by selective OFDMA relaying with only symbol detection at each relay. This is highly attractive as the processing complexity and decoding delay incurred are very small. In the literature, the error performance of multi-hop networks was investigated in

narrowband channels for only serial topology without MRC with only AF relaying. We are going to investigate the performance of the network with an MRC receiver over different fading environments in narrowband, CDMA, and OFDM systems using AF and DF relaying with different topologies.

1.4 Thesis Contributions

The contributions of this thesis can be summarized as follows:

- We investigate the performance of both uncoded and convolutionally coded multi-hop networks over narrowband fading channels. The end-to-end probability of error of both the uncoded and the convolutionally coded multihop networks is derived when employing AF relaying for both the serial and parallel topologies.

- The performance of multi-hop relaying in uncoded CDMA networks is derived. In particular, we analyze the end-to-end probability of error of the network under different topologies and fading distributions. Finally, we investigate the effect of different network parameters such as the spreading gain and the number of users on the performance of the network.

- Finally, we investigate the effect of relaying on the error performance of convolutionally coded multi-hop networks employing OFDM transmission. The error performance of the network is studied when using serial, parallel, and selection relaying over two different wideband fading channels. Additionally, the effect of the number of carriers and the path loss exponent on the network performance is investigated.

1.5 Thesis Outline

In Chapter 2, we investigate the performance of both uncoded and convolutionally coded multi-hop networks over a narrowband fading channels. We derive the error performance of the system with serial and parallel relaying, using AF for both the coded and the uncoded cases.

In Chapter 3, we investigate the performance of multi-hop relaying in CDMA networks. A brief background on spread spectrum techniques is given. We use the standard Gaussian approximation to derive the probability of error of the CDMA-based network with diversity. The probability of error of the system when using serial and parallel relaying is derived. Additionally, we investigate the error performance of systems with serial, parallel and selection relaying over different values of spreading gain and number of users.

In Chapter 4, we investigate the performance of convolutionally coded multi-hop networks in OFDM wireless environments. We consider the different forwarding techniques and the multi-hop topologies used in the literature. The performance of the system using serial, parallel, and selection relaying over different wideband fading channels is investigated. Finally, the effect the number of carriers has on the system, and the effect of the path loss exponent are investigated.

Finally in Chapter 5, the main conclusions from the thesis and possible future research directions are discussed.

Chapter 2

Narrowband Networks

In multi-hop networks, ordinary mobile terminals are used to relay the data from the source to the destination without the need for a base station. The relaying improves the system because it acts like a space diversity scheme. Other advantages for multi-hop networks include larger coverage area, flexible routing capability, low power consumption, and better quality of service in poor fading channel conditions [14].

In this chapter, we investigate the performance of multi-hop networks over narrowband channels with Rayleigh fading. We will derive the error performance of both the uncoded and the convolutionally coded systems when using AF relaying in different network topologies.

The rest of the chapter is organized as follows. Section 2.1 gives a brief description of the system model we are using. Section 2.2 shows the performance analysis of the

uncoded system. Section 2.3 shows the performance analysis of the convolutionally coded system. Finally Section 2.4 presents the chapter's conclusion.

2.1 System Model

The discrete-time signal model of the received signal at the relay for the single-relay serial network is given by

$$y_r = \sqrt{d_{sr}^{-n}}\alpha_{sr}x_s + \eta_{sr}, \tag{2.1}$$

where y_r is the received signal at the relay, α_{sr} is the channel fading amplitude between the source and the relay, x_s is the transmitted signal from the source, d_{sr} is the distance between the source and the relay usually measured in meters, n is the path loss exponent which depends on the environment, and finally η_{sr} is the AWGN component at the relay. The relay amplifies and forwards the signal to the destination node. The received signal at the destination node using AF scheme is given by

$$y_d = G\sqrt{d_{rd}^{-n}}\alpha_{rd}y_r + \eta_{rd}, \tag{2.2}$$

where d_{rd} is the distance between the relay and the destination, and η_{rd} is the AWGN component at the destination. The most widely used formula for the forwarding gain G is given by [21]:

$$G^2 = \frac{E_r}{E_s d_{sr}^{-n}\alpha_{sr}^2 + N_{0_{sr}}}, \tag{2.3}$$

where E_r is the average transmitted energy at the relay, E_s is average transmitted energy from the source, α_{sr} is the fading amplitude of the first hop, and $N_{0_{sr}}$ is the noise average power of the first hop. The gain aims to invert the fading and path loss effects of the first hop, while limiting the output power of the relay if the fading amplitude of the first hop is low.

At the destination, maximum ratio combining (MRC) is employed to combine the data received from the source and the relays. For L-branch MRC receiver, the total received signal-to-noise-ratio (SNR) at the output of the MRC combiner is given by [3]

$$\gamma_T = \sum_{l=1}^{L} \gamma_l, \tag{2.4}$$

where γ_l is the SNR for the branch l. For coherent BPSK, the conditional bit error probability (BEP) of the L-branch MRC receiver is given by

$$P_b(E|\{\gamma_l\}_{l=1}^{L}) = Q(\sqrt{2\gamma_T}), \tag{2.5}$$

where $P(E)$ is the probability of an error event at the receiver, and the subscript b means a bit error. In order to find the average end-to-end BEP of the system, the conditional BEP in (2.5) has to be averaged over the distribution of the random variables $\{\gamma_l\}_{l=1}^{L}$. For this purpose, we need to find the probability distribution function (PDF) of the total SNR γ_T and to average (2.5) over this PDF as follows:

$$P_b(E) = \int_0^{\infty} Q(\sqrt{2\gamma_T}) p_{\gamma_T}(\gamma_T) d\gamma_T. \tag{2.6}$$

An alternative expression for the Gaussian Q-function can be found in [31] as

$$Q(x) = \frac{1}{\pi}\int_0^{\pi/2} \exp\left(-\frac{x^2}{2\sin^2(\phi)}\right) d\phi. \tag{2.7}$$

Using (2.7) in (2.5) yields

$$P_b(E|\{\gamma_l\}_{l=1}^L) = \frac{1}{\pi}\int_0^{\pi/2} \exp\left(-\frac{2\gamma_T}{\sin^2(\phi)}\right) d\phi = \frac{1}{\pi}\int_0^{\pi/2} \prod_{l=1}^{L} \exp\left(-\frac{2\gamma_l}{\sin^2(\phi)}\right) d\phi. \tag{2.8}$$

By averaging (2.8) over the PDFs of the random variables $\{\gamma_l\}_{l=1}^L$ independently, the average end-to-end BEP can be written as

$$P_b(E) = \underbrace{\int_0^{\infty}\int_0^{\infty}\cdots\int_0^{\infty}}_{L fold} \frac{1}{\pi}\int_0^{\pi/2} \prod_{l=1}^{L} \exp\left(-\frac{2\gamma_l}{\sin^2(\phi)}\right) p_{\gamma_l}(\gamma_l) d\phi d\gamma_1 d\gamma_2 \cdots d\gamma_L \tag{2.9}$$

By interchanging the integrals in (2.9), we can combine the terms with index l. Thus an expression for the average end-to-end BEP for BPSK can be written as

$$P_b(E) = \frac{1}{\pi}\int_0^{\pi/2} \prod_{l=1}^{L} M_{\gamma_l}\left(\frac{-1}{\sin^2(\phi)}\right) d\phi, \tag{2.10}$$

where $M_{\gamma_l}(s) = \int_0^{\infty} p_{\gamma_l}(\gamma_l)\exp(s\gamma_l) d\gamma_l$ is the moment generating function (MGF) of the SNR per symbol associated with the diversity path l.

A general expression for the average end-to-end BEP for M-PSK with Grey coding was derived in [32] as

$$P_b(E) = \frac{1}{\pi\log_2(M)}\int_0^{(M-1)\pi/M} \prod_{l=1}^{L} M_{\gamma_l}\left(\frac{-\sin^2(\pi/M)}{\sin^2(\phi)}\right) d\phi, \tag{2.11}$$

where M is the number of constellation points composing the M-PSK modulation scheme, and $\log_2(M)$ is the number of bits/symbol.

For M-QAM, a general expression for the average end-to-end BEP was also derived in [32] as

$$P_b(E) = \frac{4}{\pi \log_2(M)} \left(1 - \frac{1}{\sqrt{M}}\right) \int_0^{\pi/2} \prod_{l=1}^{L} M_{\gamma_l} \left(\frac{-3}{2(M-1)\sin^2(\phi)}\right) d\phi - \frac{4}{\pi \log_2(M)} \left(1 - \frac{1}{\sqrt{M}}\right)^2 \int_0^{\pi/4} \prod_{l=1}^{L} M_{\gamma_l} \left(\frac{-3}{2(M-1)\sin^2(\phi)}\right) d\phi \quad (2.12)$$

2.2 Uncoded System

In this section we derive the performance of an uncoded multi-hop network using AF relaying with serial and parallel topologies over narrowband Rayleigh fading channels.

2.2.1 Serial Relaying

In serial relaying with AF relaying, the source transmits the data to a relay, which in turn amplifies and forwards it to the destination or another relay. The destination combines the received signal from both the source and each of the relays using MRC. The serial topology used in this section is shown in Figure 2.1, while Figure 2.2 shows the time allocation of all the transmissions. For simplicity, we consider the relays are positioned at an equal distance between the source and the destination nodes. Also, in order to be fair in comparing the relayed transmission and the direct transmission in terms of energy and bandwidth, we use QPSK for the single-relay network and

8PSK for the two-relay network. By doing this, we make sure that the total number of bits transmitted and the energy per bit is the same in all cases. Table 2.1 shows the parameters of the serial network used.

For the single-relay serial network, the received signal at the relay and the destination were shown in (2.1) and (2.2) respectively. If the gain is chosen as (2.3), the equivalent SNR at the destination can be written as [20]

$$\gamma_{eq} = \frac{\gamma_{sr}\gamma_{rd}}{\gamma_{sr} + \gamma_{rd} + 1}, \tag{2.13}$$

where $\gamma_{sr} = \frac{E_s d_{sr}^{-n} \alpha_{sr}^2}{N_{0_{sr}}}$ and $\gamma_{rd} = \frac{E_r d_{rd}^{-n} \alpha_{rd}^2}{N_{0_{rd}}}$ are respectively the SNRs from the source to the relay and from the relay to the destination nodes. After the receiver combines the signals from the source and the relay using MRC, the total received SNR at the destination γ_d becomes

$$\gamma_d = \gamma_{sd} + \frac{\gamma_{sr}\gamma_{rd}}{\gamma_{sr} + \gamma_{rd} + 1}, \tag{2.14}$$

where $\gamma_{sd} = \frac{E_s d_{sd}^{-n} \alpha_{sd}^2}{N_{0_{sd}}}$ is the end-to-end SNR from the source to the destination nodes.

Hasna *etal.* in [20] have showed that for J relays serial relaying using the gain

Number of relays	**Modulation scheme**
0	BPSK
1	QPSK
2	8PSK

Table 2.1: Network parameters of uncoded serial relaying scheme.

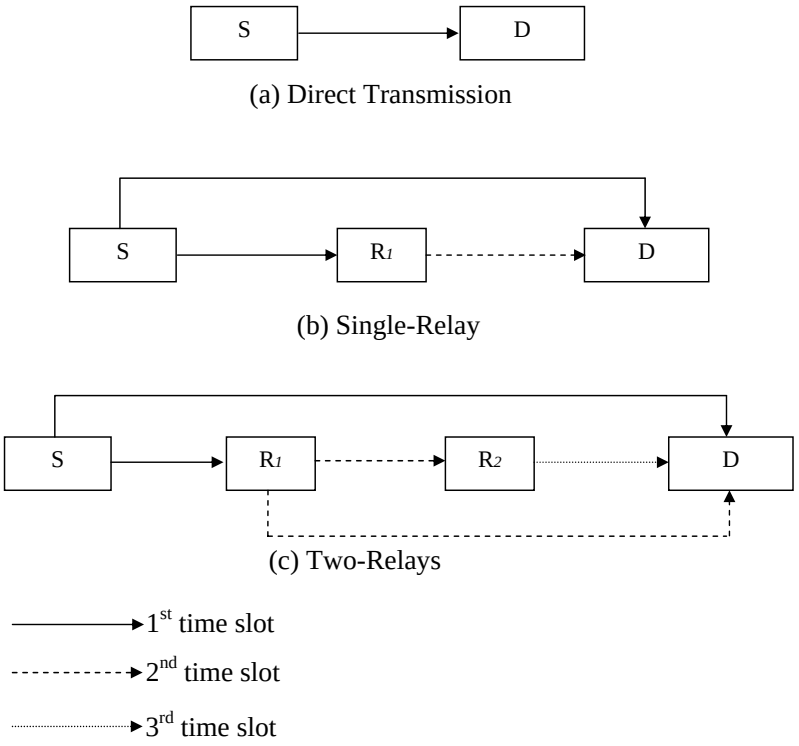

Figure 2.1: Serial multihop topology. (a) Direct transmission, (b) Single-relay network, and (c) Two-relay network.

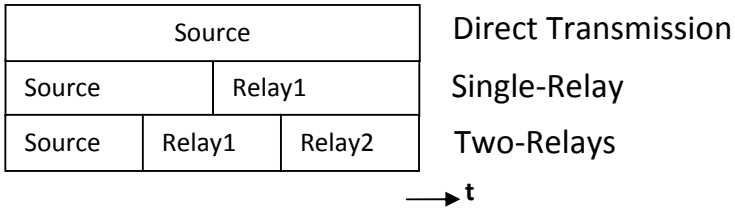

Figure 2.2: Time Allocation of the serial relaying scheme.

formula for relay j as

$$G_j^2 = \frac{E_{j+1}}{E_j d_j^{-n} \alpha_j^2 + N_{0_j}}, \tag{2.15}$$

the end-to-end SNR can be shown to be

$$\gamma_{eq} = \left[\prod_{j=1}^{J+1} \left(1 + \frac{1}{\gamma_j} \right) - 1 \right]^{-1}, \tag{2.16}$$

where $\gamma_j = \frac{E_j d_j^{-n} \alpha_j^2}{N_{0_j}}$ is the SNR of the j-th hop.

Combining (2.4) and (2.16), the equivalent SNR of a serial relaying system with J relays after the MRC at the destination becomes

$$\gamma_d = \gamma_{sd} + \left[\prod_{j=1}^{J+1} \left(1 + \frac{1}{\gamma_j} \right) - 1 \right]^{-1}. \tag{2.17}$$

Thus, the end-to-end SNR for the single-relay serial network can be written as

$$\gamma_d = \gamma_{sd} + \left[\left(1 + \frac{1}{\gamma_{sr}} \right) \left(1 + \frac{1}{\gamma_{rd}} \right) - 1 \right]^{-1}. \tag{2.18}$$

And for the two-relay serial network as

$$\begin{aligned} \gamma_d = \gamma_{sd} &+ \left[\left(1 + \frac{1}{\gamma_{sr1}} \right) \left(1 + \frac{1}{\gamma_{r1d}} \right) - 1 \right]^{-1} \\ &+ \left[\left(1 + \frac{1}{\gamma_{sr1}} \right) \left(1 + \frac{1}{\gamma_{r1r2}} \right) \left(1 + \frac{1}{\gamma_{r2d}} \right) - 1 \right]^{-1}. \end{aligned} \tag{2.19}$$

Using (2.10), we can calculate the average BEP of the network. The MGF of the first term in (2.17) for Rayleigh fading is easily found from [32] to be

$$M_{\gamma_{sd}}(s) = (1 - s\bar{\gamma_{sd}})^{-1}. \tag{2.20}$$

As for the second term in (2.17), a lower bound for its MGF was derived in [20] for Rayleigh fading for J relays as

$$M_{\gamma_{eq}}(s) = \left[1 + s\left[\sum_{j=1}^{J+1} \frac{1}{\bar{\gamma}_j}\right]^{-1}\right]^{-1}. \tag{2.21}$$

Applying the MGF approach in (2.10) for equations (2.20) and (2.21), we can find the average BEP of the single-relay serial case with QPSK transmission as

$$P_b(E) = \frac{1}{2\pi}\int_0^{3\pi/4} \left(1 + \frac{\sin^2(\pi/4)}{\sin^2(\phi)\left(\frac{1}{\bar{\gamma}_{sr}} + \frac{1}{\bar{\gamma}_{rd}}\right)}\right)^{-1} \left(1 + \frac{\sin^2(\pi/4)\bar{\gamma}_{sd}}{\sin^2(\phi)}\right)^{-1} d\phi, \tag{2.22}$$

and for the two-relays serial case with 8PSK transmission

$$P_b(E) = \frac{1}{3\pi}\int_0^{7\pi/8} \left(1 + \frac{\sin^2(\pi/8)}{\sin^2(\phi)\left(\frac{1}{\bar{\gamma}_{sr_1}} + \frac{1}{\bar{\gamma}_{r_1 d}}\right)}\right)^{-1} \times \left(1 + \frac{\sin^2(\pi/8)}{\sin^2(\phi)\left(\frac{1}{\bar{\gamma}_{sr_1}} + \frac{1}{\bar{\gamma}_{r_1 r_2}} + \frac{1}{\bar{\gamma}_{r_2 d}}\right)}\right)^{-1} \left(1 + \frac{\sin^2(\pi/8)\bar{\gamma}_{sd}}{\sin^2(\phi)}\right)^{-1} d\phi. \tag{2.23}$$

Figure 2.3 shows the error performance of the direct, single-relay, and two-relay serial BPSK, QPSK, and 8PSK transmission, respectively, over Rayleigh fading channels with path loss exponent n=3. The figure shows that the simulation results and the analytical results from equations (2.22) and (2.23) are very close. Also, the figure shows that relaying improves the performance of the network by more than 5 dB even with the SNR loss from the change in the transmission technique. The diversity gain in each case can be seen from the change in the slope of the curve. Figure 2.4 shows the effect of the path loss exponent on the performance of the single-relay serial scheme. The case where $n = 0$ means that the distance is not taken into

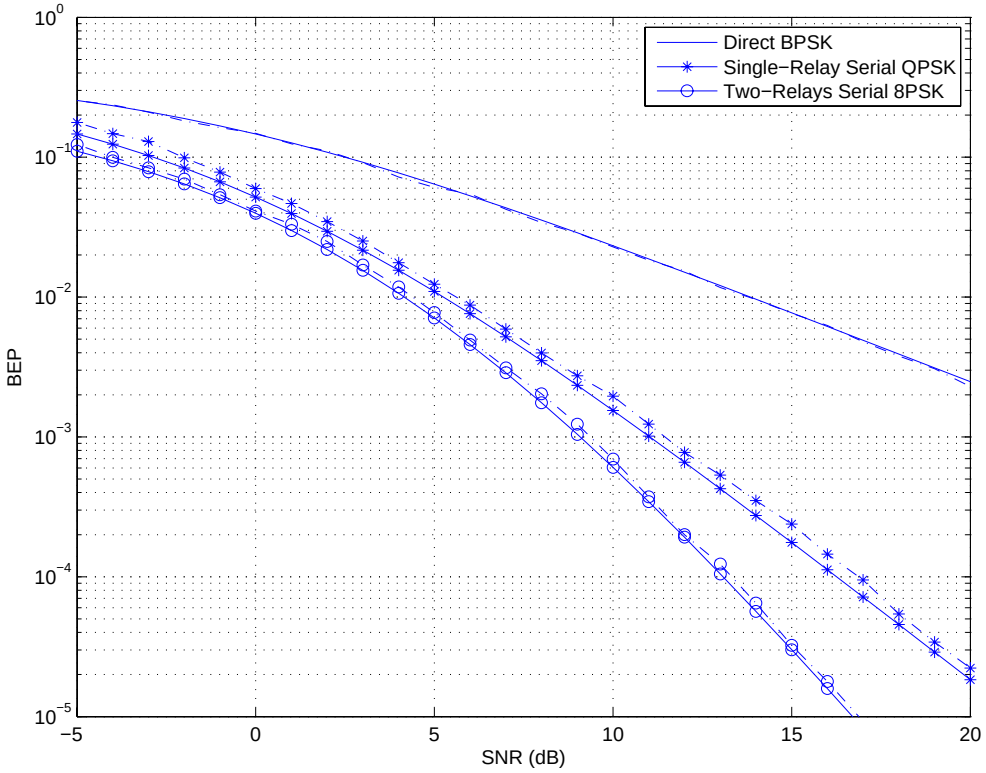

Figure 2.3: Performance of the direct BPSK transmission, single-relay serial QPSK transmission, and two-relay serial 8PSK transmission over Rayleigh fading channels: (solid) analysis, (dashed) simulation.

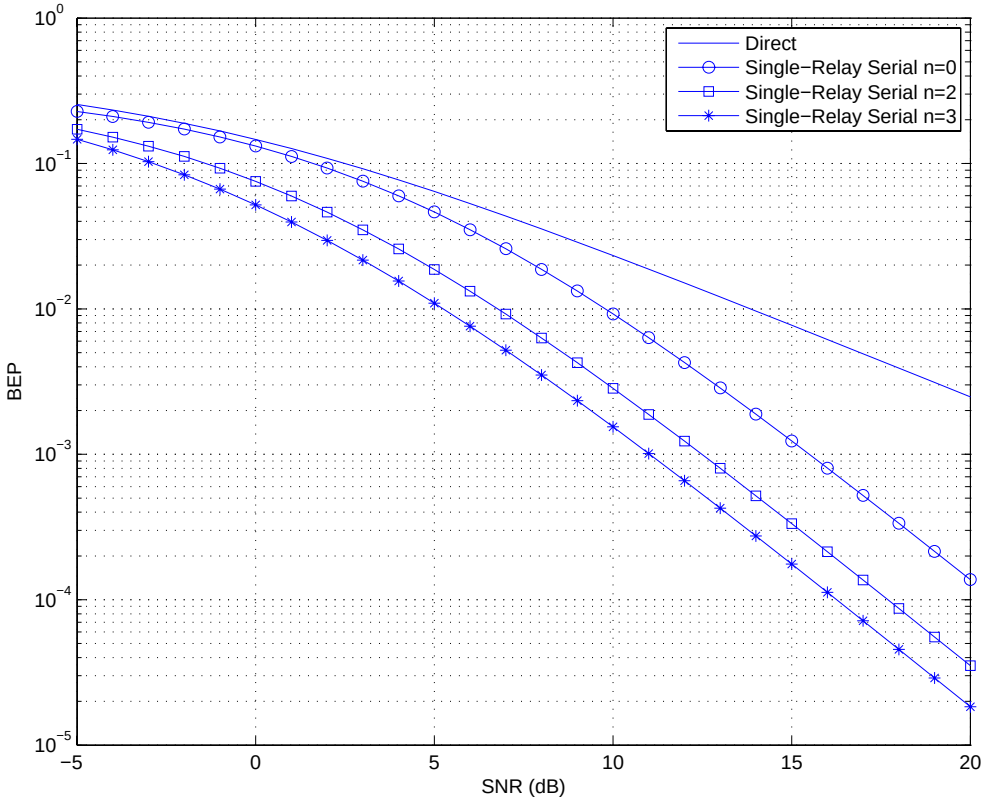

Figure 2.4: Effect of the path loss exponent on the performance of the single-relay serial scheme with $n = 0, 2$, and 3.

consideration. We can see from the figure that the relaying gain increases as the path loss exponent increases. In high path loss exponent environments, sending the data over short distances saves more energy than doing the same in low path loss exponent environments.

2.2.2 Parallel Relaying

In parallel relaying using AF, the source transmits the data to all the relays, which amplify and forward the signal to the destination node. The destination combines the received signal from the source and the relays using MRC. The parallel topology used in this chapter is shown in Figure 2.5. The time allocation of the system is the same as in the serial schemes shown in Figure 2.2. It is as if the destination is receiving the data from the source and from J links of single-relay serial transmissions.

For simplicity, we consider the relays are positioned in the middle between the source and the destination nodes. Also, in order to be fair in comparing the relayed transmission and the direct transmission in terms of energy and bandwidth, we use 8PSK for the two-relay network and 16QAM for the three-relay network. This ensures that the total number of bits transmitted and the energy per bit is the same in all cases. Table 2.2 shows the parameters of the network network used.

Using the same procedure as in the serial relaying, we can find the total received

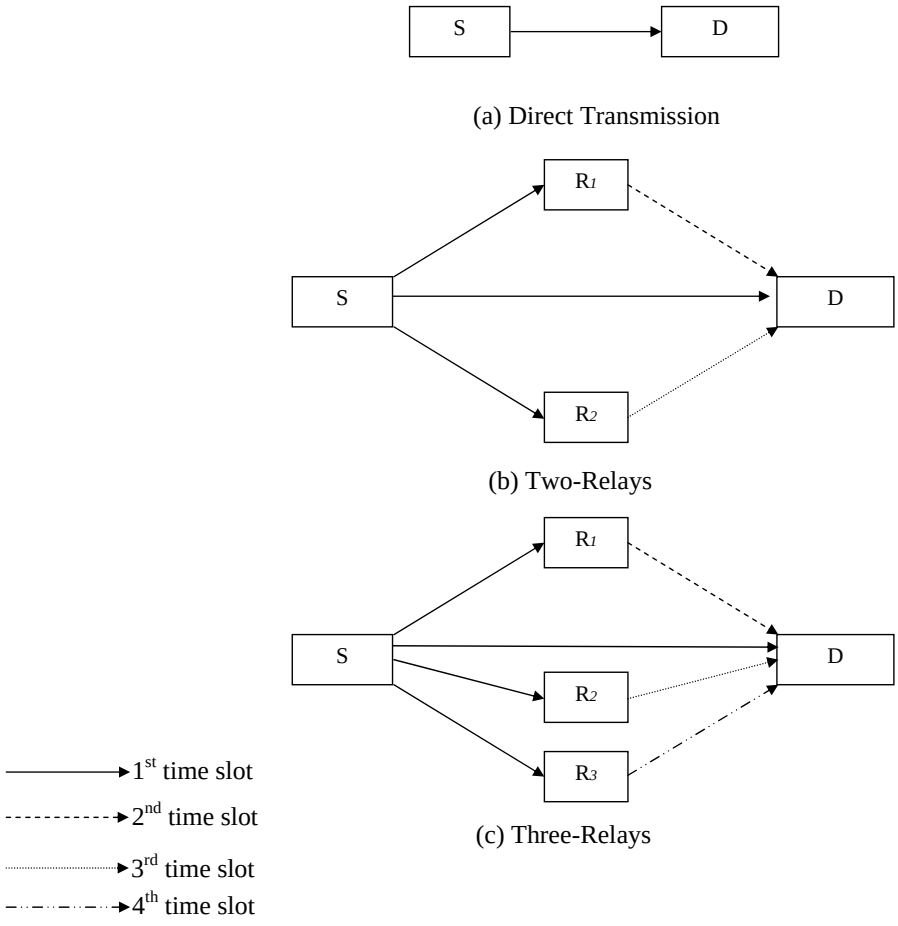

Figure 2.5: Parallel Topology. (a) Direct transmission, (b) Two-relay network, and (c) Three-relay network.

Number of relays	**Modulation scheme**
0	BPSK
2	8PSK
3	16QAM

Table 2.2: Network parameters of uncoded parallel relaying scheme.

SNR at the destination for the two-relay parallel scheme:

$$\gamma_d = \gamma_{sd} + \frac{\gamma_{sr_1}\gamma_{r_1d}}{\gamma_{sr_1} + \gamma_{r_1d} + 1} + \frac{\gamma_{sr_2}\gamma_{r_2d}}{\gamma_{sr_2} + \gamma_{r_2d} + 1}. \tag{2.24}$$

and for the three-relay parallel scheme:

$$\gamma_d = \gamma_{sd} + \frac{\gamma_{sr_1}\gamma_{r_1d}}{\gamma_{sr_1} + \gamma_{r_1d} + 1} + \frac{\gamma_{sr_2}\gamma_{r_2d}}{\gamma_{sr_2} + \gamma_{r_2d} + 1} + \frac{\gamma_{sr_3}\gamma_{r_3d}}{\gamma_{sr_3} + \gamma_{r_3d} + 1}. \tag{2.25}$$

If we made $\gamma_{sr_i} = \gamma_{sr}$ and $\gamma_{r_id} = \gamma_{rd}$ for all i (i.e. the SNR of the first hop is the same in all the relays and the same for the second hop SNR) then the average BEP for the two-relay parallel scheme with 8PSK transmission can be written as:

$$P_b(E) = \frac{1}{3\pi}\int_0^{7\pi/8}\left(1 + \frac{\sin^2(\pi/8)}{\sin^2(\phi)\left(\frac{1}{\bar{\gamma}_{sr}} + \frac{1}{\bar{\gamma}_{rd}}\right)}\right)^{-2}\left(1 + \frac{\sin^2(\pi/8)\bar{\gamma}_{sd}}{\sin^2(\phi)}\right)^{-1} d\phi, \tag{2.26}$$

and for the three-relay parallel scheme with 16QAM transmission:

$$\begin{aligned} P_b(E) = {} & \frac{3}{4\pi}\int_0^{\pi/2}\left(1 + \frac{1}{10\sin^2(\phi)\left(\frac{1}{\bar{\gamma}_{sr}} + \frac{1}{\bar{\gamma}_{rd}}\right)}\right)^{-3}\left(1 + \frac{\bar{\gamma}_{sd}}{10\sin^2(\phi)}\right)^{-1} d\phi \\ & - \frac{9}{16\pi}\int_0^{\pi/4}\left(1 + \frac{1}{10\sin^2(\phi)\left(\frac{1}{\bar{\gamma}_{sr}} + \frac{1}{\bar{\gamma}_{rd}}\right)}\right)^{-3}\left(1 + \frac{\bar{\gamma}_{sd}}{10\sin^2(\phi)}\right)^{-1} d\phi \end{aligned} \tag{2.27}$$

Figure 2.6 shows the error performance of the direct, two-relay, and three-relay parallel relaying using BPSK, 8PSK, and 16QAM transmission, respectively, over Rayleigh fading channels with path loss exponent n=3. The figure shows both the simulation results and the analytical results from equations (2.26) and (2.27). Even with the SNR loss from the higher modulation scheme, the relaying clearly improves the system more than the direct transmission. The diversity gain can be

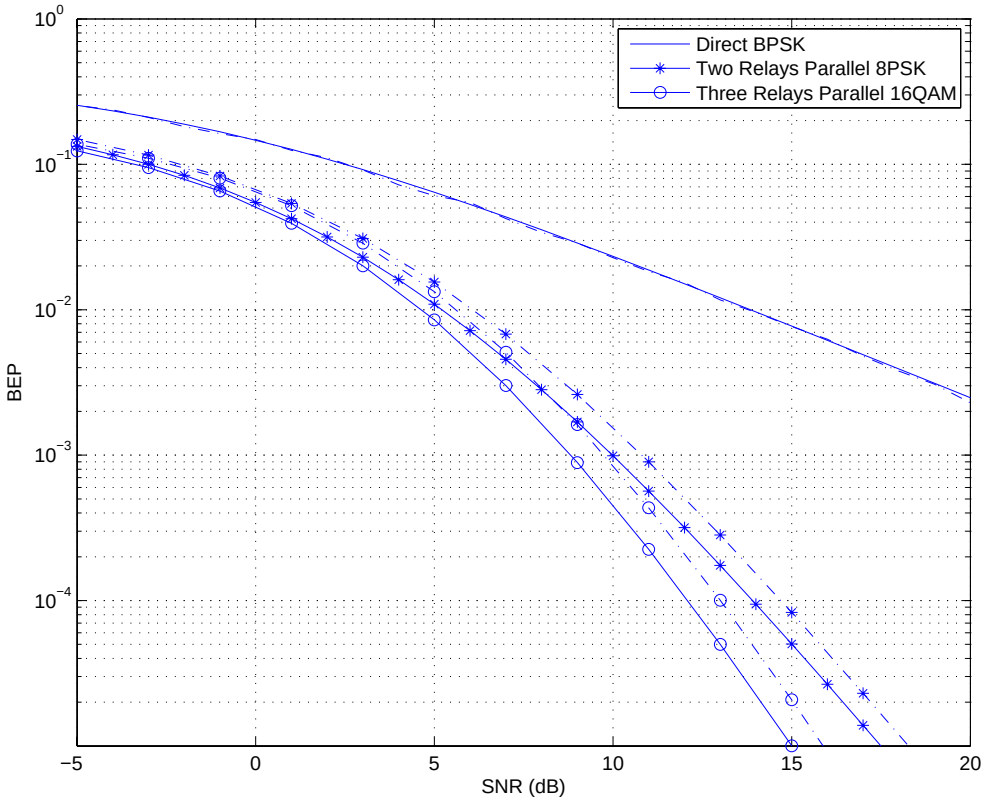

Figure 2.6: Performance of the direct BPSK transmission, two-relay parallel 8PSK transmission, and three-relay parallel 16QAM transmission over Rayleigh fading channels: (solid) analysis, (dashed) simulation.

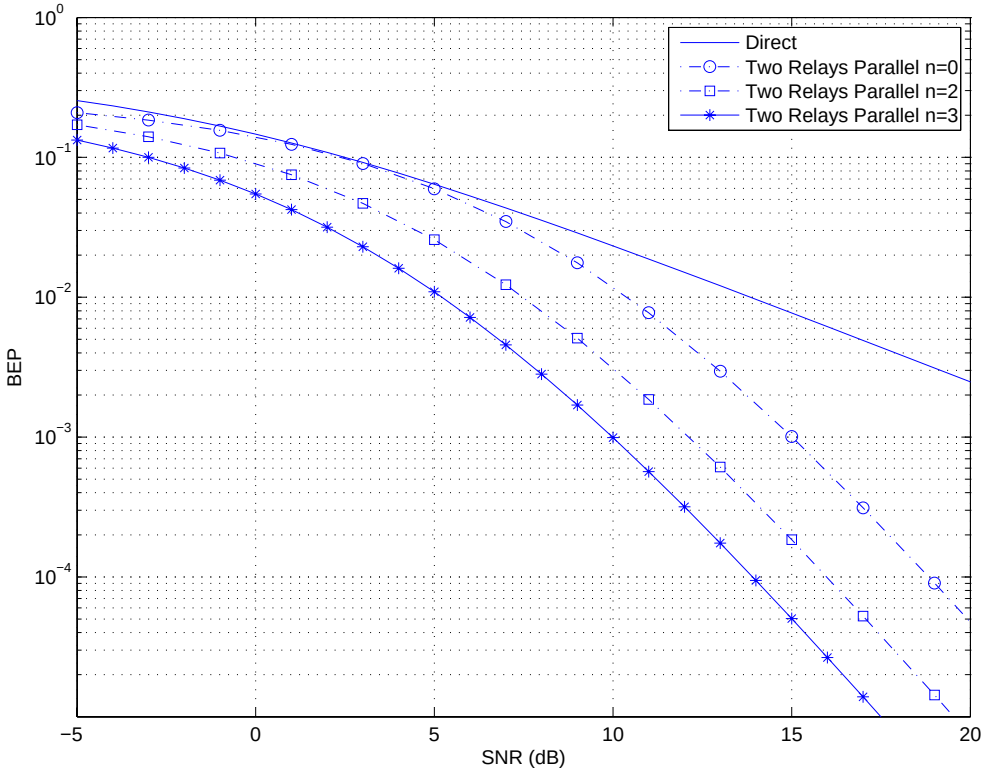

Figure 2.7: Effect of the path loss exponent on the performance of the two-relay parallel scheme with $n = 0, 2$, and 3.

seen from the change in the slope of the curve between the different cases. Figure 4.16 shows the effect of the path loss exponent on the performance of the two-relay serial scheme. We can see from the figure that, as the path loss exponent increases, the relaying gain increases. This is the same conclusion as we got from the serial.

2.3 Coded Systems

In this section we derive the performance of a convolutionally coded multi-hop network using AF with serial and parallel topologies. In convolutionally coded systems, all k source bits in a length-k vector $\mathbf{u}$ are encoded into an n-bit codeword $\mathbf{v}$. The coded vector $\mathbf{v}$ is transmitted through the channel to the receiver. The receiver uses a Viterbi decoder to retrieve the source bits [11].

When using a convolutional code with a code rate $R_c = \frac{k}{n}$, the BEP can be upper bounded using the union bound [33] as

$$P_b(\alpha) \leq \frac{1}{k} \sum_{q=q_{min}}^{\infty} c(q) P_2(q|\alpha), \tag{2.28}$$

where $c(q)$ is the number of codewords at distance q from the all-zero codeword, and q_{min} is the minimum Hamming distance of the convolutional code. The coefficients $c(q)$ are obtained from the code's generalized transfer function which defines the code's distance properties [11].

In (2.28), $P_2(d|\alpha)$ is the conditional pairwise error probability (PEP), defined as the probability of decoding a received sequence as a weight-q codeword given that the all-zero codeword was transmitted [11]. In fast fading channels with ideal interleaving of the transmitted data, each transmitted coded bit goes through an independent fading. The received signal samples can be written as

$$y_j = x_j \alpha_j + \eta_j, \tag{2.29}$$

where x_j is the j^{th} transmitted symbol with energy per transmitted symbol E_s, α_j is the fading component of the channel affecting symbol x_j, and η_j is the AWGN sample with variance $N_0/2$. When using BPSK transmission, the conditional PEP can be written as

$$P_2(q|\boldsymbol{\alpha}) = P\left(\sum_{j=1}^{q} \alpha_j^2 |s_j - \hat{s}_j|^2 \leq \eta\right), \tag{2.30}$$

where $\boldsymbol{\alpha} = (\alpha_1, \alpha_2 \cdots \alpha_q)$ are the fading components of the channel, s_j and $\hat{s}_j$ are the transmitted and the detected j^{th} symbols, respectively. For BPSK $|s_j - \hat{s}_j|^2 = 4E_s$, and hence, (2.30) can be simplified to

$$P_2(q|\boldsymbol{\alpha}) = Q\left(\sqrt{\frac{2E_s}{N_0}\sum_{j=1}^{q} \alpha_j^2}\right). \tag{2.31}$$

The average BEP can be found by averaging (2.28) over the distribution of the fading random variables $\boldsymbol{\alpha}$

$$P_b = \int_{\boldsymbol{\alpha}} P_b(\boldsymbol{\alpha}) f(\boldsymbol{\alpha}) d\boldsymbol{\alpha} \leq \frac{1}{k} \sum_{q=q_{min}}^{\infty} c(q) \int_{\boldsymbol{\alpha}} P_2(q|\boldsymbol{\alpha}) d\boldsymbol{\alpha}. \tag{2.32}$$

This analysis is appropriate for coded systems with ideal interleaving of the transmitted data, in which each coded bit goes through an independent fading. In such cases, diversity already exists in the system and so relaying will not help much. However, in slowly moving wireless terminals, where relaying can be of great benefit, the fading model can be considered to be a block fading channel [34, 35], in which the fading process is constant over a block of channel symbols and it is statistically independent between the blocks. In this chapter, we consider slow block fading, i.e.

each codeword goes through a different independent fading. In such a system, (2.30) can be rewritten as

$$P_b = \int P_b(\alpha) f(\alpha) d\alpha \leq \frac{1}{k} \sum_{q=q_{min}}^{\infty} c(q) \int P_2(q|\alpha) d\alpha. \tag{2.33}$$

This upper bound is very loose. This is because there is no dominant error event and, even at high SNR, many terms in (2.33) contribute significantly to the sum, and make the expression diverge more from the accurate result [23].

Leib *et al.* have shown in [23] a much tighter upper bound which can be obtained by limiting the conditional union upper bound on the bit error probability before averaging over the fading vector, which yield

$$P_b \leq \int_{\alpha} \min \left[\frac{1}{2}, \frac{1}{k} \sum_{q=q_{min}}^{\infty} c(q) P_2(q|\alpha) \right] f(\alpha) d\alpha. \tag{2.34}$$

The minimization in (2.34) ensures that the expression converges. However, due to the minimization, the order of the integration and the summation cannot be interchanged in (2.34), and so the integration has to be done numerically.

2.3.1 Serial Relaying

Here, the source encodes the data, and sends it to the relay which amplifies and forwards it to the destination. The destination employs MRC to combine and decode the data received from the source and the relays. The serial topology we are using in this section and the time allocation are the same as the uncoded system shown in Figures 2.1 and 2.2, respectively. For simplicity, we consider the relays are positioned

at equal distances between the source and the destination nodes. Also, in order to be fair in comparing the relayed transmission and the direct transmission in terms of energy and bandwidth, we use code rate $R_c = \frac{1}{6}$ for the direct transmission, $R_c = \frac{1}{3}$ for single-relay network and $R_c = \frac{1}{2}$ for the two-relays network, and memory order $m = 2$. By doing so, we fix the total number of transmitted symbols and the total energy used in all the cases. Table 2.3 shows the parameters of the coded serial network used.

In order to calculate the BEP numerically, we rewrite equation (2.34) in terms of the equivalent SNR γ_{eq} as

$$P_b \leq \int_{\gamma_{eq}} \min\left[\frac{1}{2}, \frac{1}{k}\sum_{q=q_{min}}^{\infty} c(q)P_2(q|\gamma_{eq})\right] f(\gamma_{eq})d\gamma_{eq}$$

$$P_b \leq \mathrm{E}\left\{\min\left[\frac{1}{2}, \frac{1}{k}\sum_{q=q_{min}}^{\infty} c(q)Q\left(\sqrt{2q\gamma_{eq}}\right)\right]\right\}, \tag{2.35}$$

where E{.} is the statistical expectation operator. For this section, we are doing semi-analysis of the system, i.e. we generate random data using the expression we derived in the uncoded case for the equivalent SNR for the single-relay serial network (2.14) and we insert them in (2.35) and take the expectation.

The same was done for the two-relay serial network but with the expression for the

Number of relays	**Code rate**
0	1/6
1	1/3
2	1/2

Table 2.3: Network parameters of the coded serial relaying scheme.

equivalent SNR (2.17) with $J = 2$. Figure 2.8 shows the analysis and simulation performance of the convolutionally coded direct and serial relaying using one and two relays with respective code rate $R_c = 1/6, 1/3$ and $1/2$ over Rayleigh fading channels. The figure shows the improvement which relaying gives to the system, and the coding gain can be seen by comparison with the uncoded serial cases in Figure 2.3. Figure 2.9 shows the effect of the path loss exponent on the performance of the convolutionally coded single-relay serial scheme. We can see from the figure that the relaying gain increases as the path loss exponent increases. In high path loss exponent environments, sending the data over short distances saves more energy than doing the same in low path loss exponent environments.

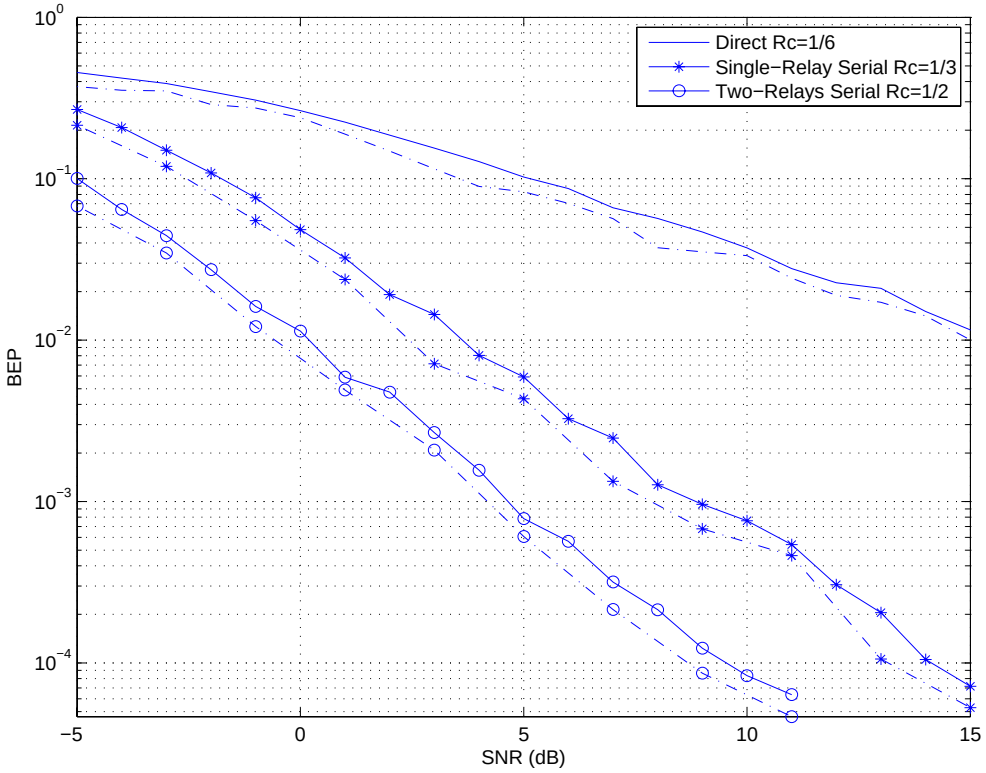

Figure 2.8: Performance of the convolutionally coded direct and serial relaying using one and two relays with $R_c = 1/6, 1/3$, and $1/2$ respectively over Rayleigh fading channels: (solid) analysis, (dashed) simulation.

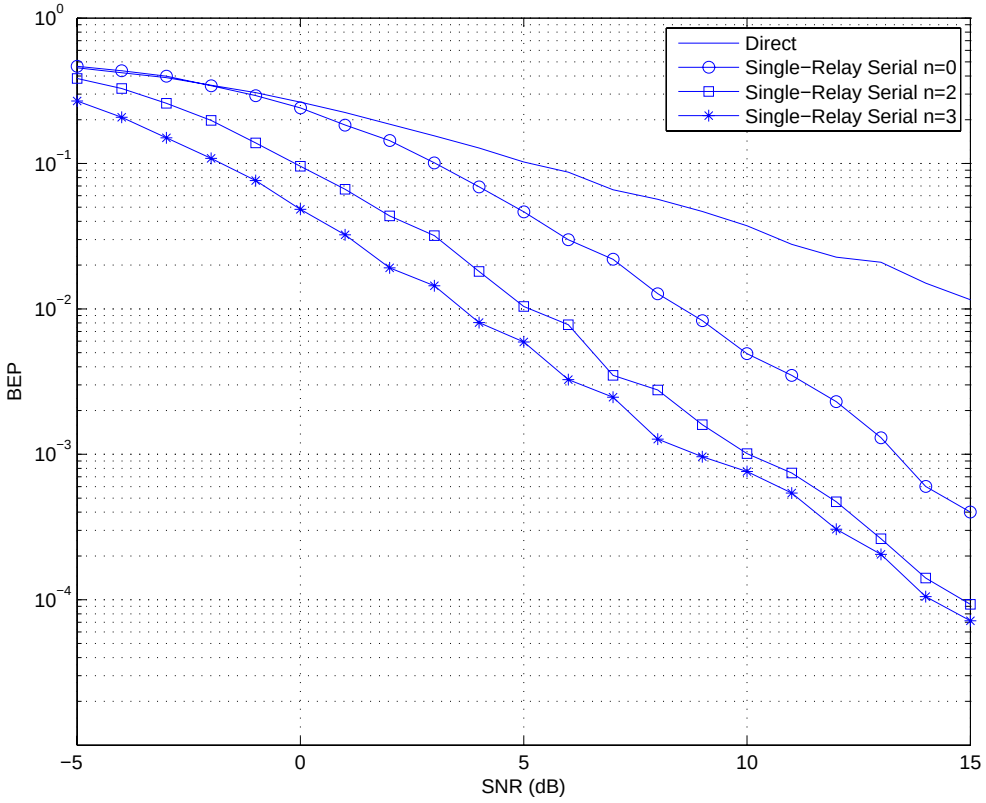

Figure 2.9: Effect of the path loss exponent on the performance of the coded single-relay serial scheme with $n = 0, 2$, and 3.

2.3.2 Parallel Relaying

Here, the source encodes the data, and sends it to all relays which then amplify and forward it to the destination at different time slots. The destination uses MRC to combine and decode the data received from the source and the relays. The parallel topology used in this section and the time allocation are the same as the uncoded system shown in Figures 2.5 and 2.2, respectively. For simplicity, we consider the relays are positioned in the middle between the source and the destination nodes. In order to be fair in comparing the relayed transmission and the direct transmission in terms of energy and bandwidth, we use code rate $R_c = \frac{1}{6}$ for the direct transmission, $R_c = \frac{1}{2}$ for two-relay network and $R_c = \frac{2}{3}$ for the three-relay network, and memory order $m = 2$. By doing so, we fix the total number of transmitted symbols and the total energy used in all the networks considered. Table 2.4 shows the network parameters of the coded parallel relaying scheme.

Number of relays	**Code rate**
0	1/6
2	1/2
3	2/3

Table 2.4: Network parameters of coded parallel relaying scheme.

Using the same procedure as in the serial relaying, Figure 2.10 shows the analysis and simulation performance of the convolutionally coded direct, two-relay parallel, and three-relay parallel cases with respective code rate $R_c = 1/6, 1/2$ and $2/3$ over Rayleigh fading channels. The figure clearly shows the improvement which the

relaying gives to the system by comparison to the direct transmission. We can also see the diversity gain from the change in the slope of the curve.

Figure 2.11 shows the effect of the path loss exponent on the performance of the convolutionally coded two-relay serial scheme. We can see from the figure that, as the path loss exponent increases, the relaying gain increases. This is the same conclusion as we got from the serial.

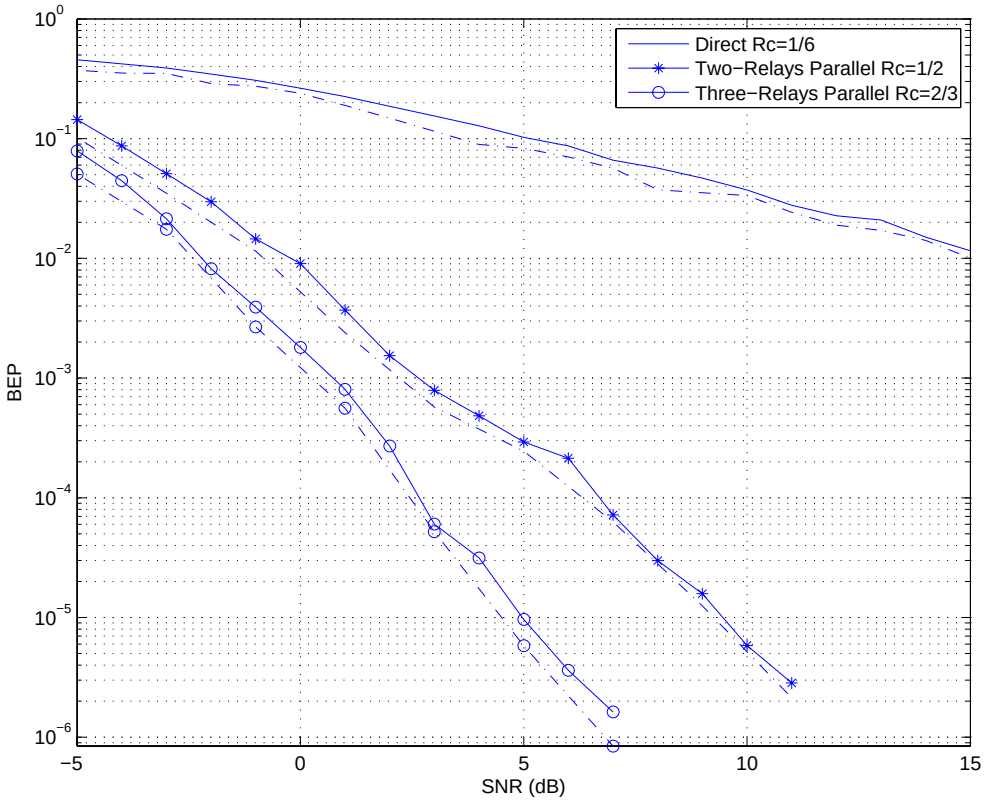

Figure 2.10: Performance of the convolutionally coded direct and parallel relaying using two and three relays with $R_c = 1/6, 1/2$, and $2/3$ respectively over Rayleigh fading channels: (solid) analysis, (dashed) simulation.

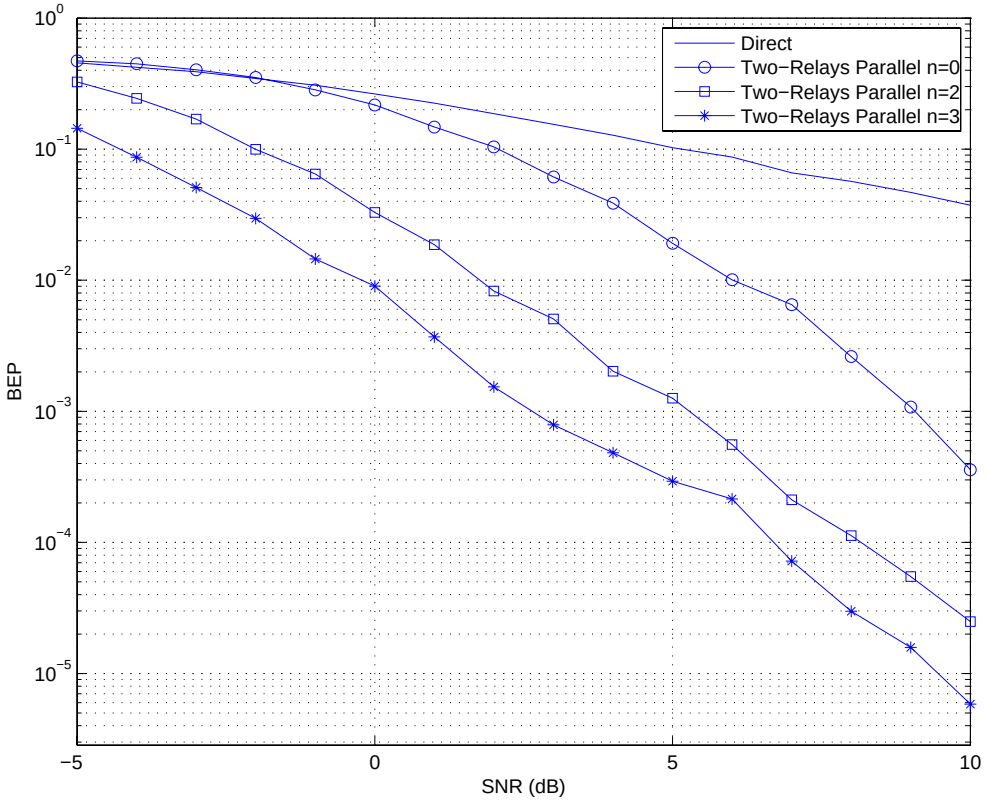

Figure 2.11: Effect of the path loss exponent on the performance of the coded two-relay parallel scheme with $n = 0, 2$, and 3.

2.4 Chapter Conclusion

In this chapter, we investigated the error performance of both coded and convolutionally coded multi-hop networks over narrowband channels over Rayleigh fading channels. We gave a brief description of the system model using AF technique, and we showed how to calculate the average BEP for M-PSK and M-QAM when using an MRC receiver. We derived the average BEP of both the uncoded system and the convolutionally coded system for the serial and the parallel networks. Results show that the relaying usefully improves the system, especially in parallel relaying schemes due to the increased diversity order.

Chapter 3

CDMA Networks

Code division multiple access (CDMA) is a channel access method utilized by various radio communication technologies. One of the basic concepts in data communication is allowing several transmitters to send information simultaneously over a single communication channel. This allows several users to share a bandwidth of frequencies. This concept is called multiple-access. CDMA employs spread-spectrum (SS) technology in which each transmitter is assigned a code to allow multiple users to be multiplexed over the same physical channel. By contrast, time division multiple access (TDMA) divides access between users by time, while frequency-division multiple access (FDMA) divides it by frequency. SS signals are distinguished by the characteristic that their bandwidth W is much greater than the information rate R in bits/sec. In other words, the bandwidth expansion factor of the signal $B_e = \frac{W}{R}$ is much greater than unity [3].

An important element employed in the design of SS signals is the pseudo-randomness, which makes the signals appear similar to random noise and difficult to demodulate by receivers other than the intended ones. This element is intimately related with the application or purpose of such signals. To be more specific, SS signals are used for

- Combatting or suppressing the detrimental effects of interference due to jamming, interference arising from other users of the channel, and self-interference due to multipath propagation and multiple-access.
- Hiding a signal by transmitting it at low power level in the spectrum, thus making it difficult for an unintended listener to detect in the presence of background noise.
- Achieving message privacy in the presence of other listeners.

Interference from the other users arises in multiple-access communication systems in which a number of users share a common channel bandwidth. At any given time, a subset of these users may transmit information simultaneously over the common channel to corresponding receivers. Assuming that all the users employ the same code for the encoding and decoding of their respective information sequences, the transmitted signals in this common spectrum may be distinguished from one another by superimposing a different pseudo-random noise (PN) pattern, also called a code, in each transmitted signal. Thus, a particular receiver can recover the transmitted

information intended for it by knowing the PN code, i.e. the key, used by the corresponding transmitter. In this chapter, we will analyze the performance of a multihop network employing CDMA on the physical layer.

The rest of this chapter is organized as follows. Section 3.1 discusses the SS technique and shows the system model used in this chapter. The performance analysis of CDMA-based multihop networks is shown in Section 3.2. Section 3.3 gives the numeric results we obtained from the simulation and the analysis. Finally, Section 3.4 presents the chapter's conclusions.

3.1 System model

Figure 3.1 shows the block diagram of a basic spread spectrum digital communication system. The modulator and demodulator are the system's basic elements, as in any other communication system. In addition, we have two identical PN code generators, one at the transmitting end and a second at the receiving end. The PN generators generate a PN binary-valued sequence, which is multiplied by the transmitted signal at the modulator and removed from the received signal at the demodulator. Synchronization of the PN sequences generated at the transmitter and the receiver is required in order to demodulate the received signal [3].

In the model shown in Figure 3.1, we assume that the information rate at the input

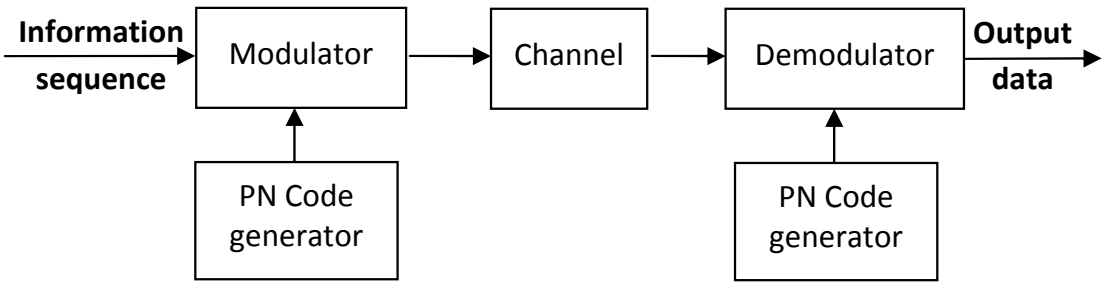

Figure 3.1: Block diagram of a SS digital communication system.

to the encoder is R bits/sec, that the available channel bandwidth is W Hz, and that the modulation is BPSK. In order to utilize the entire available channel bandwidth, the phase of the carrier is shifted pseudorandomly according to the PN code at a rate W times/sec. The reciprocal of W, denoted by T_c, defines the duration of a rectangular pulse, which is called a chip, which constitutes the basic element in a DSSS signal. Define $T_b = \frac{1}{R}$ to be the duration of a rectangular pulse corresponding to the transmission time of an information bit. Figure 3.2 shows the relationships between the PN signal and the data signal. The bandwidth expansion factor or the spreading gain V may be expressed as

$$V = \frac{W}{R} = \frac{T_b}{T_c} \tag{3.1}$$

In practical systems, the ratio $\frac{T_b}{T_c}$ is an integer, which is the number of chips per information bit. In the case of PSK, it is the number of phase shifts that occur in the transmitted signal during one bit duration.

At each user's transmitter, the information bits are multiplied by the PN code of

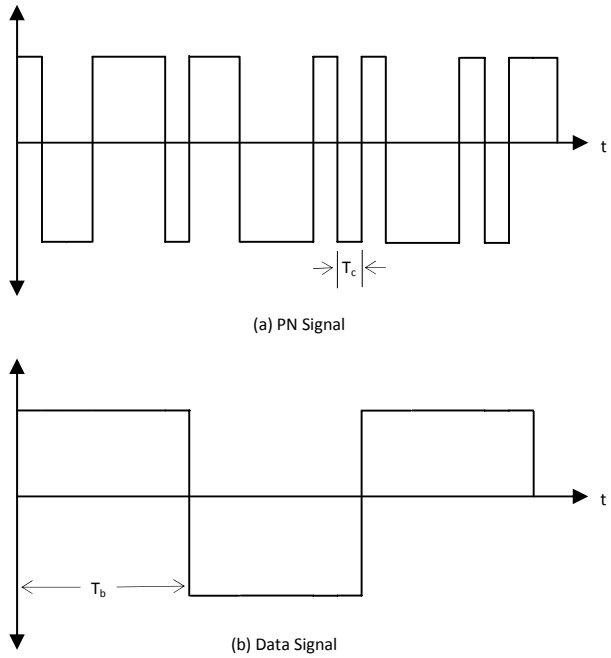

Figure 3.2: (a) PN signal, and (b) data signal.

the user at the modulator. The signal model of the transmitted signal for user k can be written as

$$s_k(t) = \sqrt{2P_k}a_k(t)b_k(t)\cos(\omega_c t + \theta_k), \tag{3.2}$$

where P_k is the power of the transmitted signal of user k, $a_k(t)$ and $b_k(t)$ are the data and spreading signals of user k respectively, ω_c is the signaling frequency and θ_k is the phase shift of user k. There are V chips of duration T_c of the PN code for each bit of duration T_b. Assuming that there are K active users in the system, the total received signal at any of the receivers can be shown as

$$r(t) = \sum_{k=1}^{K} \sqrt{2P_k}\alpha_k a_k(t-\tau_k)b_k(t-\tau_k)\cos(\omega_c t + \phi_k) + \eta(t), \tag{3.3}$$

where α_k is the fading component of user k, τ_k and ϕ_k are the phase and time delay introduced by the channel of user k, and $\eta(t)$ is the AWGN introduced at the receiver. At each user, a correlation receiver or a matched filter receiver is typically used to filter the desired user's signal from all the other users' signals which share the same channel. Figure 3.3 shows a block diagram of a typical matched filter receiver [3].

Assuming the receiver is delay and phase synchronized with the user 1, the decision statistics for this user are given by [27]

$$\begin{aligned} Z_1 &= \int_0^{T_b} r(t)b_1(t)\cos(\omega_c t)dt \\ &= \sqrt{\frac{P_1}{2}}\alpha_1 a_1 T_b + \int_0^{T_b} \sum_{k=2}^{K} \sqrt{2P_k}\alpha_k a_k(t)b_k(t)b_1(t)\cos(\omega_c t)\cos(\omega_c t + \phi_k)dt + \hat{\eta}. \end{aligned} \tag{3.4}$$

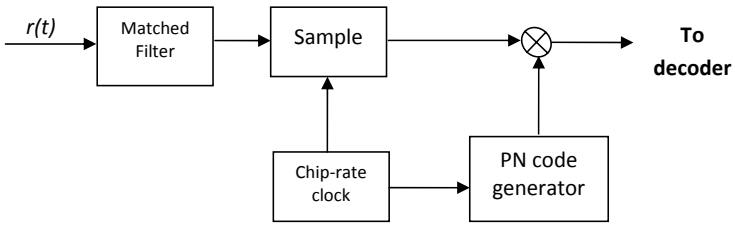

Figure 3.3: Typical demodulator for DSSS signals.

where a_1 is the information data of user 1, and $\hat{\eta}$ is an AWGN random variable with variance equal to $N_0T_b/4$. The first term in (3.4) is the desired signal component, whereas the second part is the multiple access interference, and the third part is the AWGN noise.

A method called the standard Gaussian approximation (SGA) [36] is used to derive the BEP of CDMA systems based on the argument that the decision statistic, Z_1 given in (3.4), may be modeled as a Gaussian random variable. The first component is deterministic, and the other two components are assumed to be zero-mean Gaussian random variables [27]. Assuming that the additive receiver noise $\eta(t)$ is a bandpass Gaussian noise, it is straightforward to show that $\hat{\eta}$ is also a zero-mean Gaussian random variable. The SGA then derives an expression for the bit error rate based on the assumption that the multiple access interference term may be approximated by a Gaussian random variable. The SGA method results in the conditional BEP can be written as

$$P(E)_{SGA} = Q\left[\frac{\sqrt{\frac{P_1}{2}}\alpha_1 T_b}{\sqrt{\frac{N_0T_b}{4} + \sigma_m^2}}\right], \tag{3.5}$$

where $\sqrt{\frac{P_1}{2}}\alpha_1 T_b$ is the desired signal term, $\frac{N_0 T_b}{4}$ and σ_m^2 are the respective variances of the AWGN and multiple access interference terms, and $Q[.]$ is the Gaussian Q function. We have omitted the time subscript from the analysis for simplicity.

The variance of the multiple interference was found in [27] as

$$\sigma_m^2 = \frac{T_b^2}{6V} \sum_{k=2}^{K} P_k \alpha_k^2. \tag{3.6}$$

By using (3.6) in (3.5), we get the conditional BEP for user 1 as

$$P(E|\alpha_1^2) = Q\left[\sqrt{\frac{1}{\frac{1}{3V}\sum_{k=2}^{K}\frac{P_k}{P_1}\frac{\alpha_k^2}{\alpha_1^2} + \frac{N_0}{2T_b P_1 \alpha_1^2}}}\right]. \tag{3.7}$$

In the next section, we will discuss the error performance of the CDMA-based multihop networks using the SGA approach for different network topologies.

3.2 Performance Analysis

3.2.1 Direct Transmission

In this section, we consider direct CDMA transmission with K users in the system. The conditional BEP of a DS-CDMA system using SGA is shown in (3.7). Assume the transmitted signal is a BPSK CDMA modulated signal and the PN sequences are generated randomly. In addition, assume that all the users have equal power $P_1 = P_k$ for all k, and define $E_b = T_b P_1$ as the energy per bit. If we replace these

values in (3.7) and multiply the nominator and denominator by $\frac{2\alpha_1^2 E_b}{N_0}$ we get

$$P(E|\alpha_1^2) = Q\left[\sqrt{\frac{\frac{2\alpha_1^2 E_b}{N_0}}{\frac{2E_b}{3VN_0}\sum_{k=2}^{K}\alpha_k^2 + 1}}\right]. \tag{3.8}$$

Using SGA, the term $\sum_{k=2}^{K}\alpha_k^2$ can be replaced by $K-1$ provided that K is large, and so (3.8) becomes

$$P(E|\alpha_1^2) = Q\left[\sqrt{\frac{\frac{2\alpha_1^2 E_b}{N_0}}{\frac{2E_b(K-1)}{3VN_0} + 1}}\right]. \tag{3.9}$$

When the receiver uses MRC to combine the signal of the intended user from L branches, the expression becomes [3]

$$P(E|\alpha_1^2) = Q\left[\sqrt{\frac{\sum_{i=1}^{L}\frac{2\alpha_i^2 E_b}{N_0}}{\frac{2E_b(K-1)}{3VN_0} + 1}}\right], \tag{3.10}$$

where L is the diversity order, i.e. the number of diversity branches in the system. Define the signal-to-interference-and-noise-ratio (SINR) as

$$\mathrm{SINR}(V,K) = \frac{\frac{2E_b}{N_0}}{\frac{(K-1)\frac{2E_b}{N_0}}{3V} + 1}. \tag{3.11}$$

Replacing SINR in equation (3.10), we get

$$P(E|\alpha_1^2) = Q\left[\sqrt{\mathrm{SINR}(V,K)\sum_{i=1}^{L}\alpha_i^2}\right]. \tag{3.12}$$

A widely used form of the Q function was shown in (2.7). Replacing $Q(x)$ from (2.7) into (3.12)

$$P(E|\alpha_1^2) = \frac{1}{\pi}\int_0^{\pi/2} e^{-\frac{\mathrm{SINR}(V,K)\sum_{i=1}^{L}\alpha_i^2}{2\sin^2(\theta)}} d\theta$$

$$= \frac{1}{\pi} \int_0^{\pi/2} \prod_{i=1}^{L} e^{-\frac{\mathrm{SINR}(V,K)\alpha_i^2}{2\sin^2(\theta)}} d\theta. \tag{3.13}$$

As we said before, α_i is assumed to be a Rayleigh distributed random variable, which makes α_i^2 an exponential random variable [37]. The unconditional BEP can be easily found to be

$$P_b(L,V,K) = \frac{1}{\pi} \int_0^{\pi/2} \prod_{i=1}^{L} \frac{1}{1+\frac{\mathrm{SINR}(V,K)}{2\sin^2(\theta)}} d\theta \tag{3.14}$$

If α_i was a Nakagami-m distributed random variable with unity mean, then the unconditional probability of error becomes

$$P_b(L,V,K) = \frac{1}{\pi} \int_0^{\pi/2} \prod_{i=1}^{L} \left(\frac{1}{1+\frac{\mathrm{SINR(V,K)}/m}{2\sin^2(\theta)}} \right)^m d\theta \tag{3.15}$$

Equations (3.14) and (3.15) give the average BEP of a CDMA system over Rayleigh and Nakagami-m fading channels, respectively, with L diversity order, V spreading gain, and K users. The next step is to extend this equation to include the effect of DF relaying over multihop networks with different topologies, which is shown in the next subsections.

3.2.2 Serial Relaying

In serial relaying shown in Figure 3.5, the source sends the data to the first relay, which despread it and then spread it again and forward it to the destination. This is exactly like DF but without the coding. The destination uses MRC to combine the received signals from both the relay and the source. The time allocation of the

transmission is shown in Figure 3.4. In order to be fair in comparing the relayed system with the direct system, we reduce the spreading gain in the relayed systems. By doing so, we maintain the number of bits transmitted constant in all the cases. In order to simplify the analysis, we define the next events, and we will use them in the rest of the analysis.

- E = Error event happened at the destination.
- C_i = Node i decoded correctly.
- $\bar{C}_i$ = Node i did not decode correctly.
- $P_b(L, V, K)$ = BEP of the system "Equations (3.14) or (3.15)" with diversity order L, spreading gain V, and number of users K.

For the case of single-relay as shown in Figure 3.5(b), the BEP is calculated as follows

$$P(E) = P(E|C_1)P(C_1) + P(E|\bar{C}_1)P(\bar{C}_1), \tag{3.16}$$

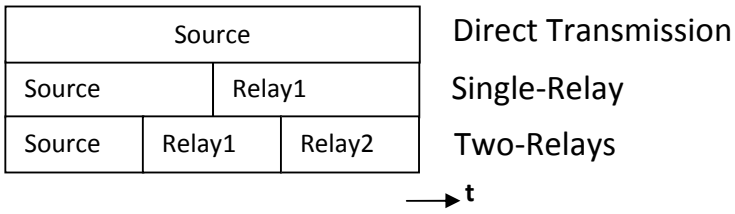

Figure 3.4: Time Allocation of the serial scheme.

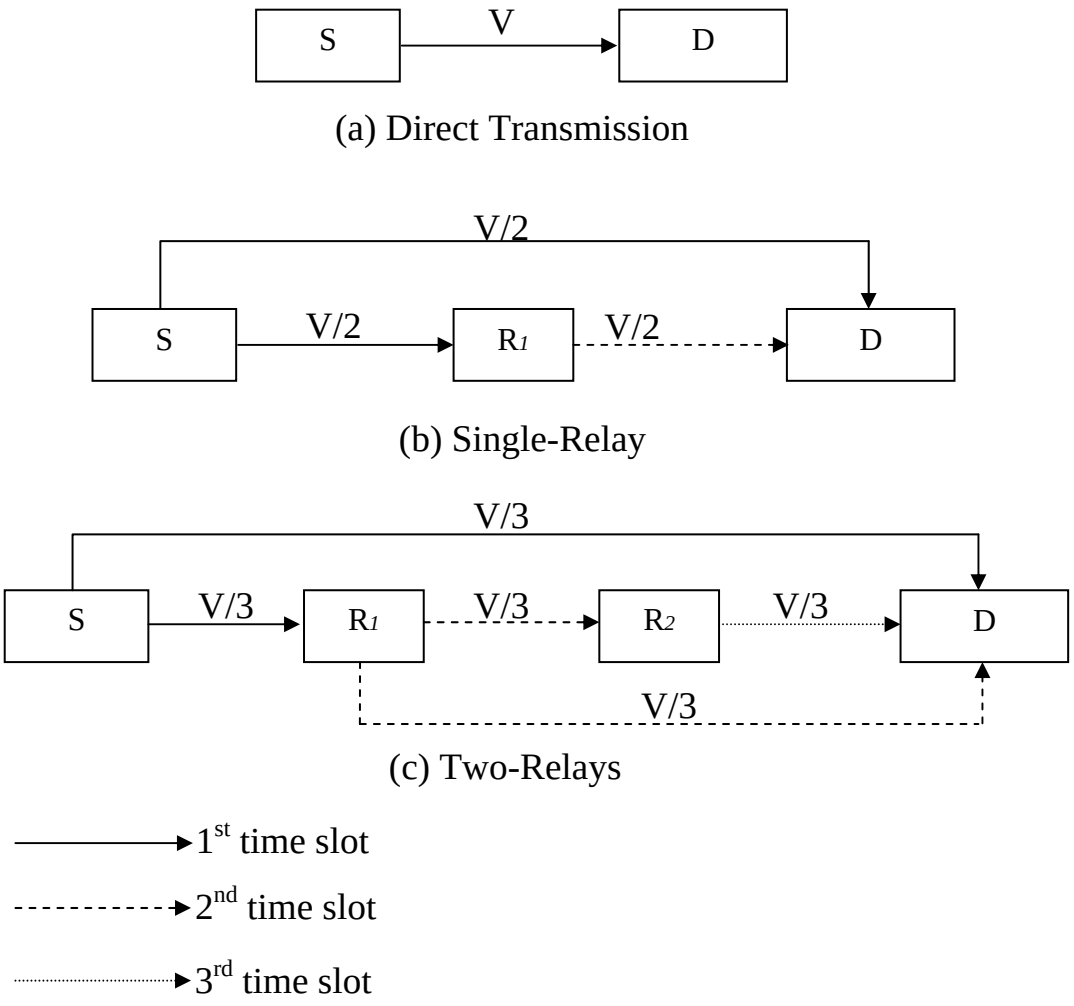

Figure 3.5: Serial multihop topology. (a) Direct transmission with spreading gain V, (b) single-relay network with spreading gain V/2, and (c) Two-relay network with spreading gain V/3.

which can be written as

$$P(E) = P_b(2, V/2, K)(1 - P_b(1, V/2, K)) + P_b(1, V/2, K)P_b(1, V/2, K), \quad (3.17)$$

which can be easily evaluated using equation (3.14) or (3.15). For the case of two-relay as shown in Figure 3.5(c), the BEP is given by

$$P(E) = P(E|C_1, C_2)P(C_1, C_2) + P(E|C_1, \bar{C_2})P(C_1, \bar{C_2}) + P(E|\bar{C_1})P(\bar{C_2}), \quad (3.18)$$

and so

$$P(E) = P_b(3, V/3, K)(1 - P_b(1, V/3, K))^2 + P_b(2, V/3, K)(1 - P_b(1, V/3, K))$$
$$\times P_b(1, V/3, K) + P_b(1, V/3, K)P_b(1, V/3, K). \quad (3.19)$$

3.2.3 Parallel Relaying

Figure 3.6 shows parallel relaying. In this case, the source sends the data to all the relays, each of which despread and then spread it again and forward it to the destination. The destination uses MRC to combine the received signal from all the relays and the source node.

We are proposing two protocols for parallel relaying:

- Protocol 1: The source sends the data to all the relays in the first time slot, and then each relay sends it in a different time slot to the destination node. In order to be fair when comparing with the direct transmission, the spreading gain is divided by the number of relays for all the transmissions, making sure that the

energy consumption and the bandwidth are the same in all the schemes. The topology is shown in Figure 3.6. The time allocation of the transmission is the same as the serial scheme shown in Figure 3.4, and the network parameters are shown in Table 3.1.

Number of relays	**Spreading gain**
0	V
2	V/3
3	V/4

Table 3.1: Network parameters for protocol 1 parallel relaying scheme.

- Protocol 2: The source sends the data to all the relays in the first time slot, and then all the relays send it in the next time slot to the destination node. In order to be fair in the comparison, the spreading gain is always $V/2$ but the energy in the second hop is divided by the number of the relays. The topology is shown in Figure 3.7, while Figure 3.8 and Table 3.2 respectively show the time allocation and the network parameters for this protocol.

Number of relays	**Spreading gain**
0	V
2	V/2
3	V/2

Table 3.2: Network parameters for protocol 2 parallel relaying scheme.

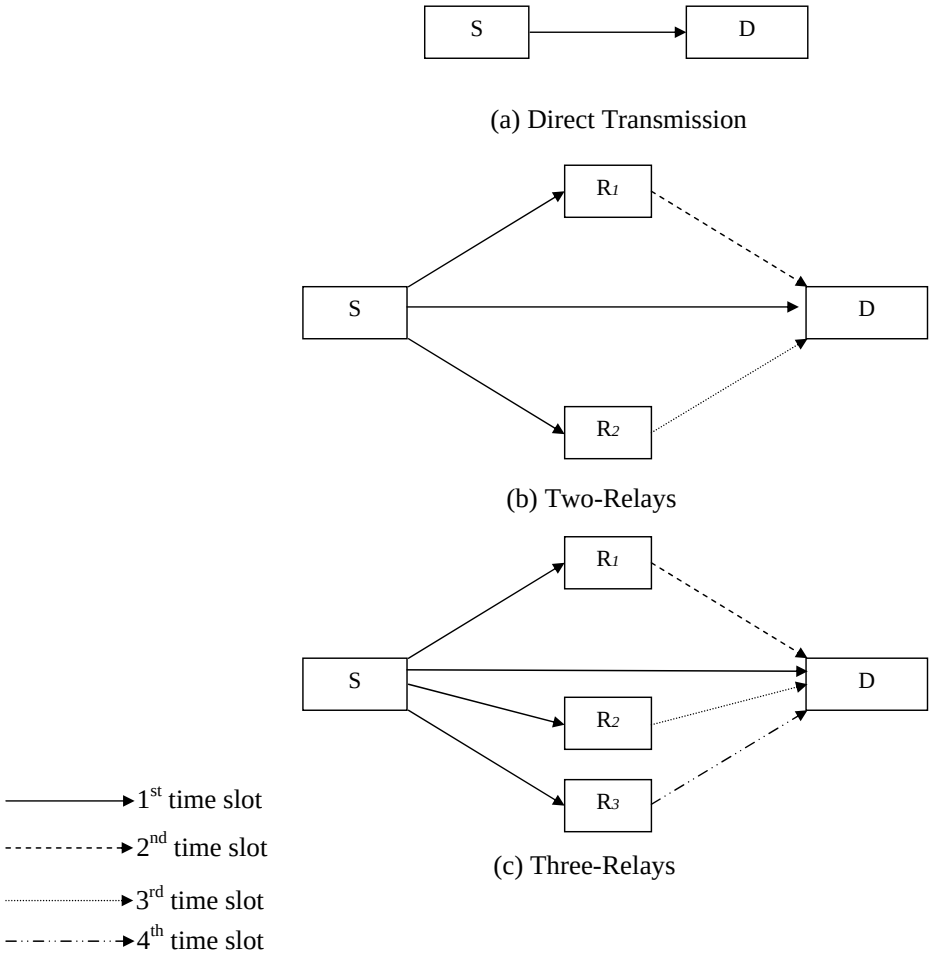

Figure 3.6: Protocol 1 of parallel multihop topology. (a) Direct transmission, (b) Two-relay, and (c) Three-relay.

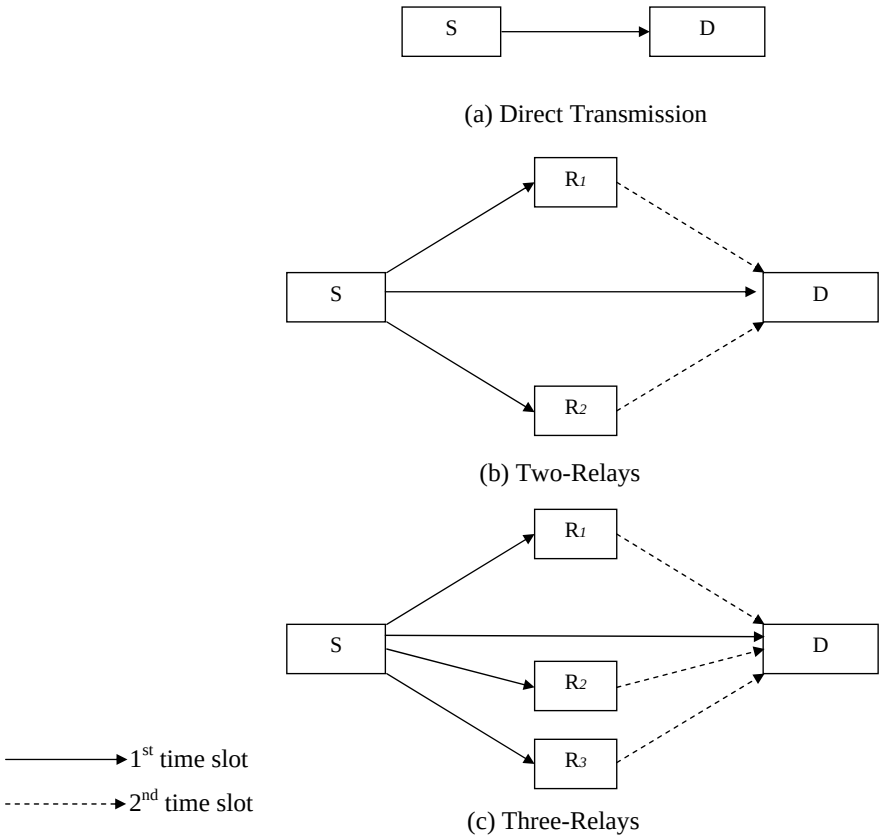

Figure 3.7: Protocol 2 of parallel multihop topology. (a) Direct transmission, (b) Two-relay, and (c) Three-relay.

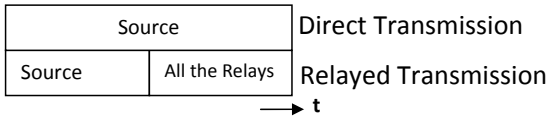

Figure 3.8: Time allocation for Protocol 2 parallel relaying.

Figures 3.9, and 3.10 show the performance of the two parallel protocols with number of users $K = 2$ and $K = 4$ respectively and $V = 128$. The results show that protocol 1 performs better than protocol 2 whenever the number of users is low. However, for higher values of number of users, protocol 2 performs better than protocol 2 in high SNR. In this chapter, we consider only protocol 1. For the case of two-relay as shown in Figure 3.6(b), the BEP is calculated as follows

$$\begin{aligned} P(E) = {} & P(E|C_1, C_2)P(C_1, C_2) + P(E|C_1, \bar{C}_2)P(C_1, \bar{C}_2) \\ & + P(E|\bar{C}_1, C_2)P(\bar{C}_1, C_2) + P(E|\bar{C}_1, \bar{C}_2)P(\bar{C}_1, \bar{C}_2). \end{aligned} \tag{3.20}$$

$$\begin{aligned} P(E) = {} & P_b(3, V/3, K)(1 - P_b(1, V/3, K))^2 + 2P_b(2, V/3, K)(1 - P_b(1, V/3, K)) \\ & \times P_b(1, V/3, K) + P_b(1, V/3, K)(P_b(1, V/3, K))^2, \end{aligned} \tag{3.21}$$

which can be easily evaluated using equation (3.14) or (3.15) where L is the diversity order, V spreading gain, and K number of users. For the case of three-relay as shown in Figure 3.6(c), the BEP can be written as

$$\begin{aligned} P(E) = {} & P(E|C_1, C_2, C_3)P(C_1, C_2, C_3) + P(E|C_1, C_2, \bar{C}_3)P(C_1, C_2, \bar{C}_3) \\ & + P(E|C_1, \bar{C}_2, C_3)P(C_1, \bar{C}_2, C_3) + P(E|\bar{C}_1, C_2, C_3)P(\bar{C}_1, C_2, C_3) \\ & + P(E|C_1, \bar{C}_2, \bar{C}_3)P(C_1, \bar{C}_2, \bar{C}_3) + P(E|\bar{C}_1, \bar{C}_2, C_3)P(\bar{C}_1, \bar{C}_2, C_3) \\ & + P(E|\bar{C}_1, C_2, \bar{C}_3)P(\bar{C}_1, C_2, \bar{C}_3) + P(E|\bar{C}_1, \bar{C}_2, \bar{C}_3)P(\bar{C}_1, \bar{C}_2, \bar{C}_3), \end{aligned} \tag{3.22}$$

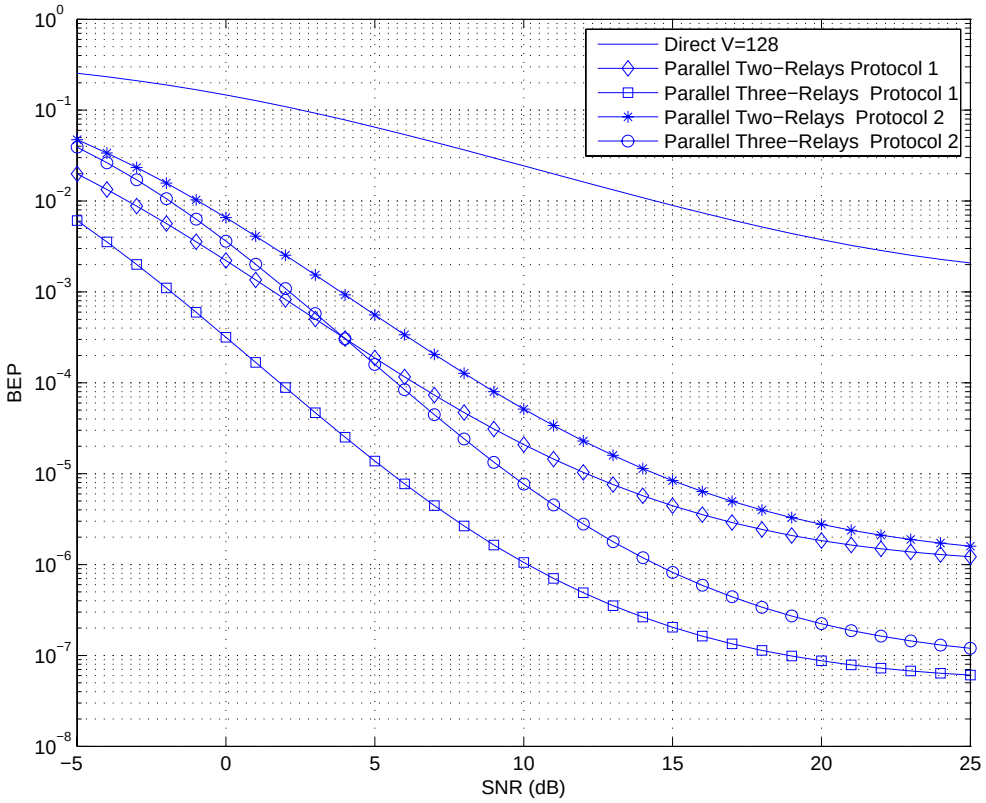

Figure 3.9: Performance of the direct, protocol 1 parallel, and protocol 2 parallel schemes with $K = 2$ and $V = 128$.

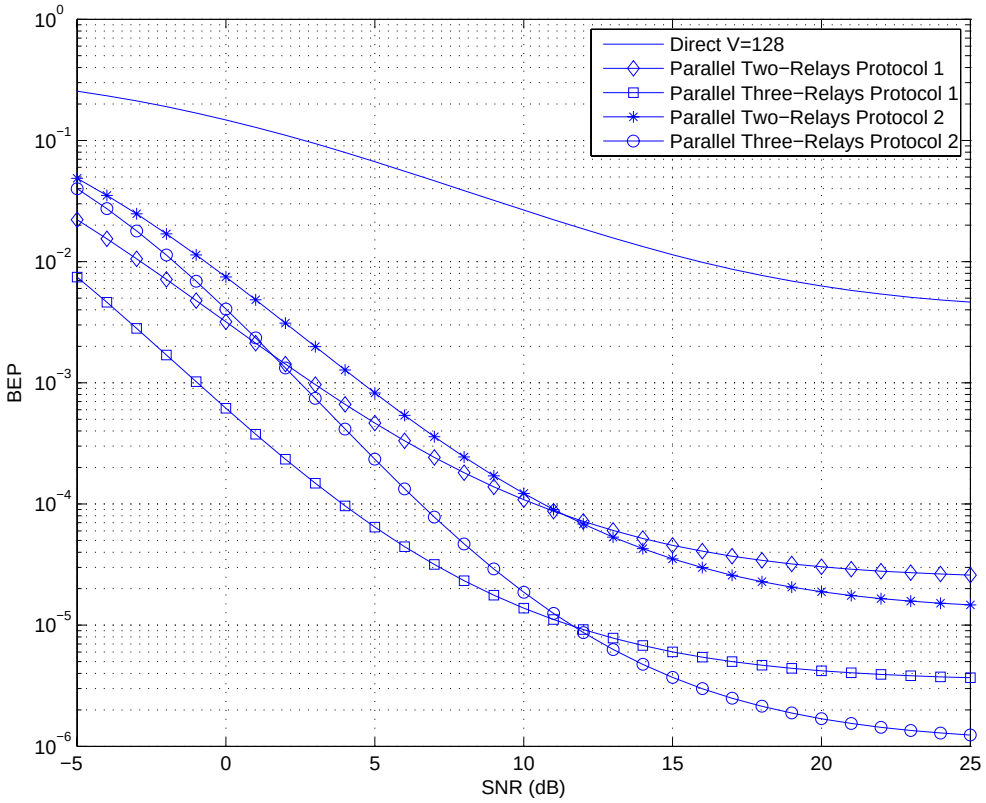

Figure 3.10: Performance of the direct, protocol 1 parallel, and protocol 2 parallel schemes with $K = 4$ and $V = 128$.

which simplifies to

$$P(E) = P_b(4, V/4, K)(1 - P_b(1, V/4, K))^3 + 3P_b(3, V/4, K)(1 - P_b(1, V/4, K))^2 \times P_b(1, V/4, K) + 3P_b(2, V/4, K)(1 - P_b(1, V/4, K))(P_b(1, V/4, K))^2 + (P_b(1, V/4, K))(P_b(1, V/4, K))^3. \quad (3.23)$$

For the case of parallel relaying, a general formula can be easily expressed as

$$P(E) = \sum_{i=0}^{J} \binom{J}{i} P_b(i{+}1, V/(J{+}1), K)(1{-}P_b(1, V/(J{+}1), K))^i (P_b(1, V/(J{+}1), K))^{L-i} \quad (3.24)$$

where J is the number of the relays.

3.2.4 Selection Relaying

In selection relaying, the topology is the same as the parallel topology in Figure 3.6 but not all of the relays forward the data to the destination. Some negotiation must be done between the source and the relays in order to select which of the relays are going to cooperate in the transmission. In this thesis, we consider the following two selection techniques:

- Threshold-based relay selection (TRS): In this case, the fading components of the links between the source and the relays are measured before each transmission. Only the relays with fading above a certain threshold α_{th} are allowed to join in the relaying. The spreading gain V is selected according to the number

of the relays joining in the transmission. For example, when only one relay is joining in the transmission, the spreading gain becomes $V/2$, in order to be fair when comparing with the direct transmission case.

- Maximum relay selection (MRS): As in threshold-based relay selection, the fading of each link between the source and the relays is measured before each transmission. Only one relay which has the maximum fading will cooperate. Here, the spreading gain is always $V/2$.

For the sake of analysis, we will use the events defined earlier in addition to the following:

- $P_{\text{out}} = \int_0^{\alpha_{th}} f(\alpha)d\alpha$ is the outage probability, i.e. the probability that the fading value α is less than the threshold α_{th}.

For the two-relay TRS scheme, the BEP is calculated as follows

$$\begin{aligned} P(E) = {} & P_b(3, V/3, K)(1 - P_{out})^2(1 - P_b(1, V/3, K))^2 \\ & + 2P_b(2, V/2, K)P_{out}(1 - P_{out})(1 - P_b(1, V/2, K)) \\ & + 2P_b(1, V/2, K)P_{out}(1 - P_{out})P_b(1, V/2, K) \\ & + P_b(1, V, K)(P_{out})^2 + P_b(1, V/3, K)(1 - P_{out})^2 P_b(1, V/3, K)^2 \quad , \end{aligned} \tag{3.25}$$

which can be easily evaluated by using equations (3.14) or (3.15). For the three-relay TRS scheme, the BEP is given by

$$\begin{aligned}
P(E) &= P_b(4, V/4, K)(1 - P_b(1, V/4, K))^3(1 - P_{out})^3 \\
&\quad + 3P_b(3, V/3, K)(1 - P_b(1, V/3, K))^2(1 - P_{out})^2 P_{out} \\
&\quad + 3P_b(2, V/3, K)(1 - P_b(1, V/3, K))P(1, V/3, K)(1 - P_{out})^2 P_{out} \\
&\quad + 3P_b(1, V/3, K)P_b(1, V/3, K)^2(1 - P_{out})^2 P_{out} \\
&\quad + 3P_b(2, V/2, K)(1 - P_b(1, V/2, K))(1 - P_{out})P_{out}^2 \\
&\quad + 3P_b(1, V/2, K)P_b(1, V/2, K)(1 - P_{out})P_{out}^2 + P_b(1, V, K)P_{out}^3 \\
&\quad + P_b(1, V/4, K)P_b(1, V/4, K)^3(1 - P_{out})^3. \qquad (3.26)
\end{aligned}$$

For the MRS, the procedure is the same as the single-relay serial but with a different direct probability of error. In order to calculate the new direct BEP, we need to devise a distribution for the random variable that is the maximum of two Rayleigh random variables for the two-relay selection scheme, and the maximum of three random variables for the three-relay scheme. Then, starting from the conditional BEP in (3.13), we can find the unconditional BEP expression.

The pdf of $Z = \max(X_1, X_2, \cdots, X_p)$ where $X_1, \cdots, X_p$, are p independent r.v.'s each with the identical pdf $f_X(x)$ and cdf $F_X(x)$ can be found from [37] as

$$f_Z(z) = p f_X(z)(F_X(z))^{p-1}. \qquad (3.27)$$

For the two-relay MRS scheme, we can get the distribution of the random variable defined as $\gamma = \max(\alpha_1^2, \alpha_2^2)$ from (3.27), with $p = 2$ and $f_{\alpha_1^2}(\alpha_1^2)$ is an exponential distribution:

$$f_\gamma(x) = \frac{1}{\sigma^2} \exp\left(\frac{-x}{2\sigma^2}\right) \left[1 - \exp\left(\frac{-x}{2\sigma^2}\right)\right] \tag{3.28}$$

By averaging the conditional BEP in (3.13) over the fading distribution in (3.28), we get the unconditional BEP to be:

$$P_b(L, V, K) = \frac{1}{\pi} \int_0^{\pi/2} \prod_{i=1}^{L} \left[\frac{2}{1 + \frac{\text{SINR(V,K)}}{\sin^2(\theta)}} - \frac{1}{1 + \frac{\text{SINR(V,K)}}{2\sin^2(\theta)}}\right] d\theta, \tag{3.29}$$

which we use in (3.17) instead of (3.14) to find the BEP of the system. For the three-relay MRS, using the same procedure, we can get the distribution for the random variable $\gamma = \max(\alpha_1^2, \alpha_2^2, \alpha_3^2)$:

$$f_\gamma(x) = \frac{3}{2\sigma^2} \exp\left(\frac{-x}{2\sigma^2}\right) \left[\exp\left(\frac{-x}{2\sigma^2}\right) - 1\right]^2 \tag{3.30}$$

By averaging the conditional BEP in (3.13) over the fading distribution in (3.30), we get the unconditional BEP to be:

$$P_b(L, V, K) = \frac{1}{\pi} \int_0^{\pi/2} \prod_{i=1}^{L} \left[\frac{3}{1 + \frac{\text{SINR(V,K)}}{\sin^2(\theta)}} - \frac{3}{1 + \frac{\text{SINR(V,K)}}{2\sin^2(\theta)}} + \frac{3}{3 + \frac{\text{SINR(V,K)}}{\sin^2(\theta)}}\right] d\theta \tag{3.31}$$

which we use in (3.17) instead of (3.14) to find the BEP of the system.

3.3 Numeric Results

In this section, we show the results we got from both the analysis and the simulation. For the sake of simplicity, we assume that the relays are at equal distances from the source and the destination. We are using random PN sequences, and BPSK transmission. The path loss exponent n is set to 3, except when we test the effect of the path loss on the system. Figure 3.11 shows the analysis and simulation results of the error performance of the direct transmission system over an AWGN channel with number of users $K = 2, 3, 4, 5$ and spreading gain $V = 24$. It is obvious that the performance gets worse as the number of interferers increases. Also the figure shows that the simulation and the analysis results are very close.

Figure 3.12 shows the analysis and simulation results of the error performance of direct transmission over Rayleigh fading channels with number of users $K = 2, 3, 4,$ and 5 and spreading gain $V = 24$. It is obvious that the performance is much worse than the AWGN case. Also the figure shows that the simulation and the analysis results are very close.

Figure 3.13 shows the analysis and simulation results of the error performance of direct transmission over Nakagami-m fading channels with two users, spreading gain $V = 24$, and $m = 1, 2$ and 3. The case of $m = 1$ means the fading is Rayleigh and as m increases, the performance gets closer to the AWGN channel performance.

Figure 3.14 shows the error performance of the direct, single-relay serial, and two-

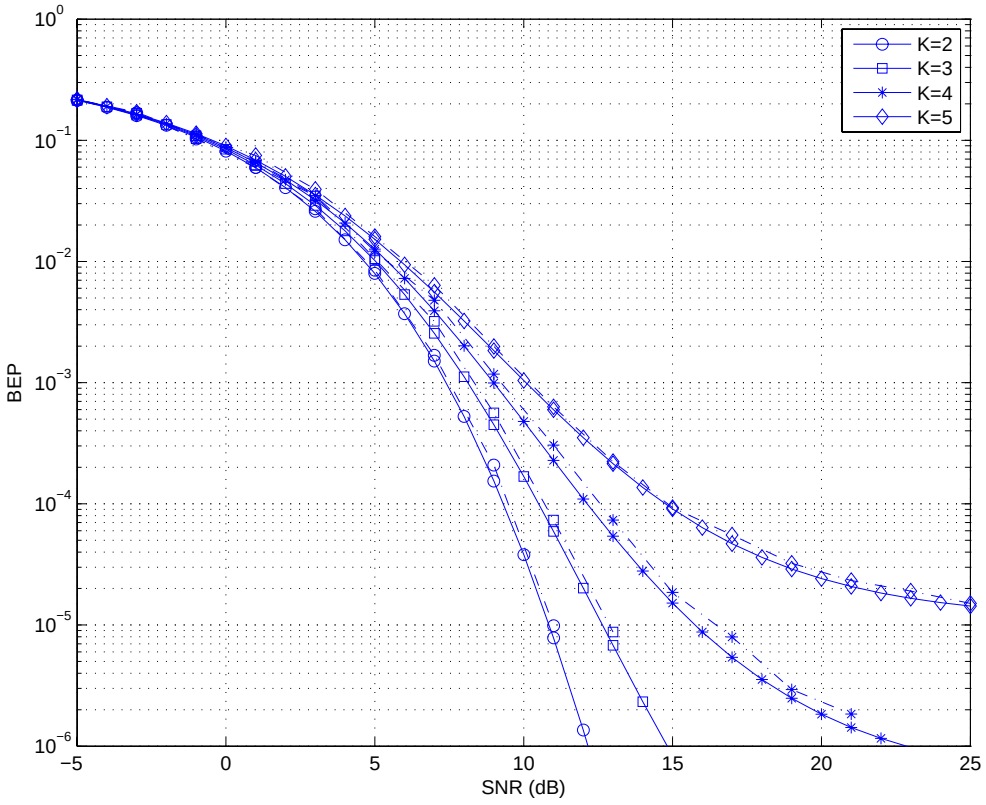

Figure 3.11: Performance of direct transmission over an AWGN channel with $K = 2, 3, 4, 5$ and $V = 24$: (solid) analysis, (dashed) simulation.

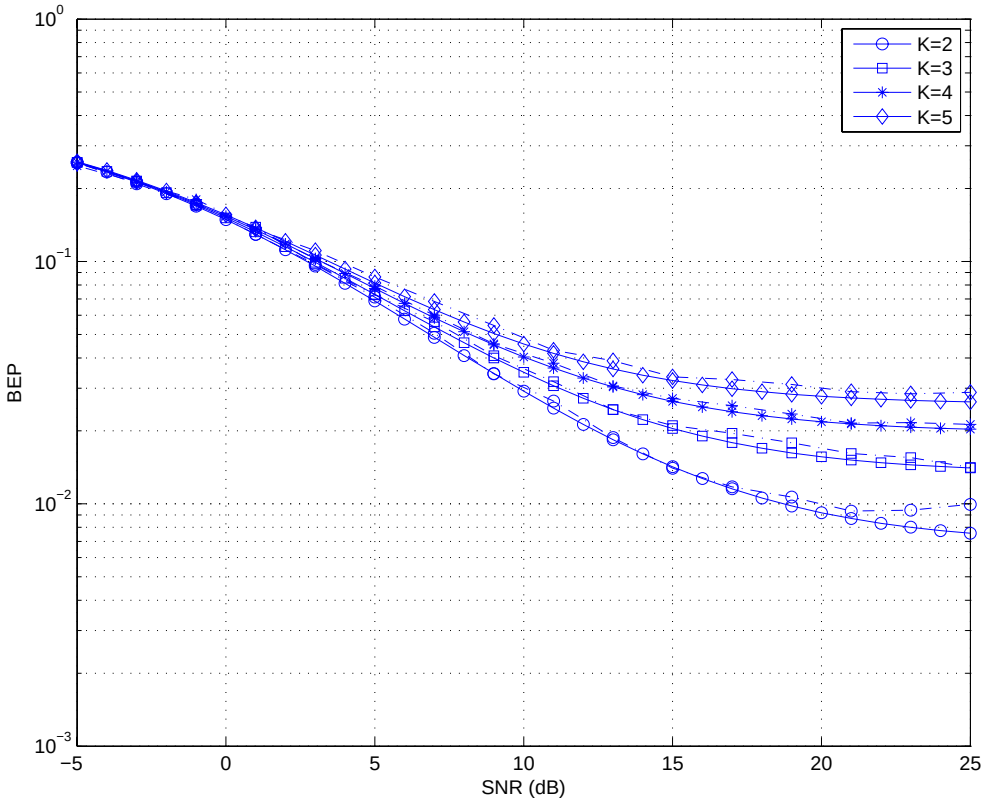

Figure 3.12: Performance of direct transmission over Rayleigh fading channels with $K = 2, 3, 4, 5$ and $V = 24$: (solid) analysis, (dashed) simulation.

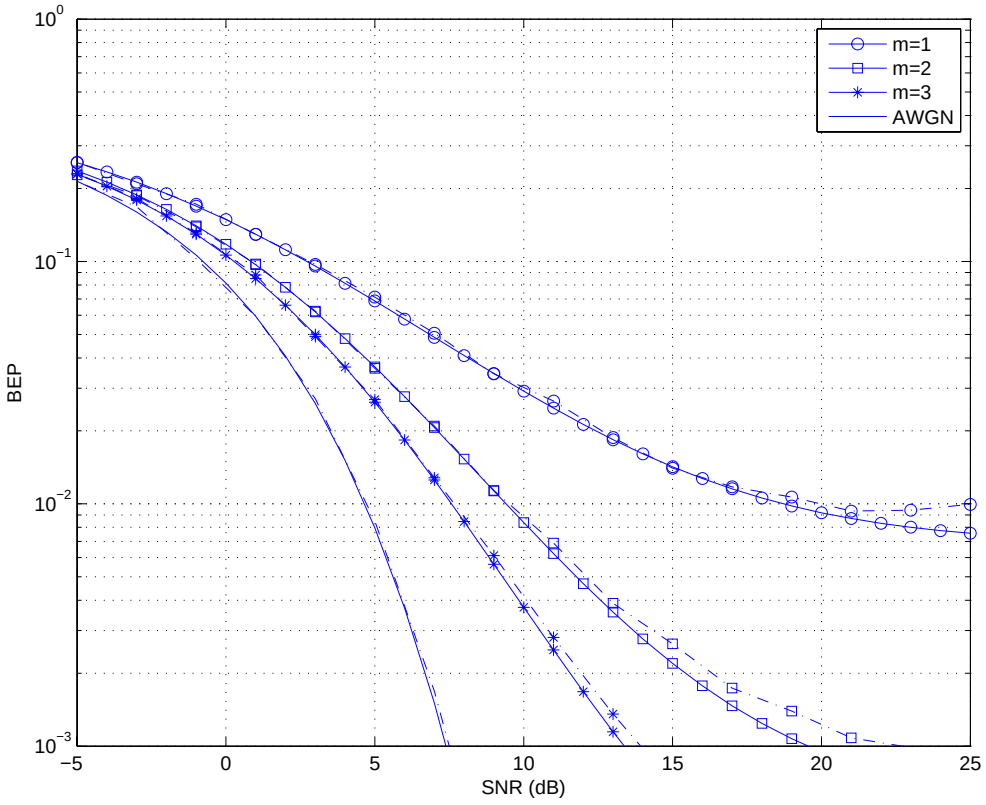

Figure 3.13: Performance of direct transmission over Nakagami-m fading channels with $K = 2$, $V = 24$, and $m = 1, 2$, and 3: (solid) analysis, (dashed) simulation.

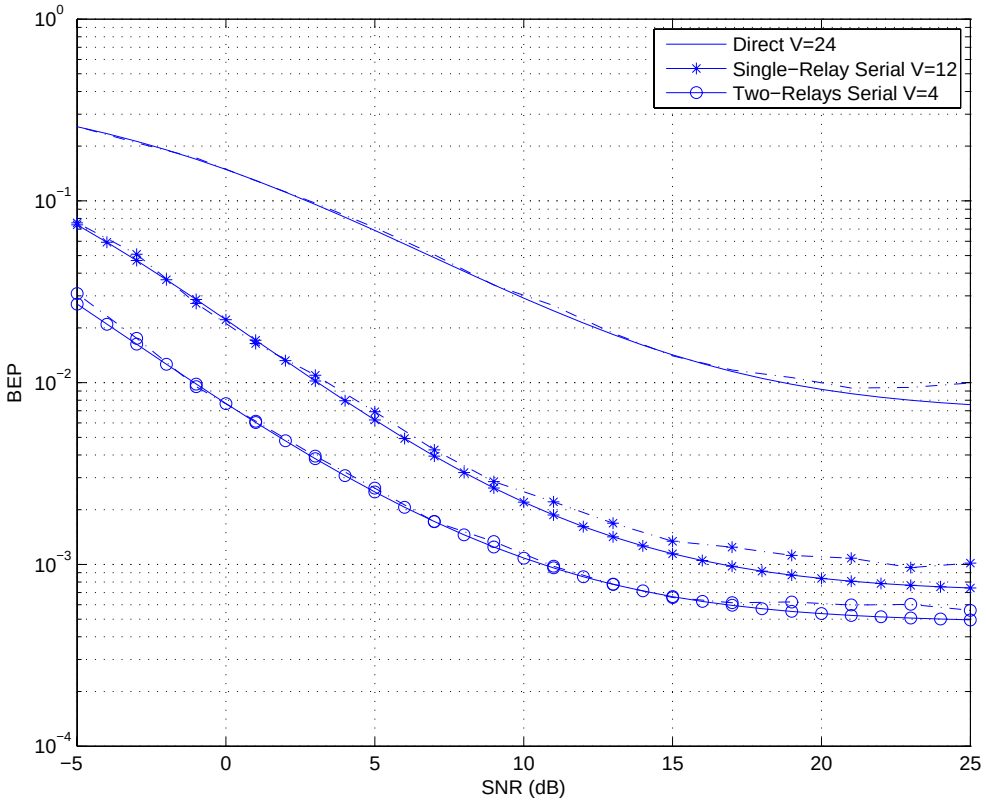

Figure 3.14: Performance of direct, single-relay serial, and two-relay serial schemes over Rayleigh fading channels with $K = 2$: (solid) analysis, (dashed) simulation.

relay serial schemes over Rayleigh fading channels with two interfering users. The figure shows the improvement given by the relaying to the system, even though the spreading gain is reduced in the relaying cases. The figure also shows the closeness of the analysis and the simulation results.

Figure 3.15 shows the analysis and simulation results of the error performance of the direct, single-relay serial, and two-relay serial schemes, over a Rayleigh channel with number of users $K = 4$. The overall performance is worse than the $K = 2$ case but relaying still improves the performance.

Figure 3.16 shows the analysis and simulation results of the error performance of the direct, two-relays parallel, and three-relays parallel cases over a Rayleigh channel with number of users $K = 2$. We notice that the error performance of the parallel relaying is much better than the serial scheme. This is due to the added diversity from the relays. Also the three-relay scheme is much better than the two-relay scheme, even though it is using lower spreading gain. This is because the diversity gain is greater than the loss from the interference.

Figure 3.17 shows the analysis and simulation results of the error performance of the direct, two-relay parallel, and three-relay parallel schemes over Rayleigh fading channels with number of users $K = 4$. The overall gain in the performance is less than the $K = 2$ case because of the additional interference, but there is still a significant improvement in the performance over the serial relaying because of the increased diversity order. Also the relaying still improves the error performance.

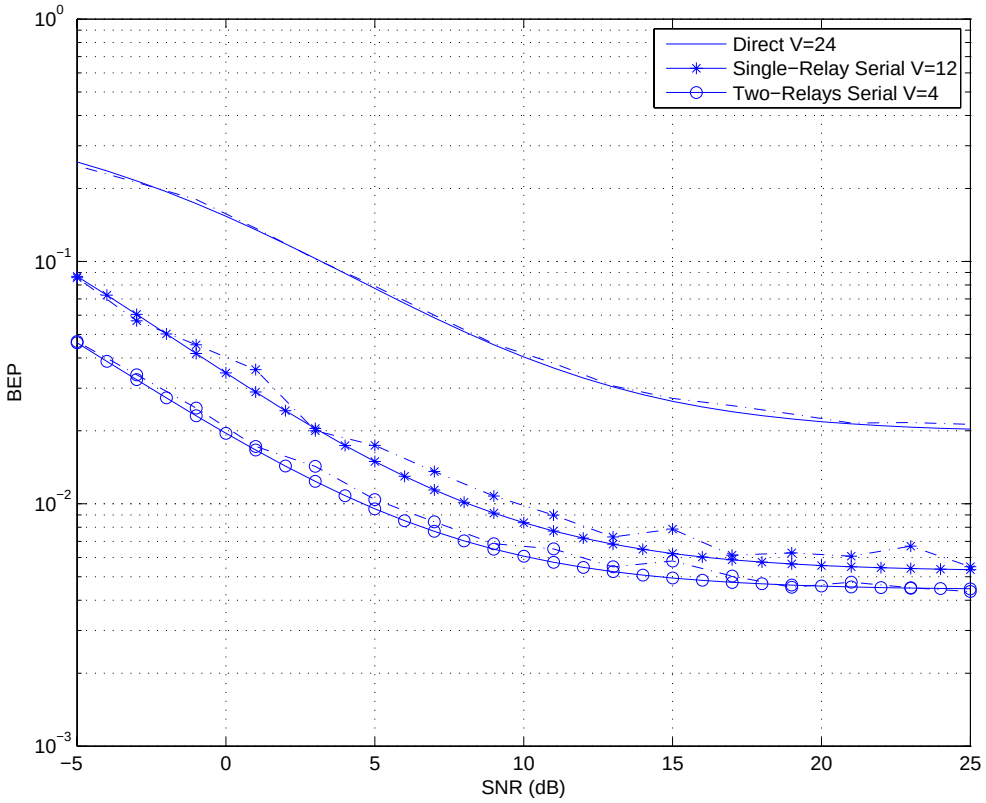

Figure 3.15: Performance of the direct, single-relay serial, and two-relay serial schemes over Rayleigh fading channels with $K = 4$: (solid) analysis, (dashed) simulation.

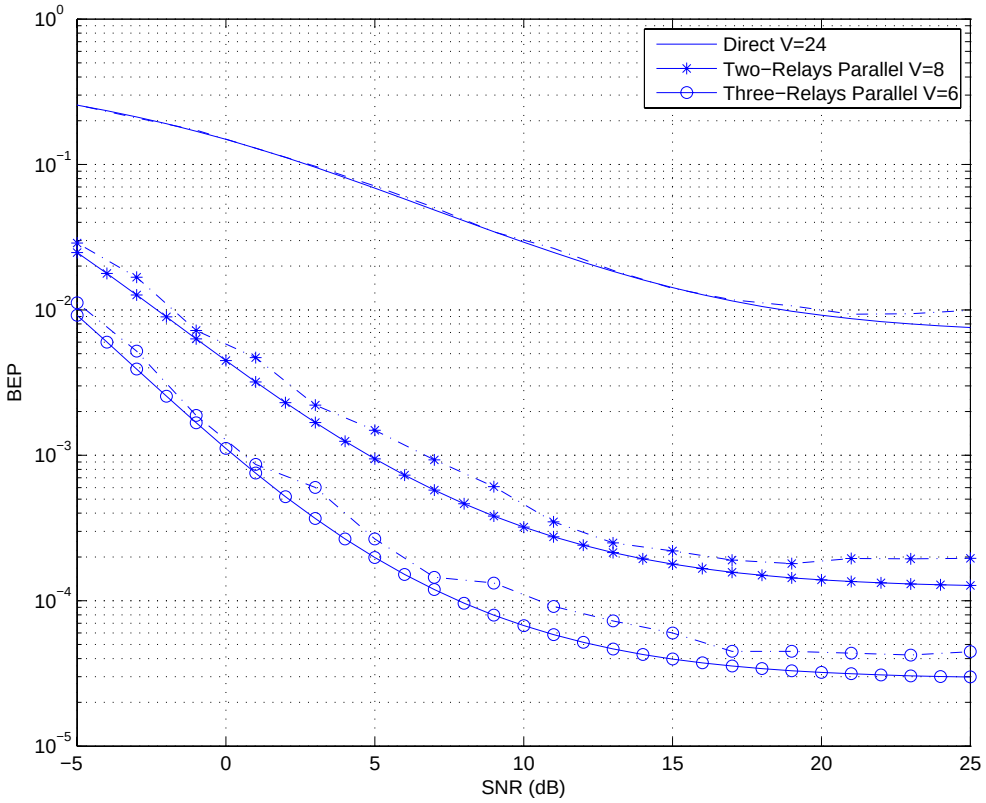

Figure 3.16: Performance of the direct, two-relay parallel, and three-relay parallel schemes over Rayleigh fading channels with $K = 2$: (solid) analysis, (dashed) simulation.

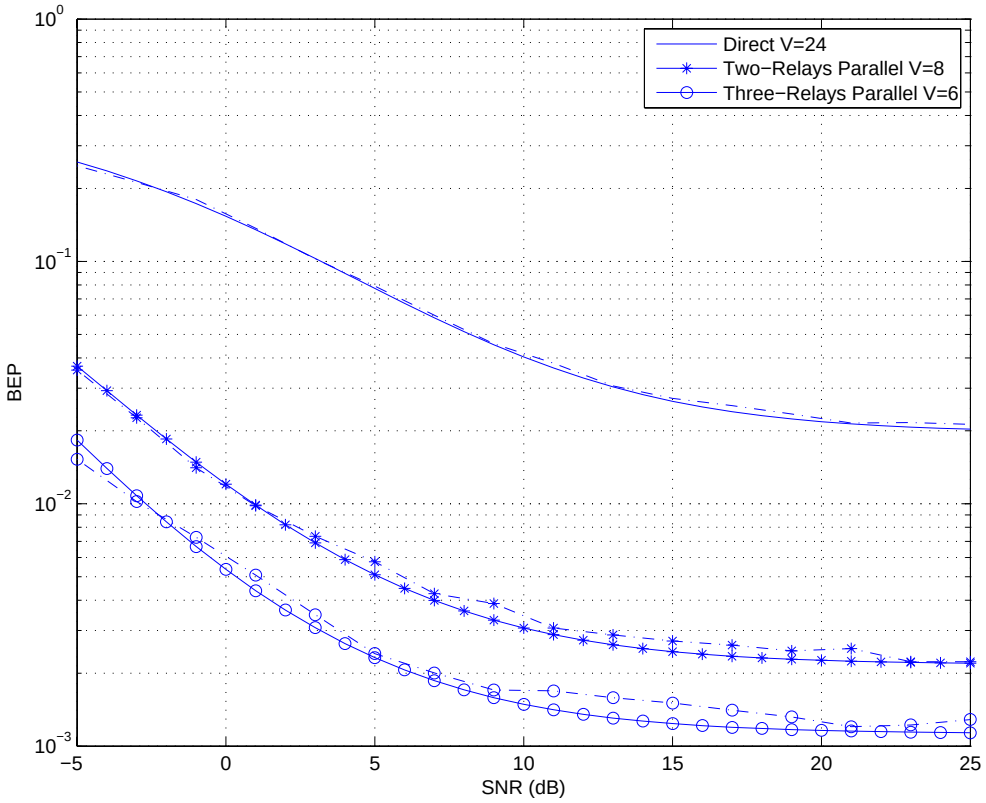

Figure 3.17: Performance of the direct, two-relay parallel, and three-relay parallel schemes over Rayleigh fading channels with $K = 4$: (solid) analysis, (dashed) simulation.

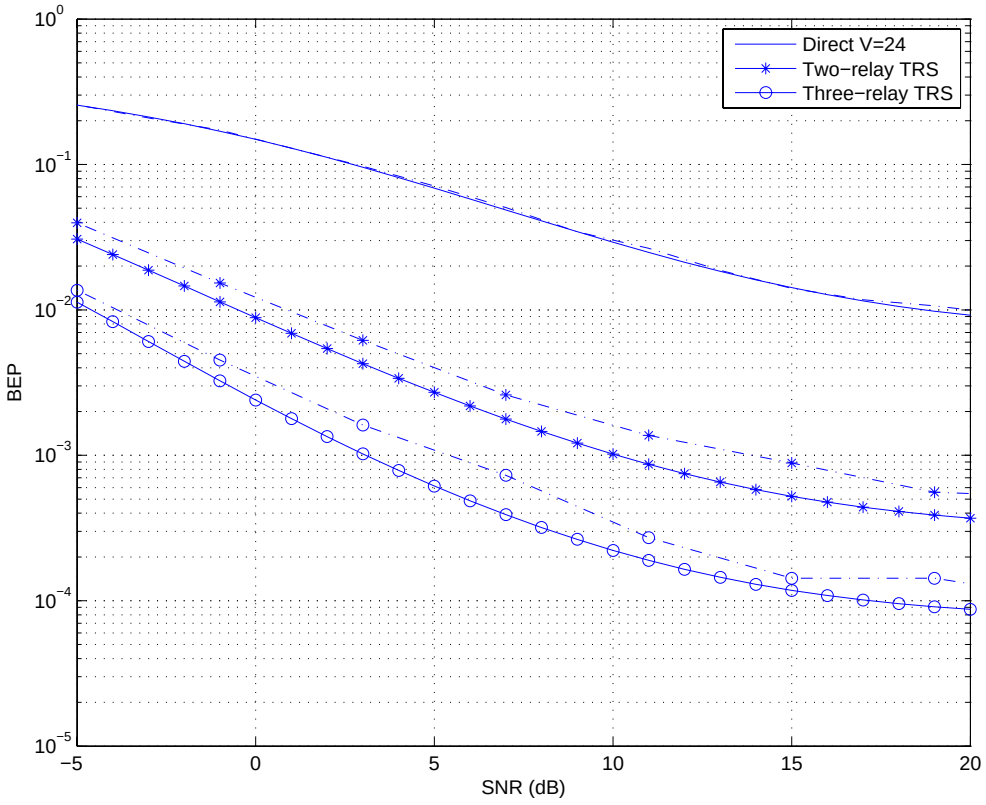

Figure 3.18: Performance of the direct, two-relay TRS, and three-relay TRS schemes over Rayleigh fading channels with $K = 2$ and $\alpha_{th} = 0.5$: (solid) analysis, (dashed) simulation.

Figure 3.18 shows the analysis and simulation results of the error performance of the direct, two-relay TRS, and three-relay TRS schemes over Rayleigh fading channels with two users and using a selection threshold of $\alpha_{th} = 0.5$. This value of $\alpha_{th} = 0.5$ is chosen so that the outage probability is 0.1175. The performance is better than the serial scheme but worse than the parallel scheme. This depends on the choice of the threshold α_{th}. As the threshold increases, fewer relays join, and so the performance approaches the serial case. On the other hand, as the threshold decreases, more relays join, and the performance approaches the parallel case.

Figure 3.19 shows the error performance of the direct, two-relay TRS, and three-relay TRS schemes. The channels used are Rayleigh fading channels with four users in the system, and the selection threshold is chosen as $\alpha_{th} = 0.5$ i.e., P_{out}=0.1175. Due to the increase in the interference level, the performance is worse than the $K = 2$ case. However, there is still a significant gain from the relaying.

Figure 3.20 shows the error performance of the direct and the MRS schemes with two and three relays over Rayleigh fading channels and with number of users $K = 2$. It can be noticed that the performance is worse than the TRS scheme because it uses only one relay all the time and so has less diversity gain. However, it performs better than the single-relay serial scheme because the probability of going into deep fading is reduced.

Figure 3.21 shows the error performance of the direct, two-relay MRS, and three-relay MRS schemes over Rayleigh fading channels with four users in the system.

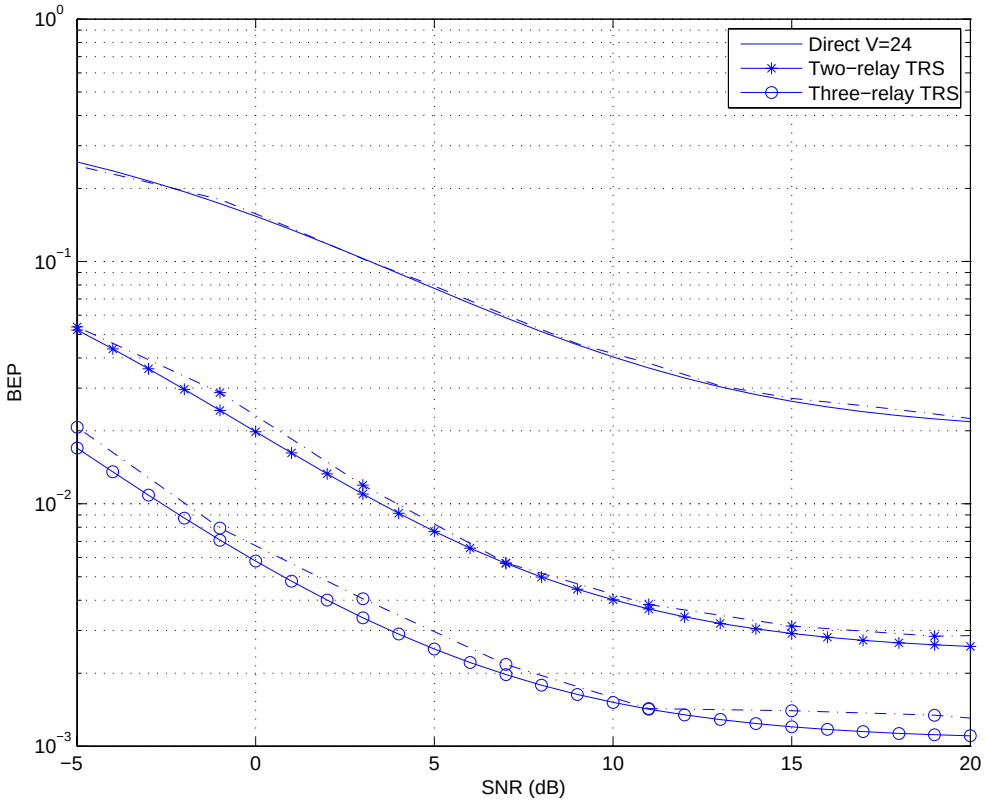

Figure 3.19: Performance of the direct, two-relay TRS, and three-relay TRS schemes over Rayleigh fading channels with K=4 and $\alpha_{TH} = 0.5$: (solid) analysis, (dashed) simulation.

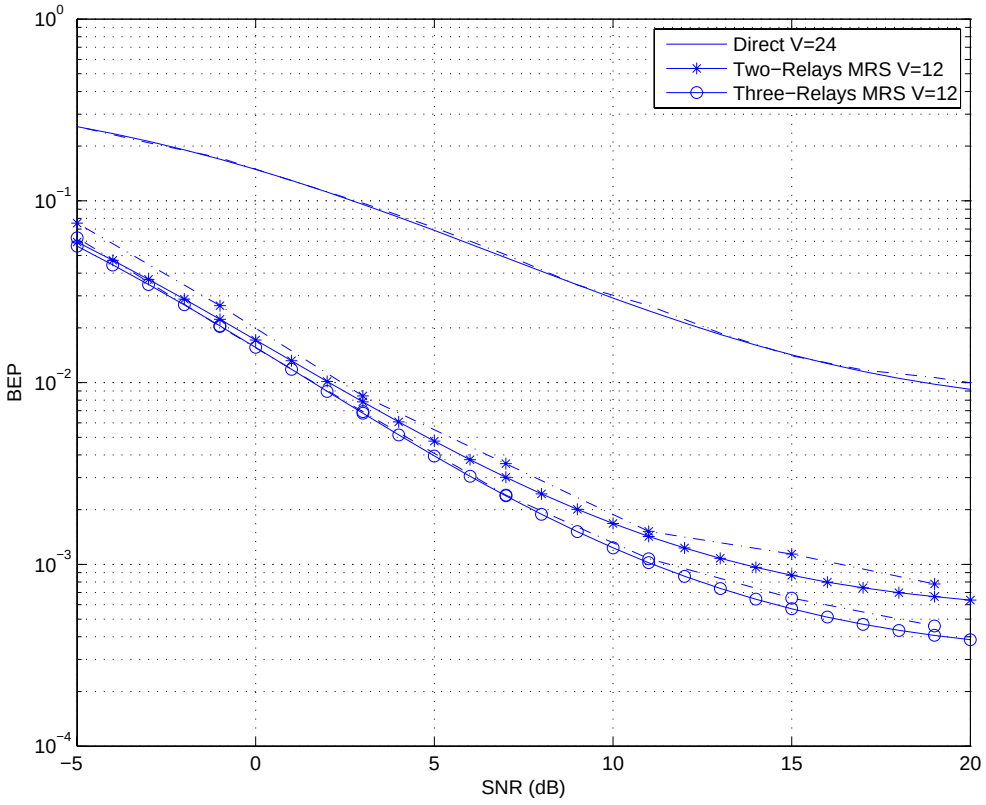

Figure 3.20: Performance of the direct, two-relay MRS, and three-relay MRS schemes over Rayleigh fading channels with $K = 2$: (solid) analysis, (dashed) simulation.

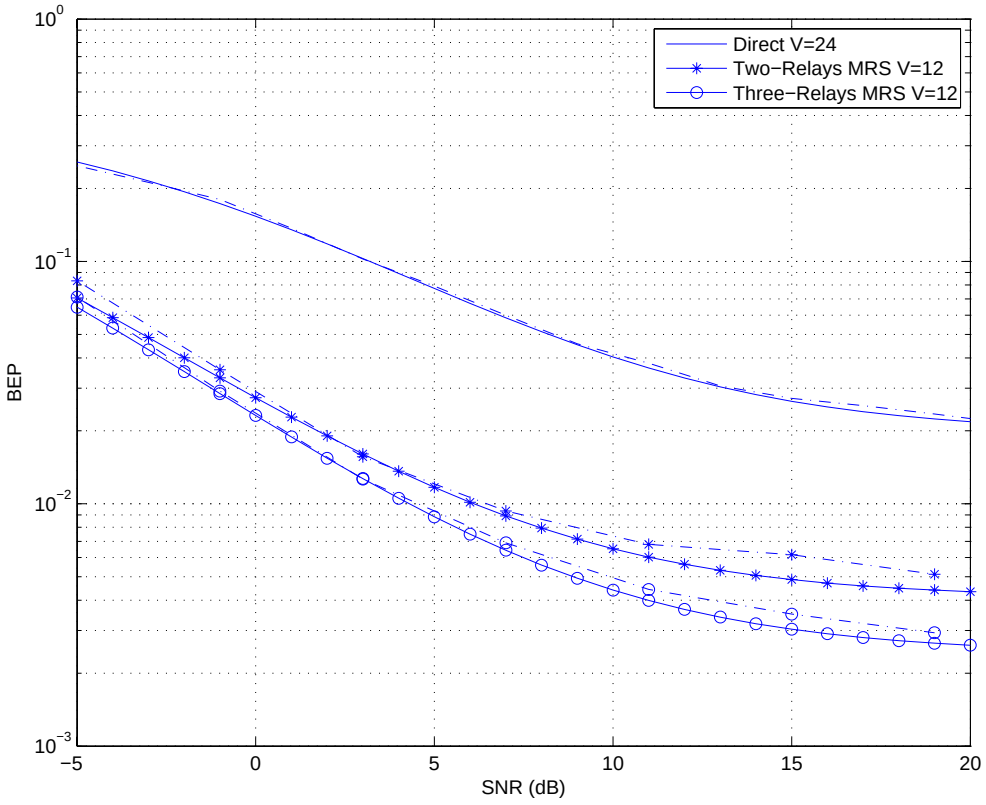

Figure 3.21: Performance of the direct, two-relay MRS, and three-relay MRS schemes over Rayleigh fading channels with $K = 4$: (solid) analysis, (dashed) simulation.

We notice that the overall performance is worse than the $K = 2$ case, due to the increased interference. However, the gain from the relaying is better than in the $K = 2$ case. The system still performs as a serial system, but with better fading conditions.

In the previous figures, we have selected the spreading gain V= 24 for the sake of the simulation time. However, now that we showed that the analysis and the simulation results are close to each other, we will test different system parameters on the analysis in the next figures, using more practical values of the spreading gain such as V=128 and 256.

Figures 3.22 and 3.23 show the analysis results of the error performance of the direct, serial, and parallel relaying over Rayleigh fading channels with number of users $K = 2$ and $K = 4$, respectively. We increased the spreading gain to 128 to reduce the effect of interference, and as we can see from the figures, the performance of the system is much better than the previous cases. Also we can see the improvement given by relaying to the performance of the system. We can conclude that relaying gives the most improvement even though it uses a much lower spreading gain. On the other hand, serial relaying does not give much improvement to the performance.

Figure 3.24 shows the performance analysis of the direct and two-relay schemes of the serial, parallel , TRS, and MRS relaying over Rayleigh fading channels with number of users $K = 4$. Because the diversity order is higher in the serial and the

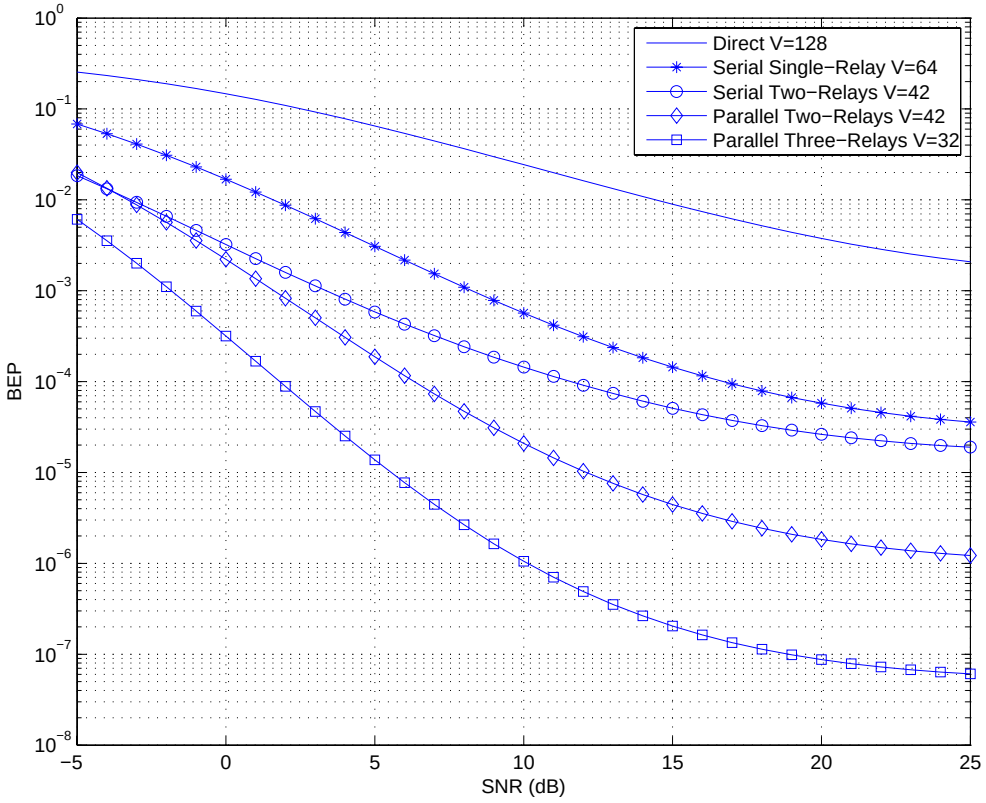

Figure 3.22: Performance of the direct, serial, and parallel relaying over Rayleigh fading channels with $K = 2$.

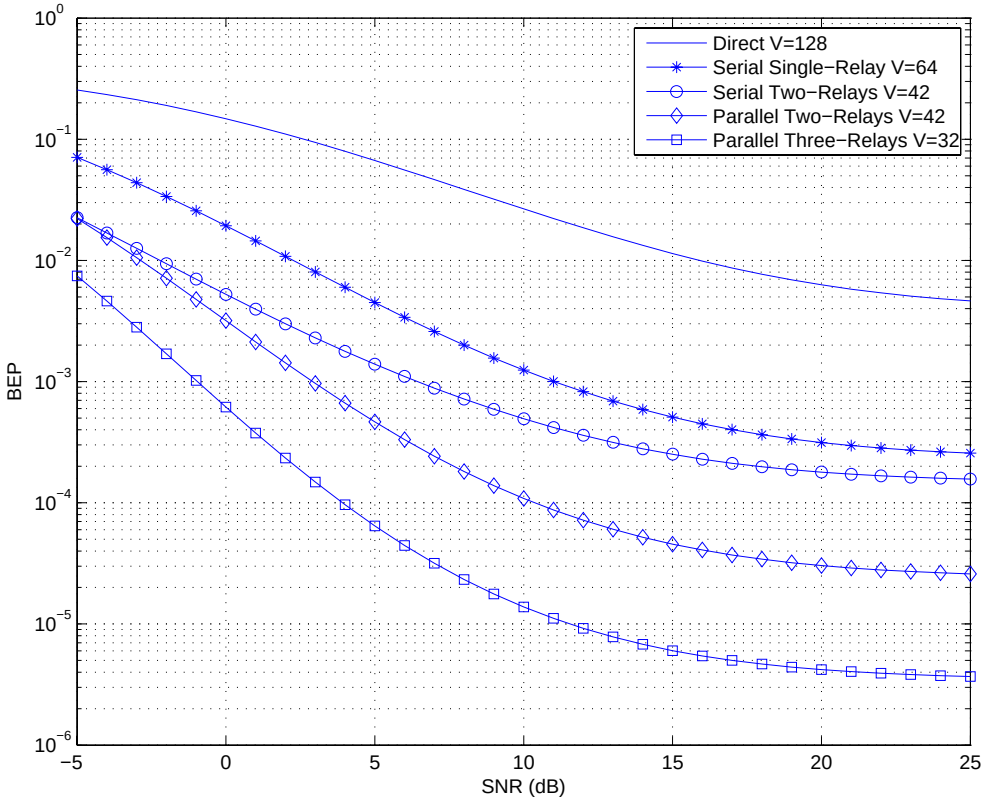

Figure 3.23: Performance of the direct, serial, and parallel relaying over Rayleigh fading channels with $K = 4$.

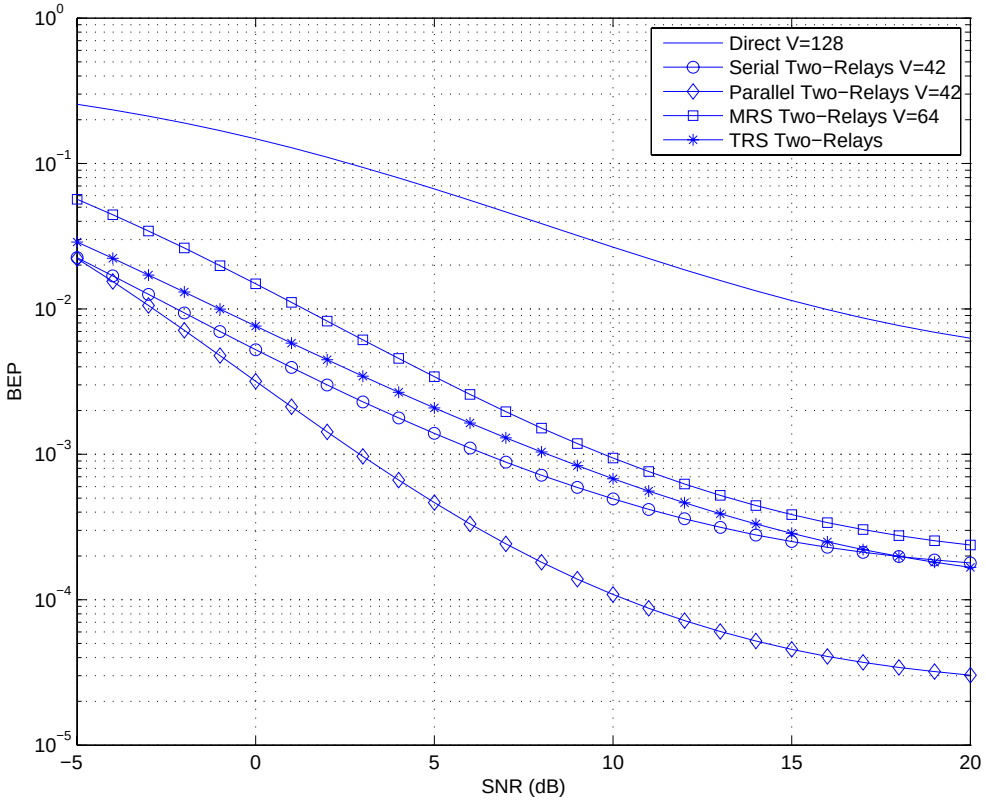

Figure 3.24: Performance of the direct, two-relays serial, parallel, TRS, and MRS relaying over a Rayleigh channel with $K = 4$.

parallel schemes, they perform better than the MRS and the TRS schemes.

Figure 3.25 shows the performance of the direct, serial and parallel relaying systems over Rayleigh fading channels against the number of users when the SNR = 20dB and spreading gain $V = 128$. We notice that both the error performance and the relaying gain decrease as the number of users increases. If we increase the spreading gain to 256 as in Figure 3.26, we notice not only an improvement in the overall performance but also an increase in the relaying gain by comparison with Figure 3.25. Increasing the spreading gain reduces the effect of interference, and hence the diversity effects becomes more visible.

Figures 3.27 and 3.28 show the performance of MRS and TRS relaying schemes in Rayleigh fading channels against the number of users when the spreading gain is 128 and 256, respectively. The SNR in both the figures is fixed at 20 dB. The figures show the improvement given by relaying to the error performance of the system. Furthermore, the gain from adding new relays to the system increases as the spreading gain increases.

In Figures 3.29, 3.30, 3.31, and 3.32 we tested the effect of the path loss exponent on the performance of the system for single-relay serial, two-relay parallel, two-relay MRS, and two-relay TRS schemes, respectively with four users and 128 spreading gain. We considered the cases when $n = 0, 2, 3$ where $n = 0$ means that the distance was not taken into consideration. Results show that the higher the path loss exponent the more improvement the system gets. In environments with high path

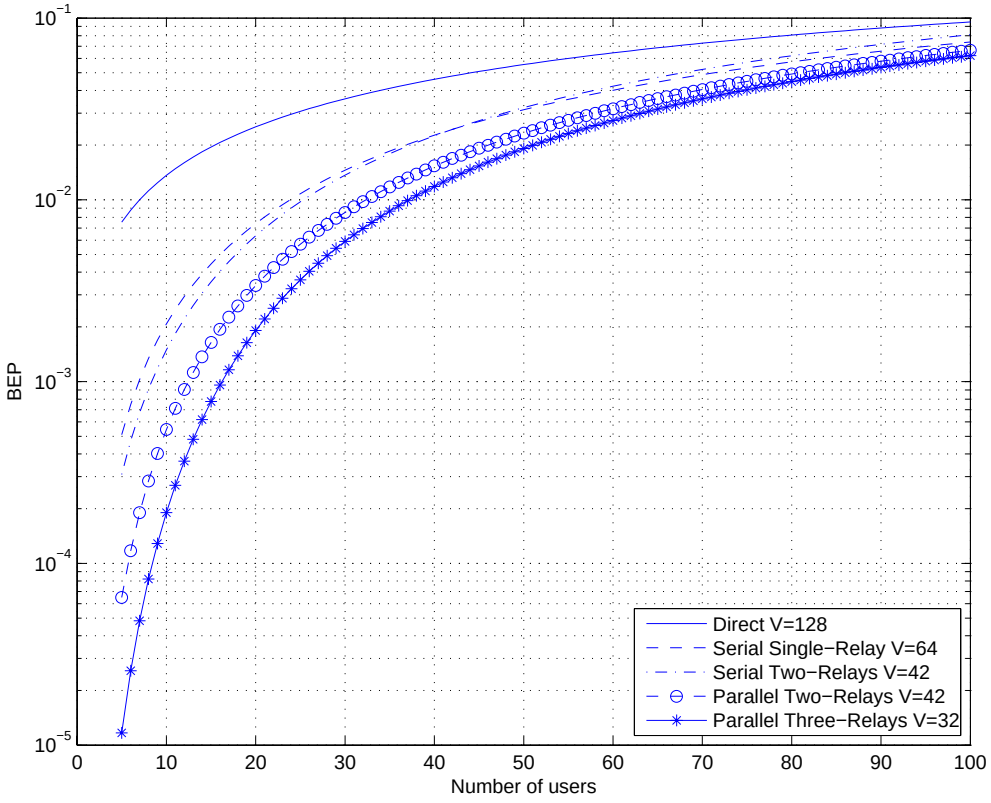

Figure 3.25: Performance for the direct, serial, and parallel relaying system in Rayleigh fading channels against K when SNR = 20dB and $V = 128$.

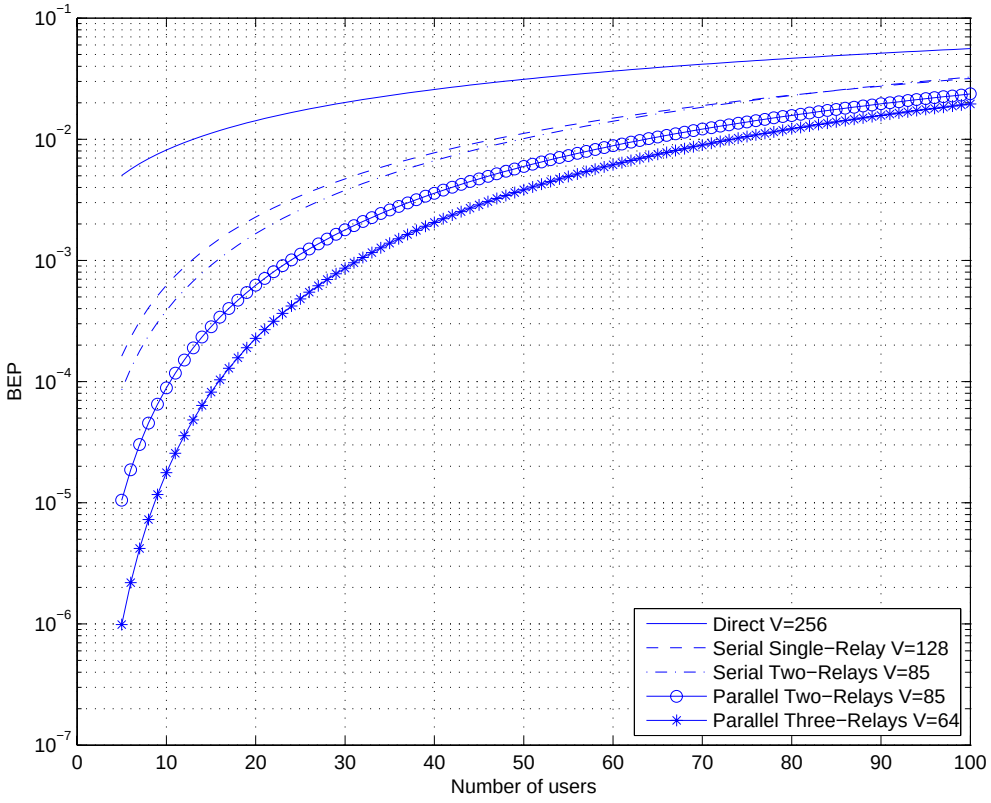

Figure 3.26: Performance for the direct, serial, and parallel relaying schemes in Rayleigh fading channels against K when SNR = 20dB and $V = 256$.

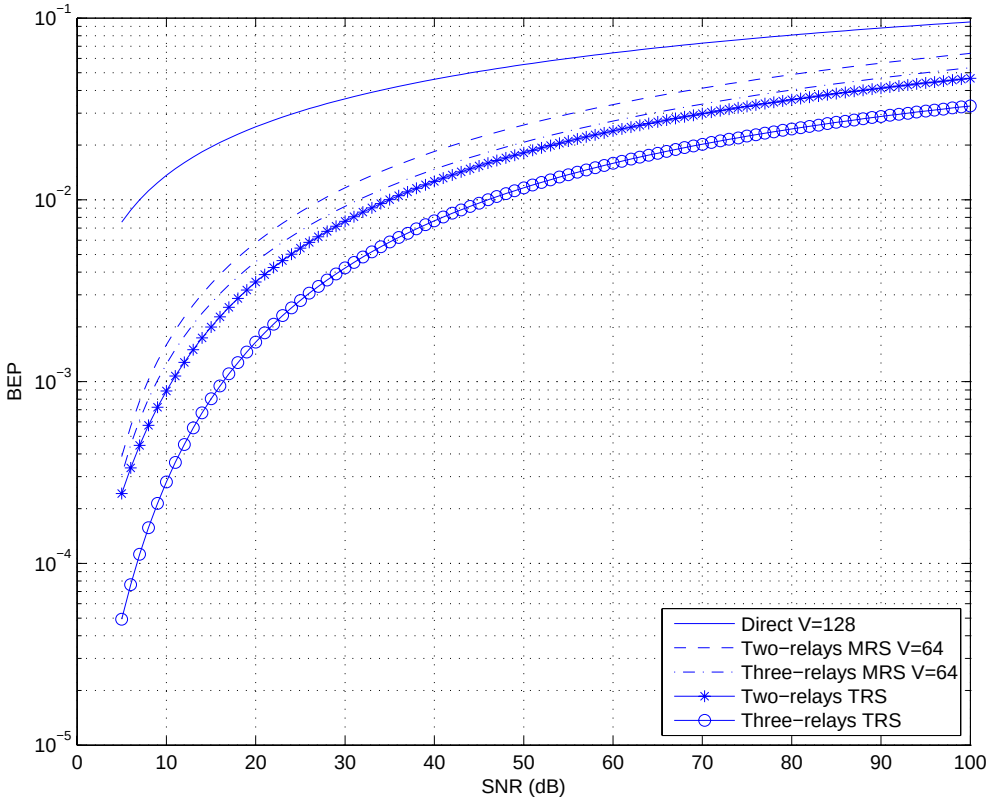

Figure 3.27: Performance for the MRS, and TRS schemes in Rayleigh fading channels against the K when SNR = 20dB and $V = 128$.

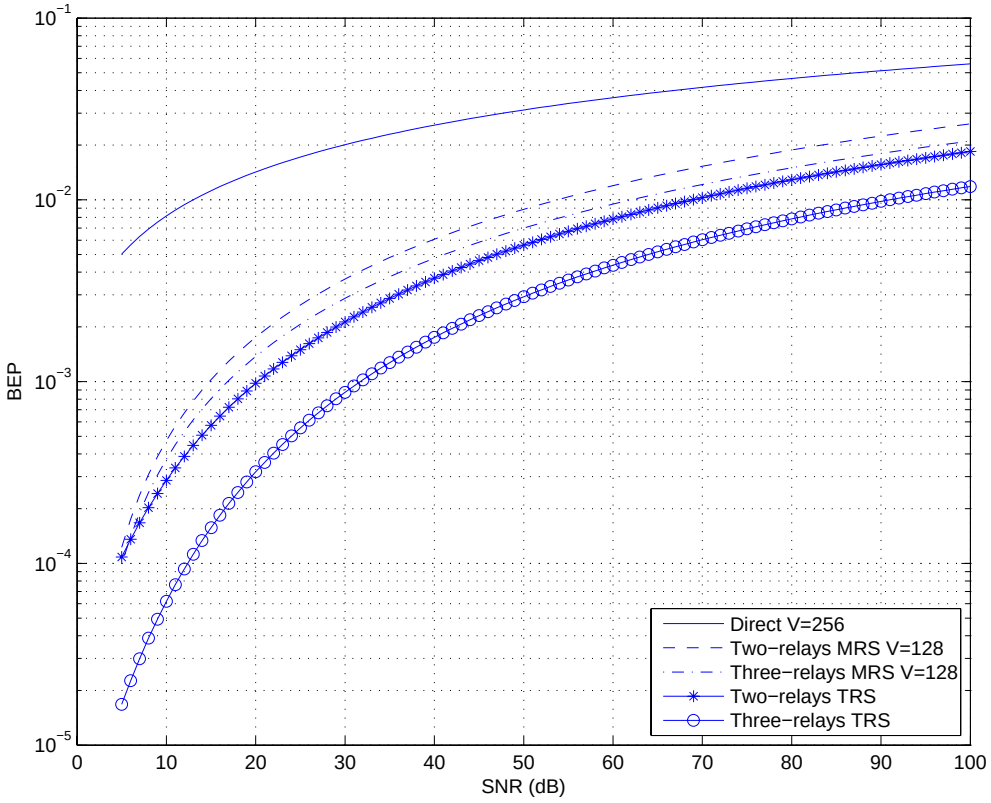

Figure 3.28: Performance for the MRS, and TRS schemes in Rayleigh fading channels against K when SNR = 20dB and $V = 256$.

loss exponent, sending the data over short distances saves more power than doing the same thing in low path loss environments. So the gain given by relaying to the system gets better as the path loss exponent increases.

3.4 Chapter Conclusions

In this chapter we investigated the performance of multi-hop networks employing CDMA transmission. A brief background on spread spectrum techniques was given. We extended the derivation of the probability of error for the CDMA system employing BPSK based on the standard Gaussian approximation to include the effect of diversity. Using this formula, we derived the probability of error of the system when using serial, parallel and two schemes based on selection relaying. We showed that both the analysis and simulation results are close to each other. Additionally, the error performance of the system with serial, parallel, and selection relaying was investigated with different values of spreading gain and number of users. Finally, the effect of the path loss exponent on the system performance for different network topologies was studied.

From the simulation and analytical results obtained in this chapter, we can conclude the following:

- Relaying greatly improves the system, especially in parallel relaying chemes.
- When the spreading gain is increased, the effect of relaying on the overall

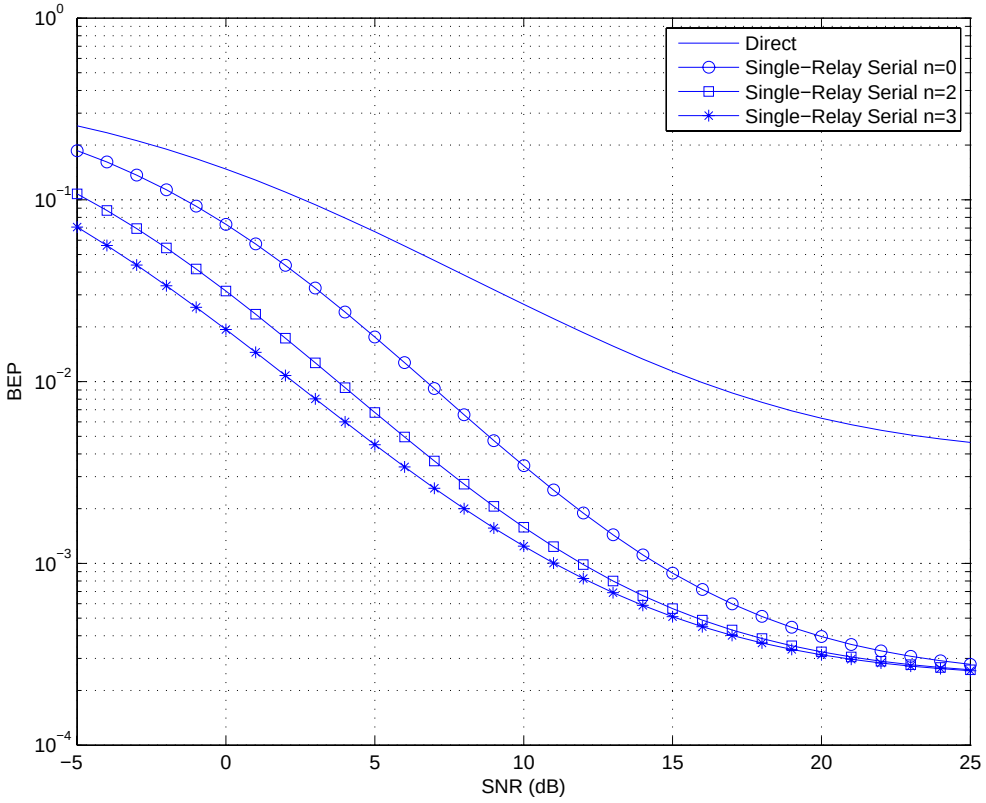

Figure 3.29: Effect of path loss exponent of the performance of the serial single-relay scheme with $K = 4$, $V = 128$, and $n = 0, 2$, and 3.

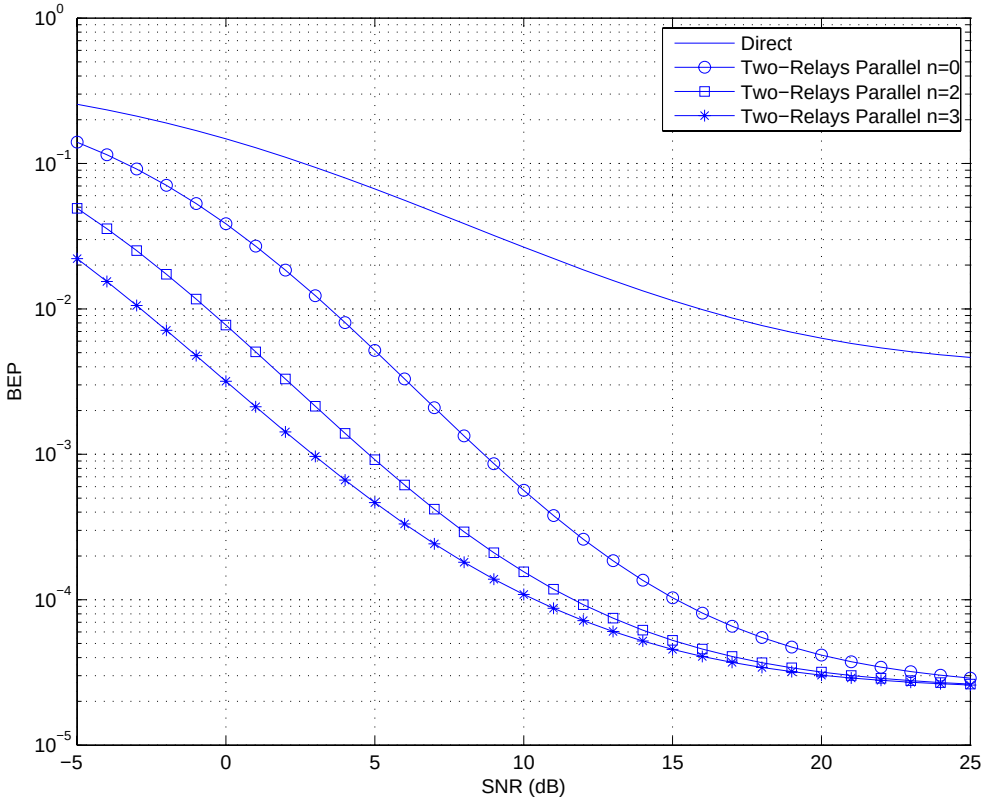

Figure 3.30: Effect of path loss exponent of the performance of the parallel two-relay scheme with $K = 4$, $V = 128$, and $n = 0, 2$, and 3.

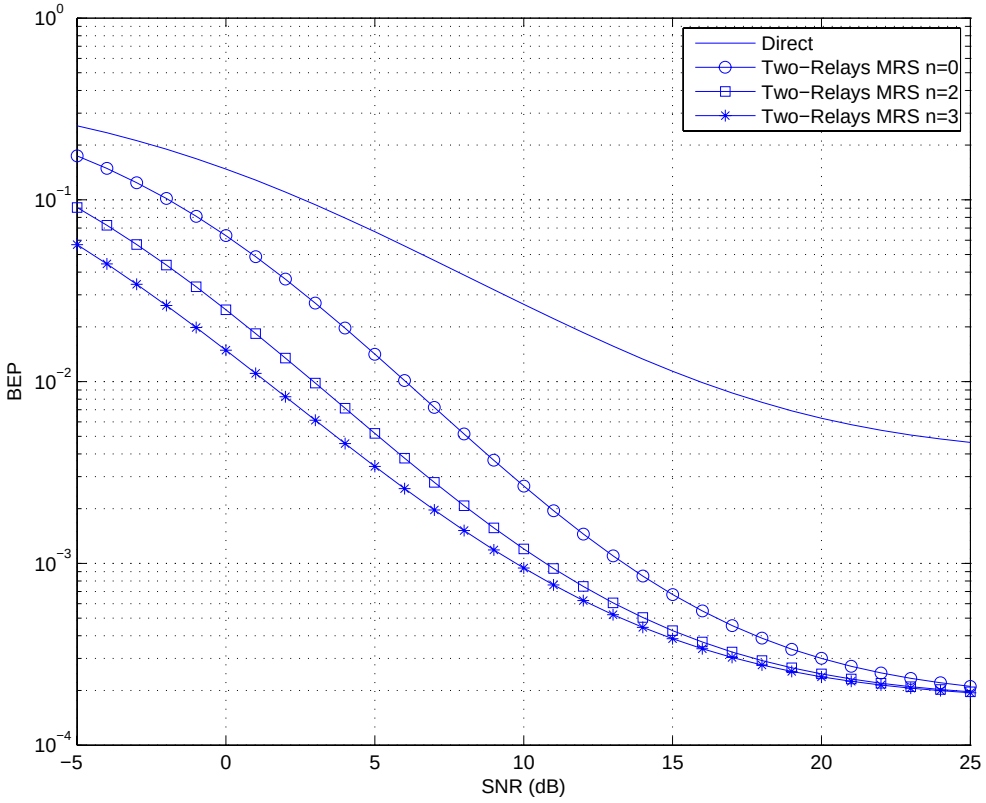

Figure 3.31: Effect of path loss exponent of the performance of the MRS two-relay scheme with $K = 4$, $V = 128$, and $n = 0, 2$, and 3.

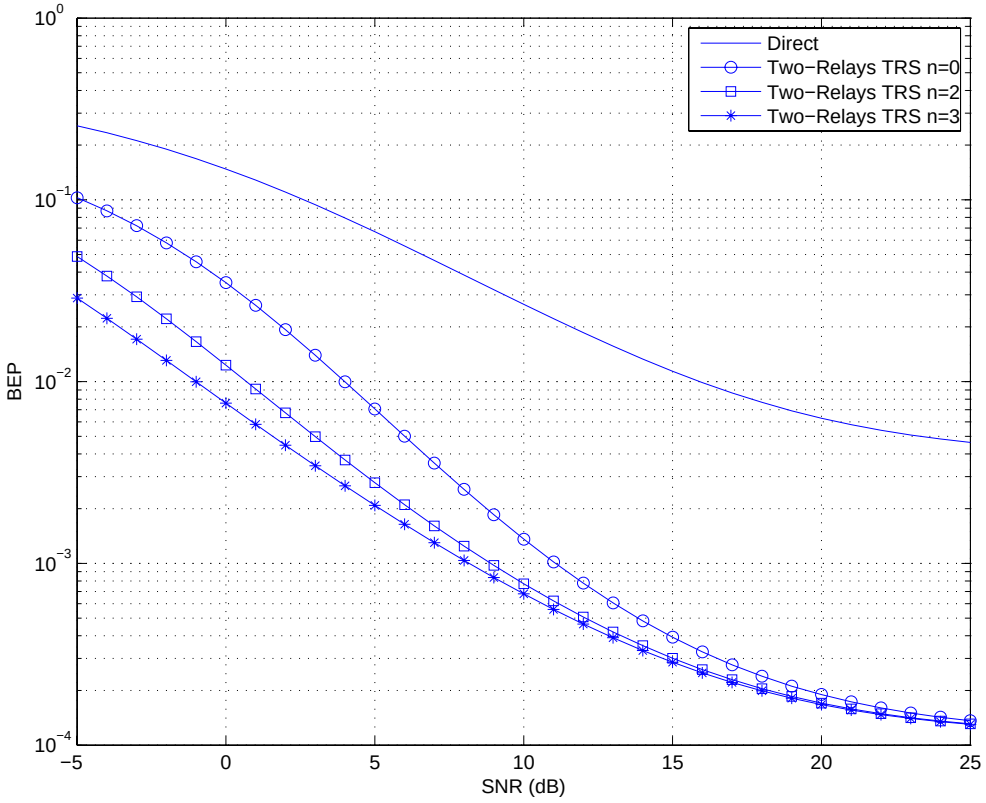

Figure 3.32: Effect of path loss exponent of the performance of the TRS two-relay scheme with $K = 4$, $V = 128$, and $n = 0, 2$, and 3.

performance increases, especially when the interference is low.

- As the number of users increases, the improvement coming from relaying decreases. However, relaying still gives significant improvement in parallel relaying because of the larger diversity order.

- The error performance of the system improves as the path loss exponent increases. In high path loss exponent environments, sending the data over short distances saves more power than doing the same thing in low path loss environments. So the gain given by relaying to the system gets better as the path loss exponent increases.

Chapter 4

Coded OFDM Networks

Orthogonal Frequency Division Multiplexing (OFDM) has been accepted as a mature technology for wireless broad-band communication links. Its design as a multicarrier system allows the support of high data rates while maintaining symbol durations longer than the channel coherence time [13]. Thus, OFDM modems can have reliable high data rate transmission in frequency-selective channels without the need for complex time-domain channel equalizers. Other advantages of OFDM systems are high spectral efficiency and low sensitivity to time synchronization errors [13].

The rest of this chapter is organized as follows. In section 4.1 we will discuss the system model we are going to use in this work. Sections 4.2, 4.3, and 4.4 respectively show the results we got from a system where serial, parallel, and selection relaying is employed. Finally Section 4.5 is the chapter's conclusion.

4.1 System Model

Figure 4.1 shows the system model of coded OFDM systems. All k source bits in a length-k vector $\mathbf{u}$ are encoded into an n-bit codeword $\mathbf{v}$. The coded vector $\mathbf{v}$ is interleaved and mapped to the N_c-symbol vectors $\{\mathbf{x}_l\}_{l=1}^{N_c}$, where $\mathbf{x}_l = (x_{l1}, x_{l2}, ..., x_{lM})$, and $x_{l,i}$ is a symbol drawn from certain signal constellation. At every time instance t, the t^{th} elements of the N_c signal vectors $\{\mathbf{x}_l\}_{l=1}^{N_c}$ are input to an IFFT block to output the t^{th} OFDM symbol s_t, whose k^{th} component is expressed as

$$s_{t,k} = G_T \sum_{l=1}^{N_c} x_{l,t} \exp\left(j2\pi \frac{kp_l}{N_{FFT}}\right), \qquad ,k = 0, ..., N_{FFT} - 1, t = 1, ..., M, \quad (4.1)$$

where G_T is the IFFT gain factor, p_l determines the corresponding subcarries of the l-th vector $\mathbf{x}_l$, and N_{FFT} is the number of the FFT points used in the OFDM modulation. The resulting signal is transmitted over a p-path fading channel with a profile $\{g_p, \tau_p\}_{p=l}^{P}$, where g_p, and τ_p, are the gain and delay of the channel's p-th path with $\sum_{p=1}^{P} g_p^2 = 1$ satisfied.

At the receiver side, the received sample for the k^{th} subcarrier at the t^{th} time instance $r_{t,k}$ is written as

$$r_{t,k} = G_T \sum_{l=1}^{N_c} \sum_{p=1}^{P} g_p \beta_p x_{l,t} H\left(j2\pi \frac{p_l}{N_{FFT}}\right) \exp\left(j2\pi \frac{(k-\tau_p)p_l}{N_{FFT}}\right) + \tilde{\eta}_{t,k} \quad (4.2)$$

$$= G_T \sum_{l=1}^{N_c} x_{l,t} \alpha_l \exp\left(j2\pi \frac{kp_l}{N_{FFT}}\right) + \tilde{\eta}_{t,k} \quad (4.3)$$

where $\{\beta_p\}_{p=1}^{P}$ are complex zero-mean Gaussian independent random variables with unit variance representing the fading coefficients of each path of the channel. Due

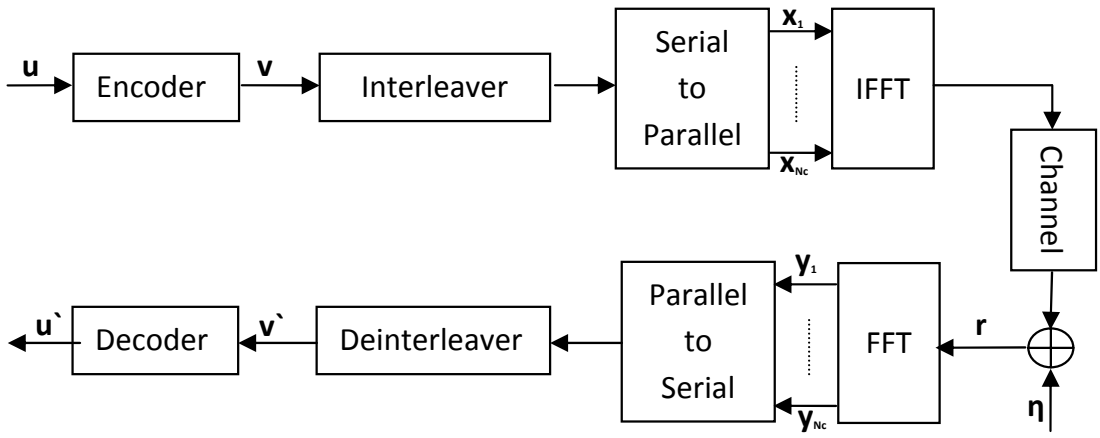

Figure 4.1: Model of coded OFDM system.

to the small packet size compared to the coherence time of fading channel, the channel condition does not vary significantly during the transmission of a packet, hence $\{\beta_p\}_{p=1}^{P}$ are assumed to be constant within a packet. In (4.3) $H(.)$ is the frequency response of the cascaded transmit and receive filters, and $\tilde{\eta}_{t,k}$ denote the noise samples filtered by the receive filter, $\eta_{t,k}$ is the independent zero-mean Gaussian noise component with variance σ_η^2. Finally $\{\alpha_l\}_{l=1}^{N_c}$ are the frequency domain fading coefficients defined as follows

$$\alpha_l = H\left(j2\pi\frac{p_l}{N_{FFT}}\right)\left(\sum_{p=1}^{P} g_p\beta_p \exp\left(-j2\pi\frac{\tau_p p_l}{N_{FFT}}\right)\right). \tag{4.4}$$

After applying the FFT to the received samples $r_{t,k}$, we get

$$y_{l,t} = G_R \sum_{k=0}^{N_{FFT}-1}\left[\sum_{i=1}^{Nc}\alpha_i x_{i,t}\exp\left(j2\pi\frac{kp_i}{N_{FFT}}\right) + \tilde{n}_{k,t}\right]\exp\left(-j2\pi\frac{kp_l}{N_{FFT}}\right) \tag{4.5}$$

$$= \alpha_l x_{l,t} + z_{l,t}, \tag{4.6}$$

where G_R is the FFT gain factor and $z_{l,t}$ is the frequency domain noise samples.

In packet switched communications such as the OFDM, the channel can be modeled as a block fading (BF) channel. In the BF channel model, the transmitted sequence is divided into blocks, and all the symbols belonging to the same block suffer the same fade. In some cases, the fade blocks are assumed to be independent from each other, but in some applications such as the OFDM system there is a considerable correlation among the fade blocks. In this case, the fading channel is referred to as correlated block fading (CBF). It was proved in [29] that OFDM systems can be simulated by using CBF.

Consider the system model shown in Figure 4.2. It iresembles the OFDM system model shown in Figure 4.1 but the blocks from IFFT to FFT are replaced with the correlated block fading system [29]. In the figure, each symbol vector $\mathbf{x}_l = (x_{l1}, x_{l2}, ..., x_{lM})$ is transmitted through a block fading subchannel with a multiplicative distortion $\boldsymbol{\alpha}_l = (\alpha_1, ..., \alpha_{N_c})$, which is a complex Gaussian random variable that stays constant during the transmission of $\mathbf{x}_l$. The fading coefficients $\{\boldsymbol{\alpha}_l\}_{l=1}^{N_c}$ are correlated with correlation matrix $C_\alpha = E[\boldsymbol{\alpha}\boldsymbol{\alpha}^H]$, where $\boldsymbol{\alpha}_l = (\alpha_1, ..., \alpha_{N_c})^T$.

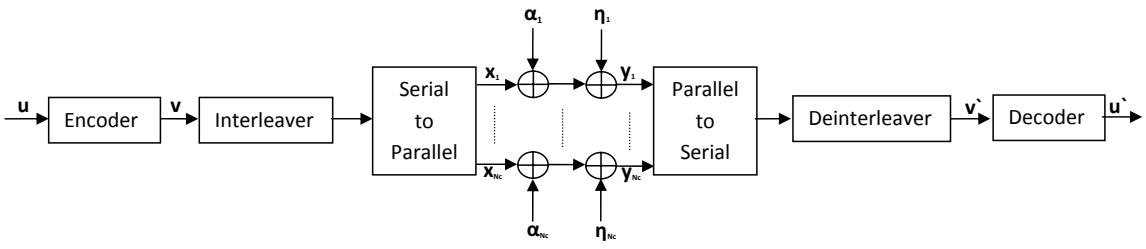

Figure 4.2: Model of a coded OFDM system over a correlated block fading channel.

The received vectors $\mathbf{y}_l = (y_{l1}, ..., y_{lM})$ corresponding to the transmission of $\mathbf{x}_l$ over the CBF channel is given by

$$\mathbf{y}_l = \boldsymbol{\alpha}_l \mathbf{x}_l + \boldsymbol{\eta}_l, \tag{4.7}$$

where the noise vector $\boldsymbol{\eta}_l$ consists of a zero-mean independent Gaussian components with variance σ_η^2. The fading vector $\boldsymbol{\alpha}_l$ can be written as $\boldsymbol{\alpha} = \mathbf{A}\boldsymbol{\beta}$ where $\mathbf{A} = [a_{l,p}]_{L\times P}$ and

$$a_{l,p} = g_p \exp\left(-j2\pi \frac{\tau_p p_l}{N_{FFT}}\right) H\left(j2\pi \frac{p_l}{N_{FFT}}\right). \tag{4.8}$$

The correlation matrix $C_\alpha = E[\boldsymbol{\alpha}\boldsymbol{\alpha}^H]$ is expressed as $C_a = \mathbf{A}\mathbf{A}^H$.

In this thesis, we consider two different fading channels, mainly by changing the gain and delay profiles of the channel, g_p, and τ_p. Figures 4.3 (a and b) are the two normalized gain profiles of the two channels we will use in all the simulations of this chapter. The delay profile is uniformly spaced in the two channels with different variance. In this chapter, we will consider two forwarding techniques, amplify-and-forward (AF) and decode-and-forward (DF), which have been discussed in Chapter 1.

4.2 Serial Relaying

In this section we will consider serial relaying, shown in Figure 4.4. In the first time slot, the source sends the data to the relay, which in turn forwards it to the destination in the next time slot, and so on. Figure 4.5 shows the time allocation of

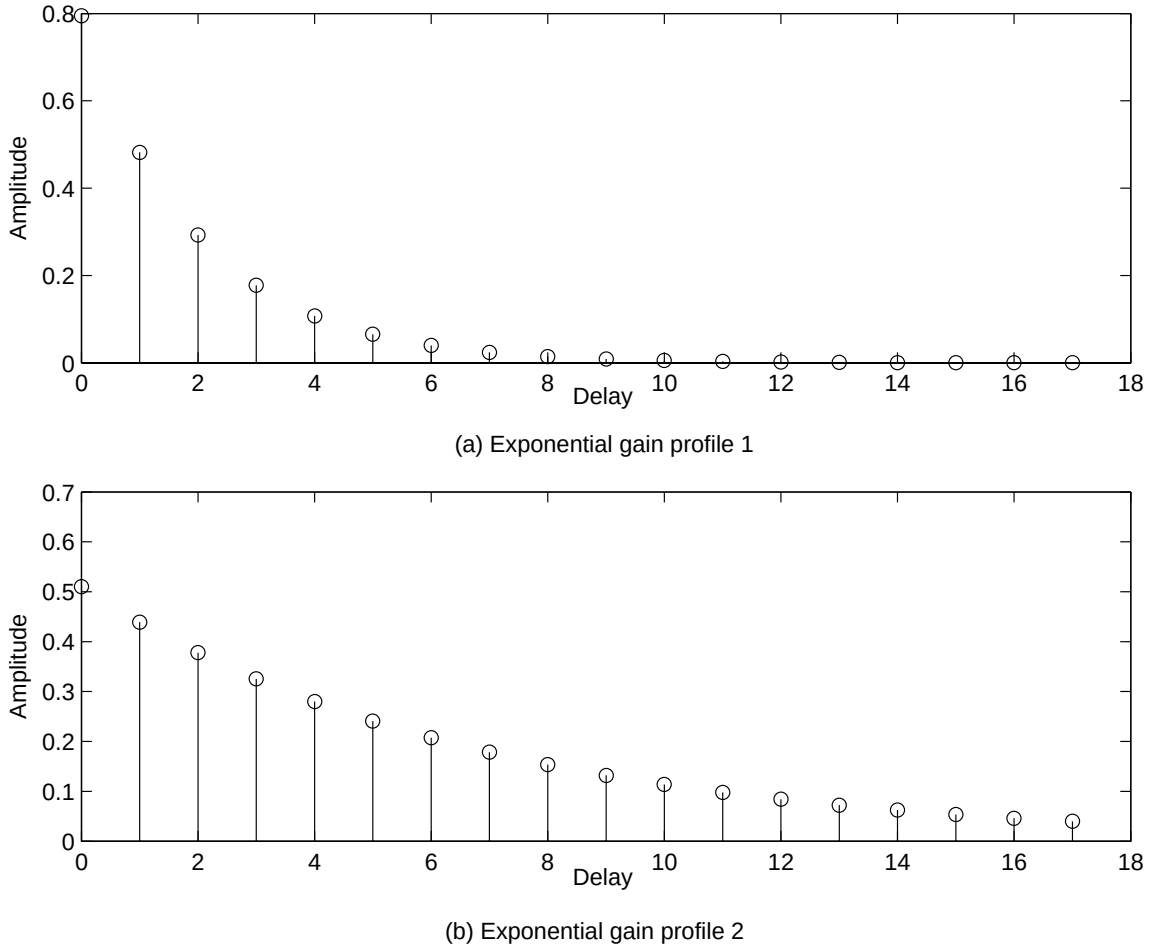

Figure 4.3: Channel Spread Profiles. (a) Exponential Channel 1. (b) Exponential Channel 2.

the transmission.

The discrete-time signal model of the received signal at the relay is given by

$$y_r = \sqrt{d_{sr}^{-n}}\alpha_{sr}x_s + \eta_r, \tag{4.9}$$

where y_r is the received signal at the relay, α_{sr} is the channel fading amplitude between the source and the relay, x_s is the transmitted signal from the source, d_{sr} is the distance between the source and the relay usually measured in meters, n is the path loss exponent which depends on the environment, and finally η_{sr} is the AWGN component at the destination. The relay then forwards the signal to the destination. The received signal at the destination node using the DF scheme is given by

$$y_d = \sqrt{d_{sr}^{-n}}\alpha_{rd}\hat{y}_r + \eta_{rd}, \tag{4.10}$$

where $\hat{y}_r$ is the signal after being encoded by the relay node.

The destination then uses maximum ratio combining (MRC) to combine the data received from the source and the relays. To implement MRC in our system, we change the metric of the Viterbi decoder to $(y_{s,d}-\sqrt{d_{sd}^{-n}}\alpha_{sd}x_d)^2+(y_{r,d}-\sqrt{d_{rd}^{-n}}\alpha_{rd}x_d)^2$, where the receiver uses the signals coming from both the source and the relay together.

For the sake of simplicity, we assume that the relays are equally spaced between the source and the destination. In order to be fair when comparing the different scenarios, we change the coding rate at the transmitter and relays, in order to fix the total number of transmitted symbols and the total energy used. In the case of direct transmission we use $\frac{1}{6}$ code rate, while in the single-relay scheme we use

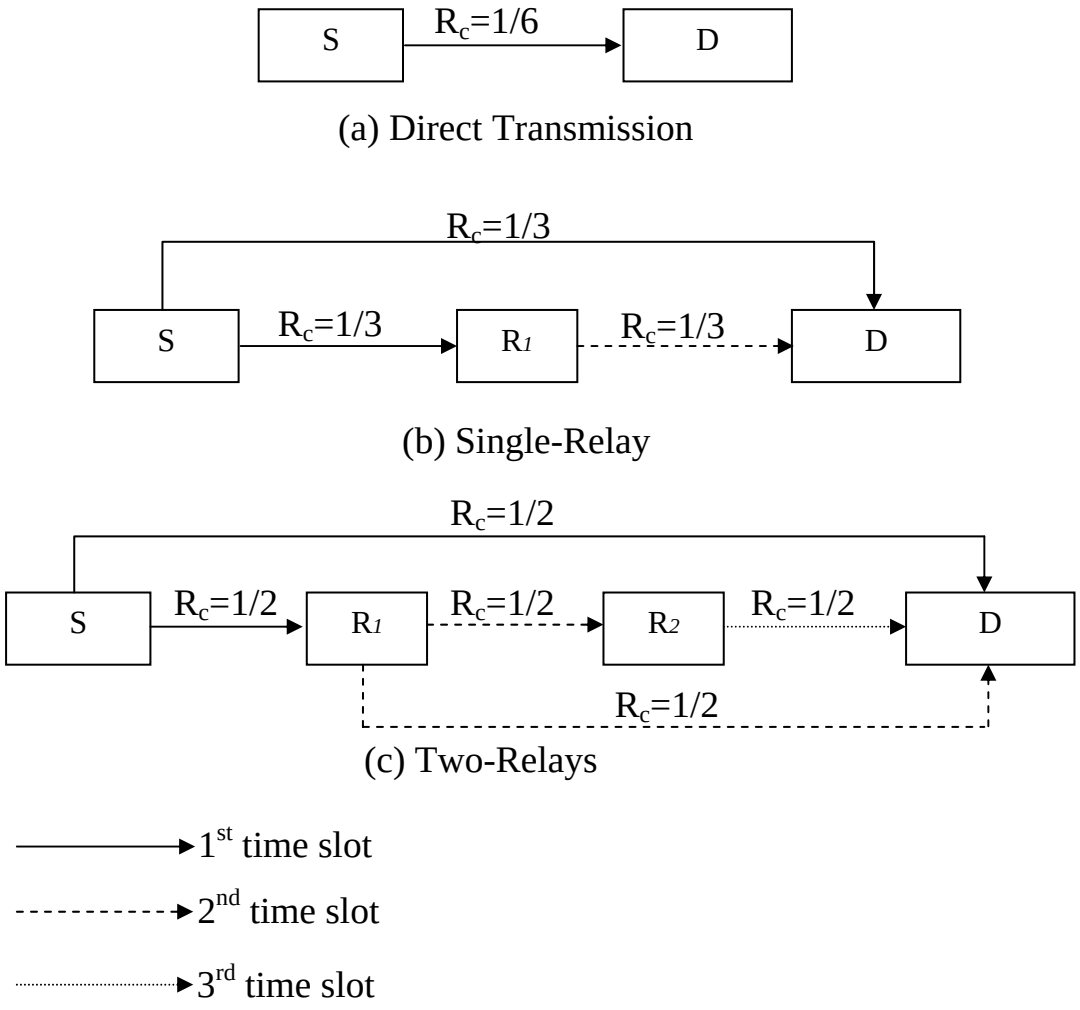

Figure 4.4: Serial Topology. (a) Direct Transmission with rate=1/6, (b) Single-relay scheme with rate=1/3, and (c) Two-relay scheme with rate=1/2.

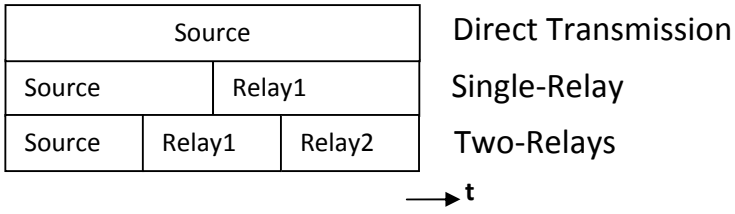

Figure 4.5: Time Allocation of the serial scheme.

$\frac{1}{3}$ code rate, and finally in the two-relay scheme we use $\frac{1}{2}$ code rate. The number of OFDM subcarriers is set to $N_c = 64$ in all cases, and the path loss exponent is $n = 3$. In the following we discuss various simulation results for different system parameters for serial relaying. We tested the effect of the channel, the effect of OFDM bandwidth by changing the number of subcarriers, and the effect of the environment by changing the path loss exponent.

Figure 4.6 shows the error performance of a convolutionally coded multi-hop network using serial relaying and DF and AF forwarding over OFDM with exponential channel 1 and number of subcarriers $N_c = 64$. The figure clearly shows the improvement given by relaying to the system, in terms of not only SNR gain but also diversity gain. The diversity gain is coming from both the coding and from using DF, and it can be seen in the change of the slope of the curve, which is steeper in the case of DF. Also we can deduce that DF performs better than AF in medium to high SNR.

Figure 4.7 shows the error performance of a convolutionally coded multi-hop network using serial relaying and DF and AF forwarding over OFDM with exponential channel 2 and number of subcarriers $N_c = 64$. By using a more frequency-selective channel, we introduce more frequency diversity gain to the system. This diversity gain affects the performance of the whole system, but it has less effect on the DF case because it already gains diversity from the coding and the forwarding technique. Finally we can see that DF always performs better than AF.

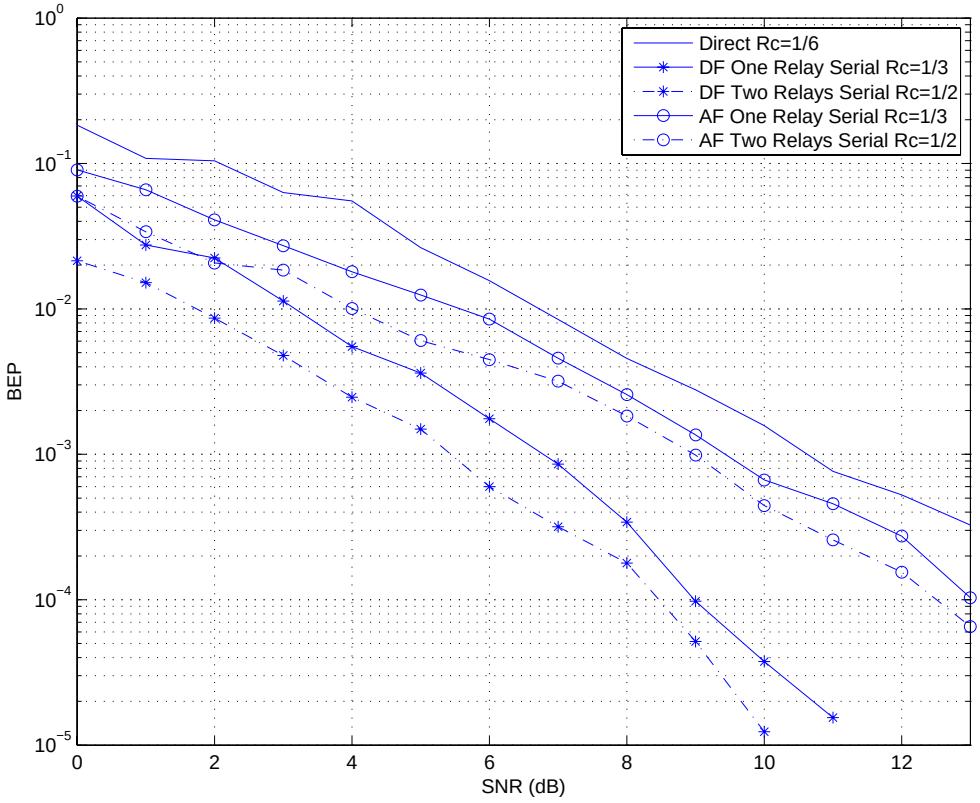

Figure 4.6: Performance of convolutionally coded OFDM multi-hop network using serial relaying and DF and AF forwarding over exponential channel 1 with $N_c = 64$.

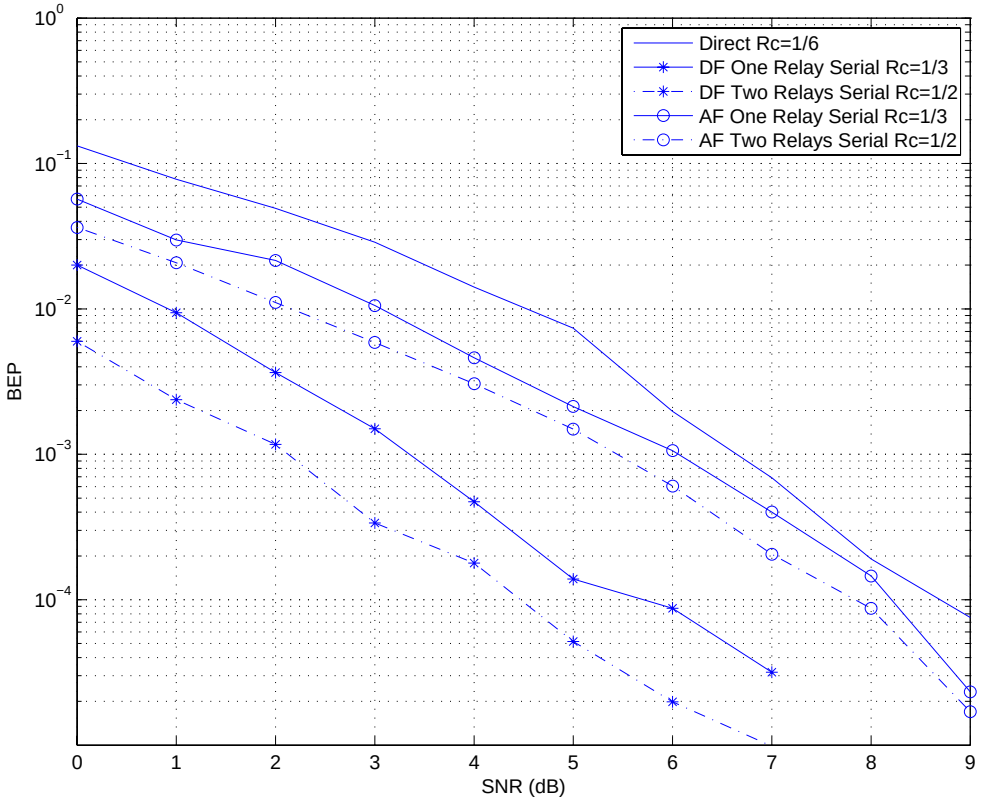

Figure 4.7: Performance of convolutionally coded OFDM multi-hop network using serial relaying and DF and AF forwarding over exponential channel 2 with $N_c = 64$.

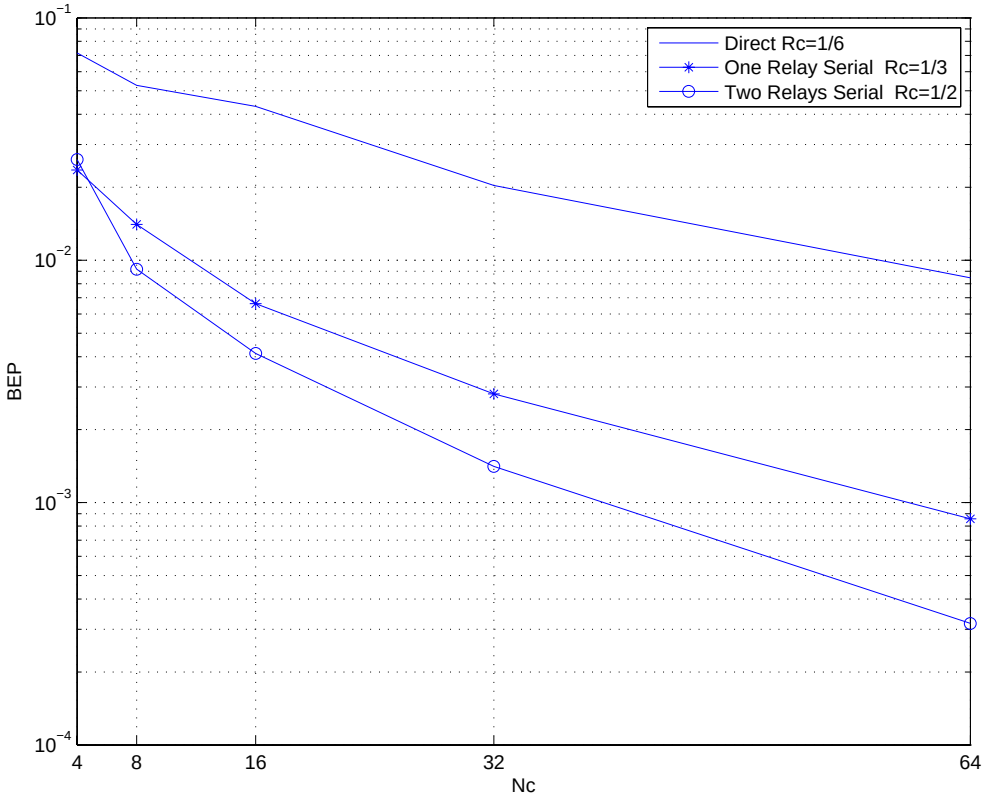

Figure 4.8: Performance of convolutionally coded OFDM multi-hop network using serial relaying and DF forwarding over exponential channel 1 with $N_c = 4, 8, 16, 32,$ and 64, and SNR = 7 dB.

Further, we tested the effect of the bandwidth used in OFDM by changing the number of subcarriers N_c. Figure 4.8 shows the error performance of a convolutionally coded multi-hop network using serial relaying and DF forwarding over OFDM with exponential channel 1 with $N_c = 4, 8, 16, 32, 64$, and SNR=7 dB. The figure clearly shows the improvement given by the increase in number of carriers to the error performance. By increasing the number of subcarriers, we add more frequency diversity to the system, which in turn improves the system's error performance. We can notice from the figure that the increase in gain is reduced as the number of subcarriers becomes high. This is because the increase in diversity gain is reduced as its order increases.

Finally we investigated how the system is affected by changing the path loss exponent. Figure 4.9 shows the error performance of a convolutionally coded OFDM multi-hop network using one relay serial relaying over exponential channel 1 with number of subcarriers $N_c = 64$, and path loss exponent $n = 0, 2, 3$. The $n = 0$ case means the distance is not taken into account. We can see from the figure that the performance improves as the path loss exponent increases. In high path loss exponent environments, sending the data over short distances saves more power than doing the same thing in low path loss environments. So the gain given by relaying to the system gets better as the path loss exponent increases.

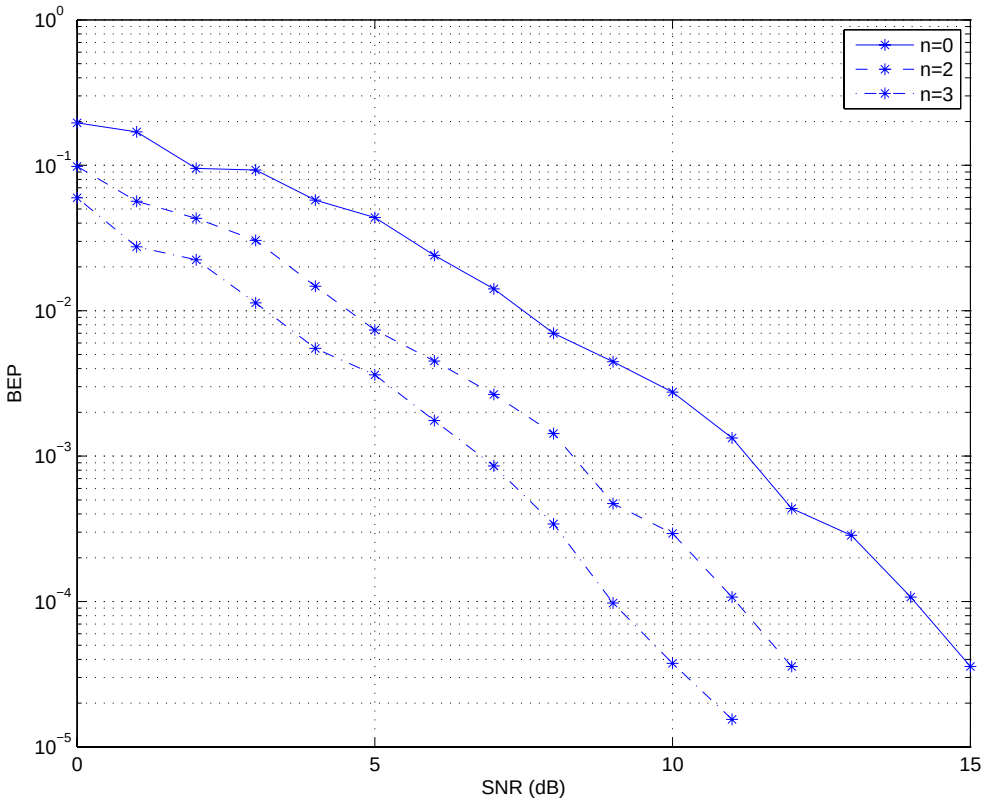

Figure 4.9: Performance of convolutionally coded OFDM multi-hop network using one relay serial relaying using DF forwarding over exponential channel 1 with $N_c = 64$, and path loss exponent $n = 0, 2$, and 3.

4.3 Parallel Relaying

Here we are considering parallel relaying. In this section, we consider the relays are equally spaced for the sake of simplicity. Here the transmitter sends the data to all the relays, and each forwards it to the destination. The parallel topology is shown in Figure 4.10. We considered the following two relaying schemes:

- The relays send the data in the same time slot but they share the bandwidth. Each relay uses a portion of the subcarriers N_c for fair comparison with the direct transmission system. The topology is shown in Figure 4.10, while the network parameters are shown in Table 4.1 and the time allocation is shown in Figure 4.11. This scheme is referred to here as variable carrier relaying (VCR).

- The relays take turns at forwarding the data in different time slots, but they send with reduced code rates. In order to be fair when comparing with the direct transmission, the number of subcarriers is 64 in all the schemes. The topology is shown in Figure 4.12, while the network parameters are shown in Table 4.2 and the time allocation is the same as in the serial scheme shown

Number of relays	**Code rate**	N_c **in the first hop**	N_c **in the second hop**
0	1/6	64	-
2	1/3	64	32
3	1/3	64	16

Table 4.1: Network parameters of VCR scheme.

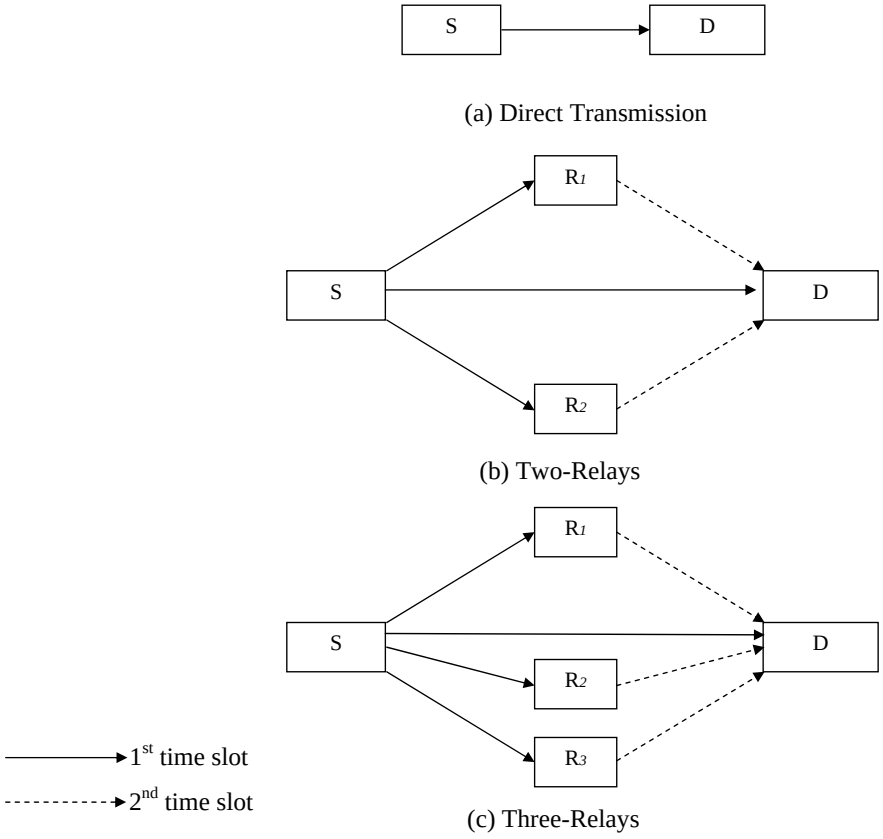

Figure 4.10: VCR parallel Topology.

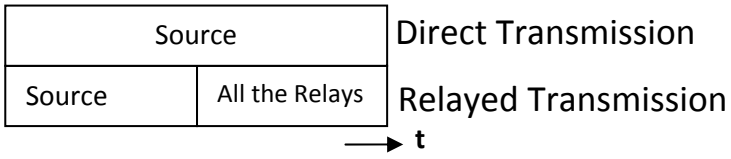

Figure 4.11: Time allocation for VCR scheme.

before in Figure 4.5. This scheme is referred to here as variable code rate relaying (VRR).

Next are the simulation results for the VCR for the two channels with gain profiles shown in 4.3. Figure 4.13 shows the performance of a convolutionally coded OFDM multi-hop network using VCR and DF and AF forwarding over exponential channel 1. We can see from the results that the two-relays scheme is much better than the direct scheme. However, adding another relay to the system does not improve the gain as much. This happens because the increase in space diversity gain is less when the diversity order increases i.e. from the two-relay scheme to three-relay scheme, and because in this case the relays share the bandwidth which reduces the frequency diversity gain added to the system. We also notice in this case that AF and DF perform close to each other. This is because the diversity gain coming from the coding is not adding much to the gain from the space diversity.

Figure 4.14 shows the performance of a convolutionally coded OFDM multi-hop network using VCR and DF and AF forwarding over exponential channel 2. The frequency diversity coming from the channel can be seen in the increase of the overall performance of the whole system. But this frequency diversity reduces the

Number of relays	**Code rate**
0	1/6
2	1/2
3	2/3

Table 4.2: Network parameters of VRR scheme.

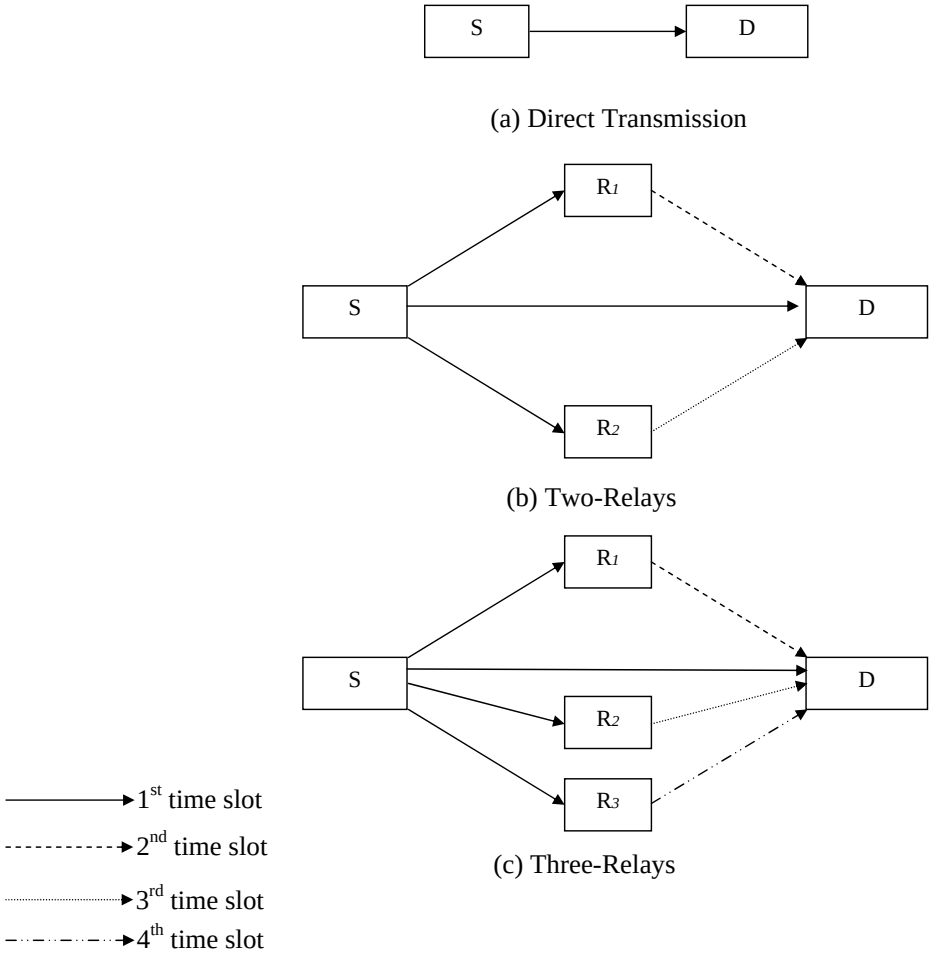

Figure 4.12: VRR parallel Topology.

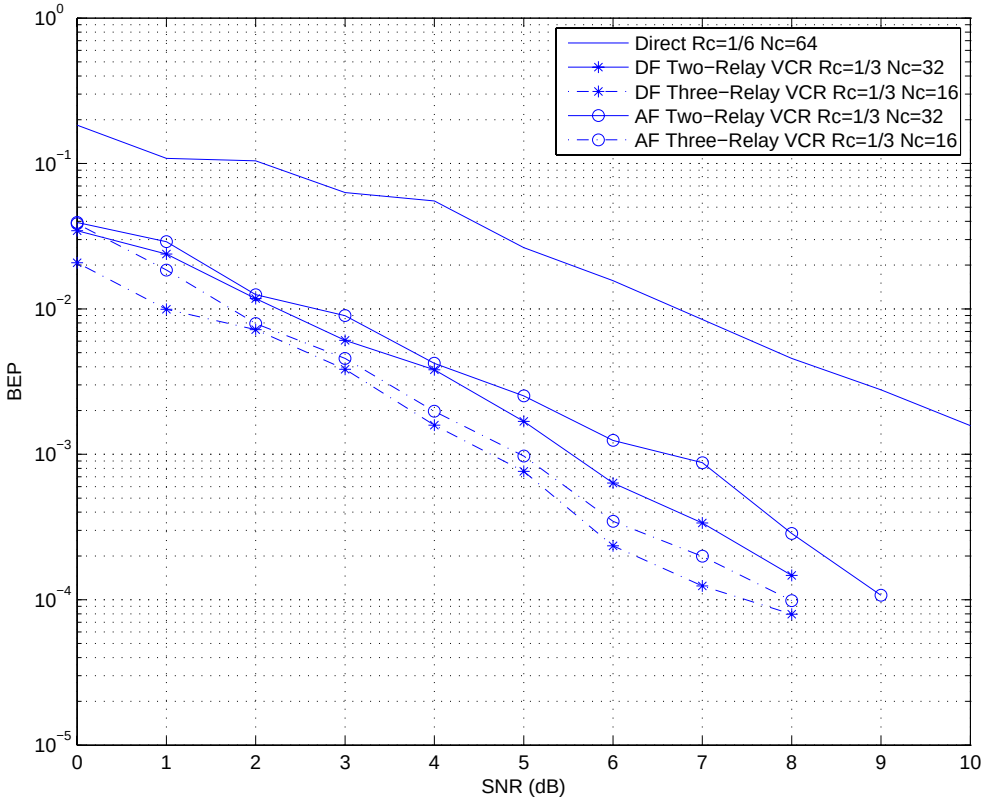

Figure 4.13: Performance of convolutionally coded OFDM multi-hop network using VCR and DF and AF forwarding over exponential channel 1.

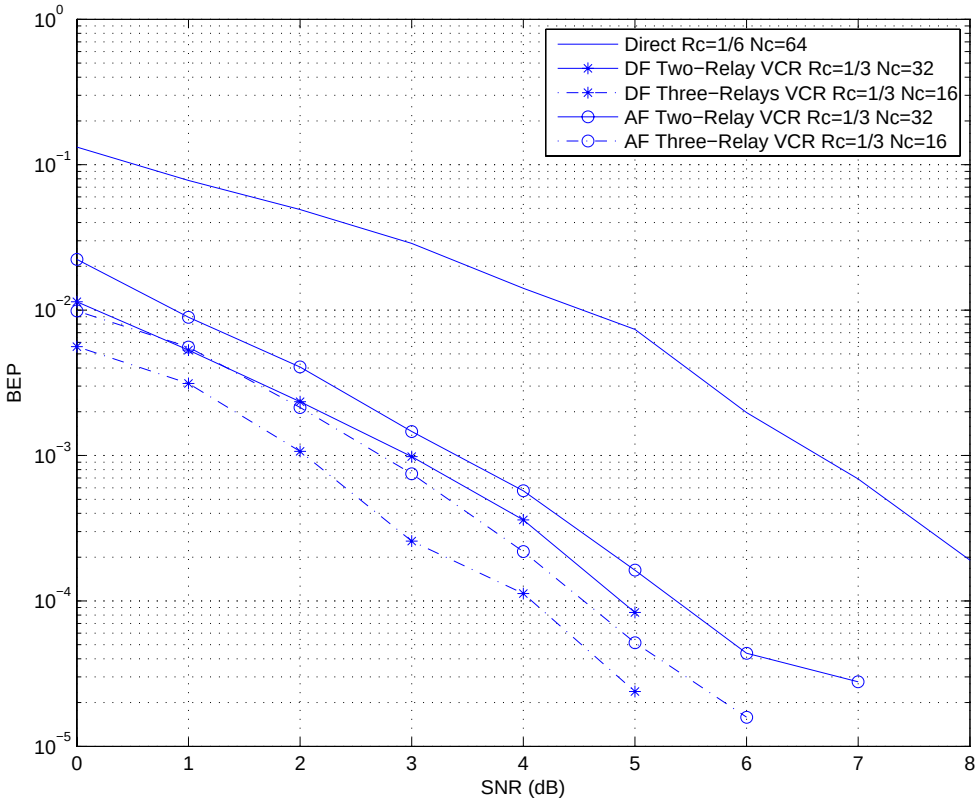

Figure 4.14: Performance of convolutionally coded OFDM multi-hop network using VCR and DF and AF forwarding over exponential channel 2.

effect of the space diversity gain coming from the relaying. So we can see that the difference between the two-relay scheme and the three-relay scheme is almost the same as when using exponential channel 1. Figure 4.15 shows the performance of a convolutionally coded OFDM multi-hop network using VCR and DF forwarding over exponential channel 1 with number of subcarriers 4,8,16,32,64, and SNR = 7 dB. The results show an improvement in the error performance when compared with the serial topology. It is also clear that adding another relay makes the system perform better, but this improvement does not increase much when the number of subcarriers increases. Also, because the relays share the bandwidth, increasing the number of subcarriers gives more improvement to the error performance without saturating as in the serial case.

Figure 4.16 shows the performance of a convolutionally coded OFDM multi-hop network using VCR with two relays and DF forwarding over OFDM with exponential channel 1 with 64 subcarrier, and path loss exponent $n = 0, 2, 3$. The $n = 0$ means the distance is not taken into account. We can see that the improvement in the performance from changing the path loss exponent is almost the same as in the serial case. However, the overall performance is better than the serial case.

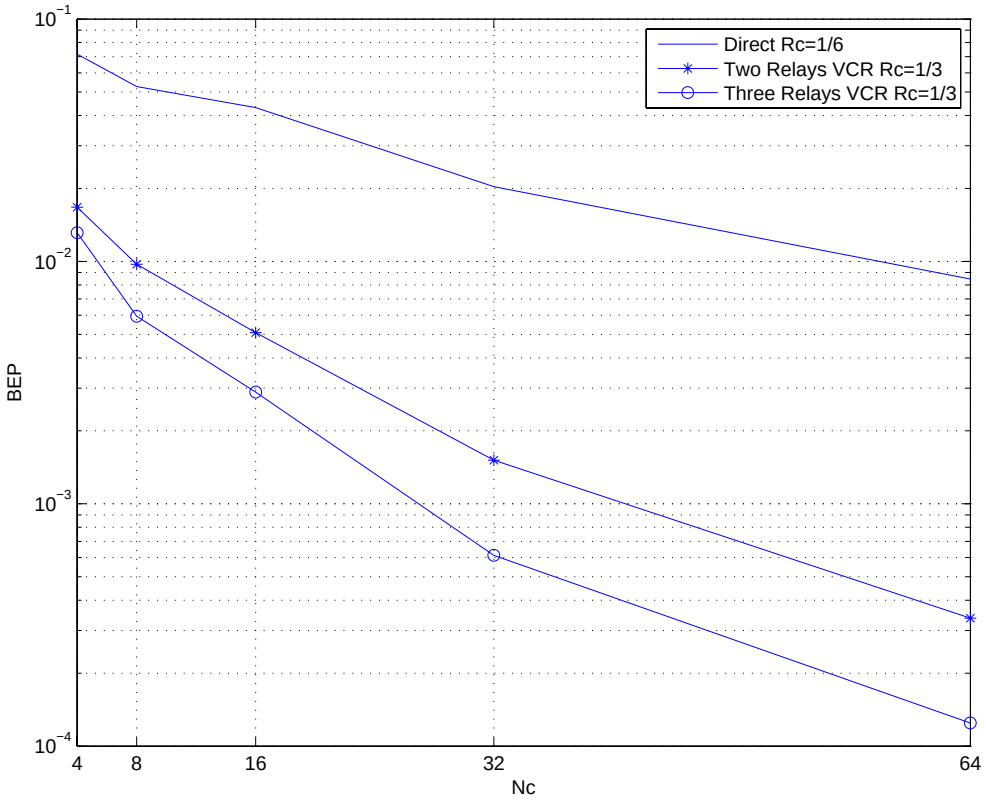

Figure 4.15: Performance of convolutionally coded OFDM multi-hop network using VCR and DF forwarding over exponential channel 1 with $N_c = 4, 8, 16, 32$, and 64, and SNR= 7 dB.

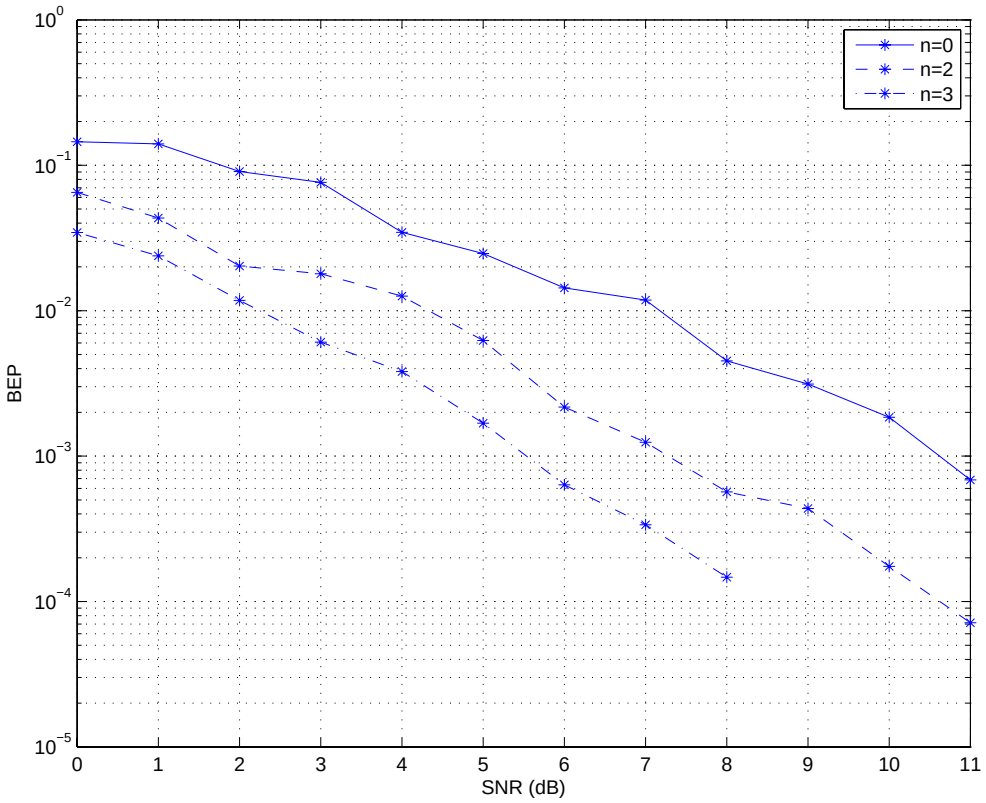

Figure 4.16: Performance of convolutionally coded OFDM multi-hop network using VCR with two relays and DF forwarding over exponential channel 1 with $N_c = 64$, and $n = 0, 2$, and 3.

The simulation results for the VRR are shown next. Figure 4.17 shows the error performance of a convolutionally coded OFDM multi-hop network using VRR and DF and AF forwarding over exponential channel 1. There is not much difference between this case and the VCR case for the two-relay scheme. However, we notice a change in the slope of the curve in the three-relay scheme. This is because we change the code rate, which adds some diversity to the system and so changes the slope of the curve. Figure 4.18 shows the error performance of a convolutionally coded multi-hop network using VRR and DF and AF forwarding over OFDM with exponential channel 2. There is not much difference between the DF and AF systems, but we get a small improvement in the three-relay scheme in both DF and AF, and this comes from the code rate change.

Clearly the change of the channel does not give much improvement in the system in either of the parallel schemes. Because these schemes give space diversity gain to the system, the frequency diversity gain from the channel does not add much.

Figure 4.19 shows the performance of a convolutionally coded OFDM multi-hop network using VRR and DF forwarding over OFDM with exponential channel 1 with $N_c = 4, 8, 16, 32$, and 64, and SNR = 7 dB. When comparing this to the VCR parallel relaying scheme, we notice that the two-relay schemes are similar. However, there is a good improvement in the performance of the three-relay scheme. This improvement is due to the use of all the subcarriers which give some frequency diversity to the system.

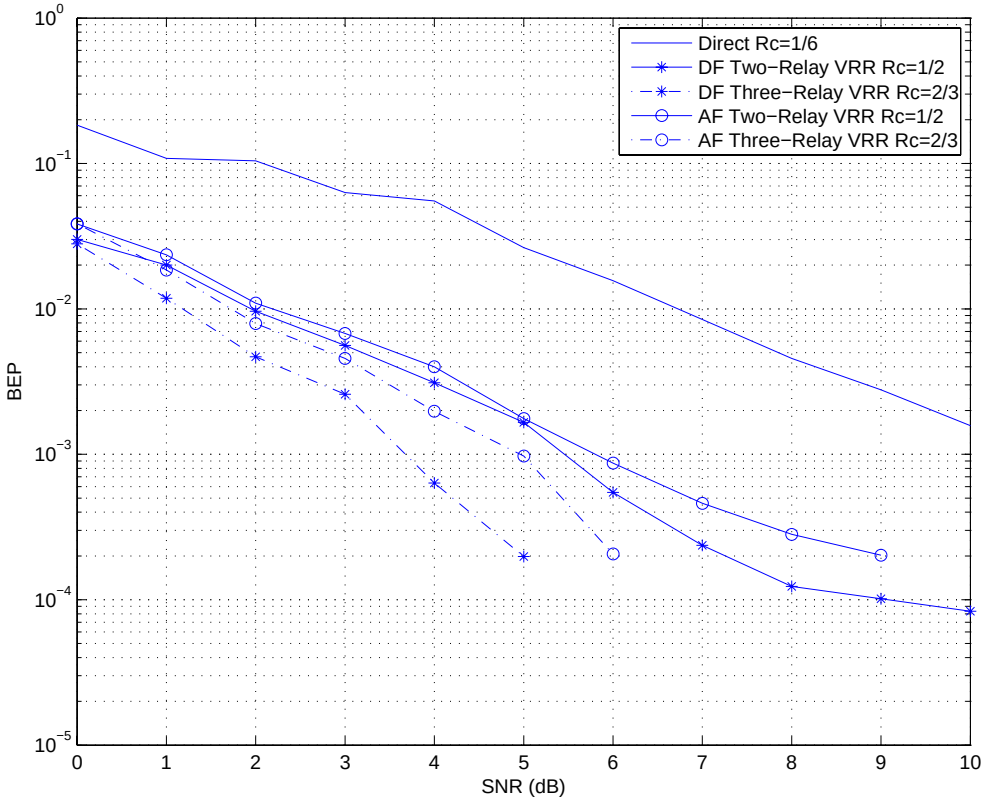

Figure 4.17: Performance of convolutionally coded OFDM multi-hop network using VRR and DF and AF forwarding over exponential channel 1.

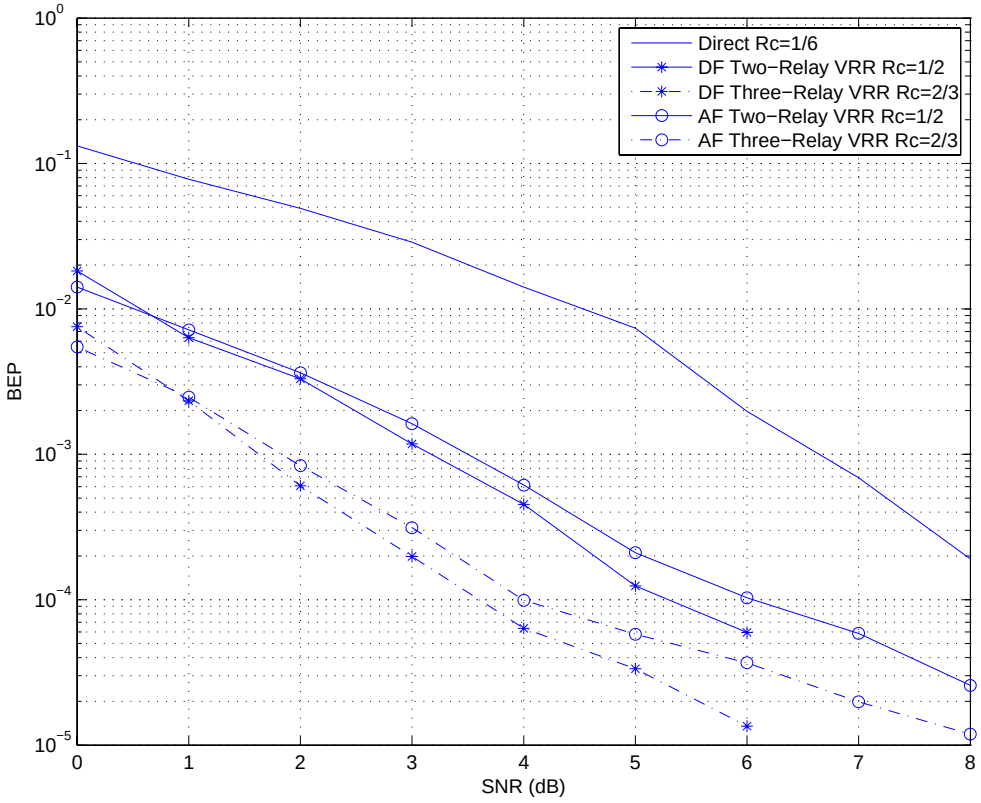

Figure 4.18: Performance of convolutionally coded OFDM multi-hop network using VRR and DF and AF forwarding over exponential channel 2.

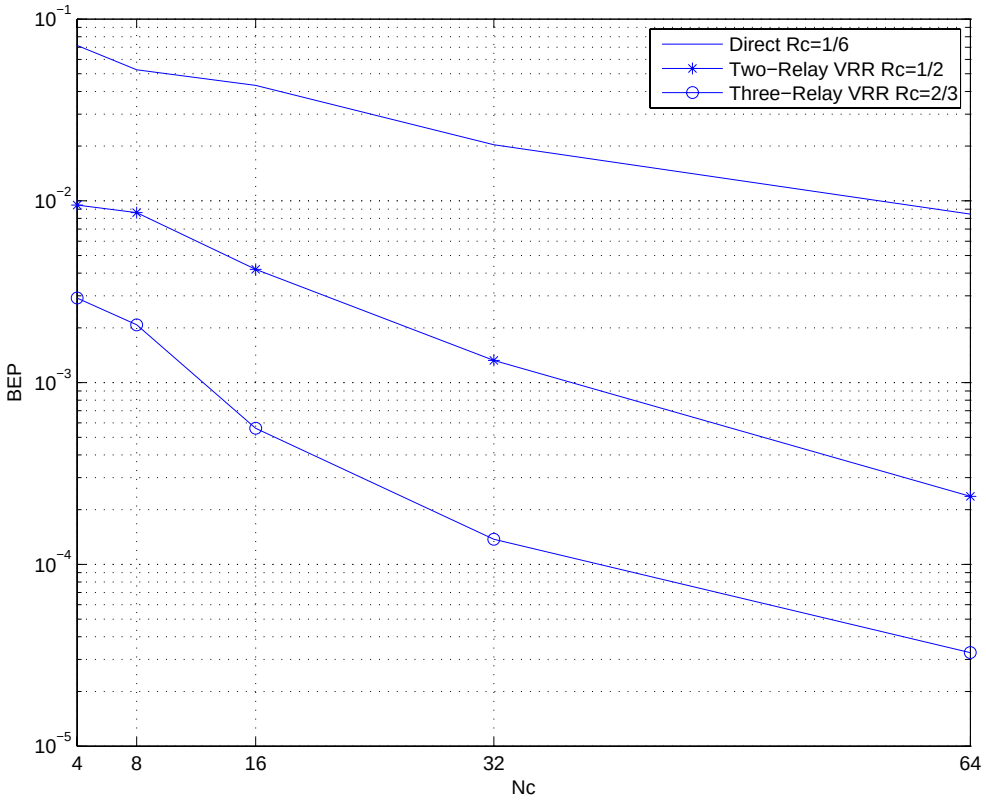

Figure 4.19: Performance of convolutionally coded OFDM multi-hop network using VRR and DF forwarding over exponential channel 1 with $N_c = 4, 8, 16, 32$, and 64, and SNR = 7 dB.

Figure 4.20 shows the performance of a convolutionally coded OFDM multi-hop network using VRR and DF forwarding over exponential channel 1 with 64 subcarriers, and path loss exponent $n = 0, 2, 3$. The $n = 0$ means we are not taking the distance into account. We can see that the improvement in the performance from changing the path loss exponent is almost the same as in the serial case. However, there is about 2dB improvement over the VCR scheme. This improvement comes from the use of the full bandwidth in the relays.

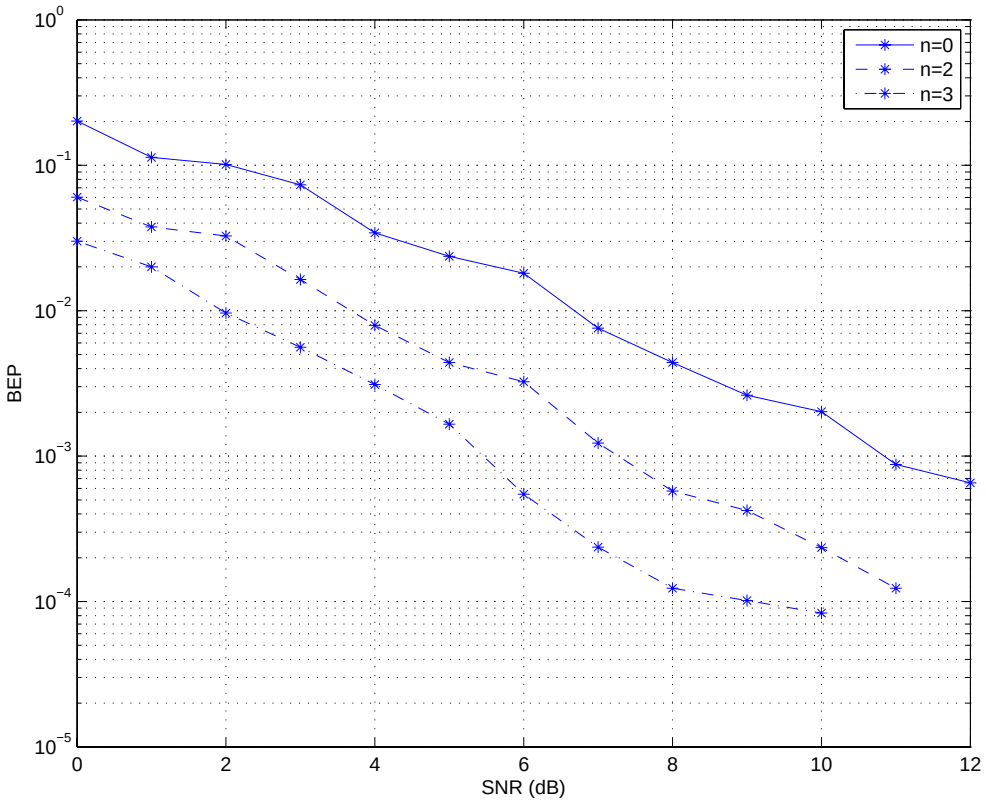

Figure 4.20: Performance of convolutionally coded OFDM multi-hop network using VRR with two-relay and DF forwarding over exponential channel 1 with $N_c = 64$, and $n = 0, 2$, and 3.

4.4 Selection Relaying

In this Section we consider selection relaying. In selection relaying, we use the parallel topology as in Figure 4.10, but we select only one relay which then forwards the data to the destination using all the subcarriers. The relay selection is based on the fading vector of both the source-relay channel and the relay-destination channel $\boldsymbol{\alpha}_{eq} = \boldsymbol{\alpha}_{sr}\boldsymbol{\alpha}_{rd}$. Three criteria were considered for the selection: the mean of the fading vector $\mu_{\boldsymbol{\alpha}_{eq}}$, the variance of the fading vector $\sigma^2_{\boldsymbol{\alpha}_{eq}}$, and the ratio between the maximum and minimum eigenvalues of the fading vector $\frac{\max(\lambda_{\boldsymbol{\alpha}_{eq}})}{\min(\lambda_{\boldsymbol{\alpha}_{eq}})}$. It was found from the simulation that the criterion which gives the best performance is the mean criterion, which corresponds with [38]. In this thesis, we selected the relay with the highest mean of its fading vector, and we used this relay to forward the data to the destination.

Next are the simulation results for the selection relaying system with two and three relays. Figure 4.21 shows the performance of a convolutionally coded OFDM multihop network using selection relaying and DF and AF forwarding over exponential channel 1 with the number of subcarriers 64. The figure clearly shows the improvement given by relaying to the system. Additionally, selection relaying gives more gain to the system, because the selection algorithm selects the best channel and uses all the subcarriers to transmit in it. Also DF has a clear gain over AF due to the diversity gain we get when using DF. However, additional communication must be

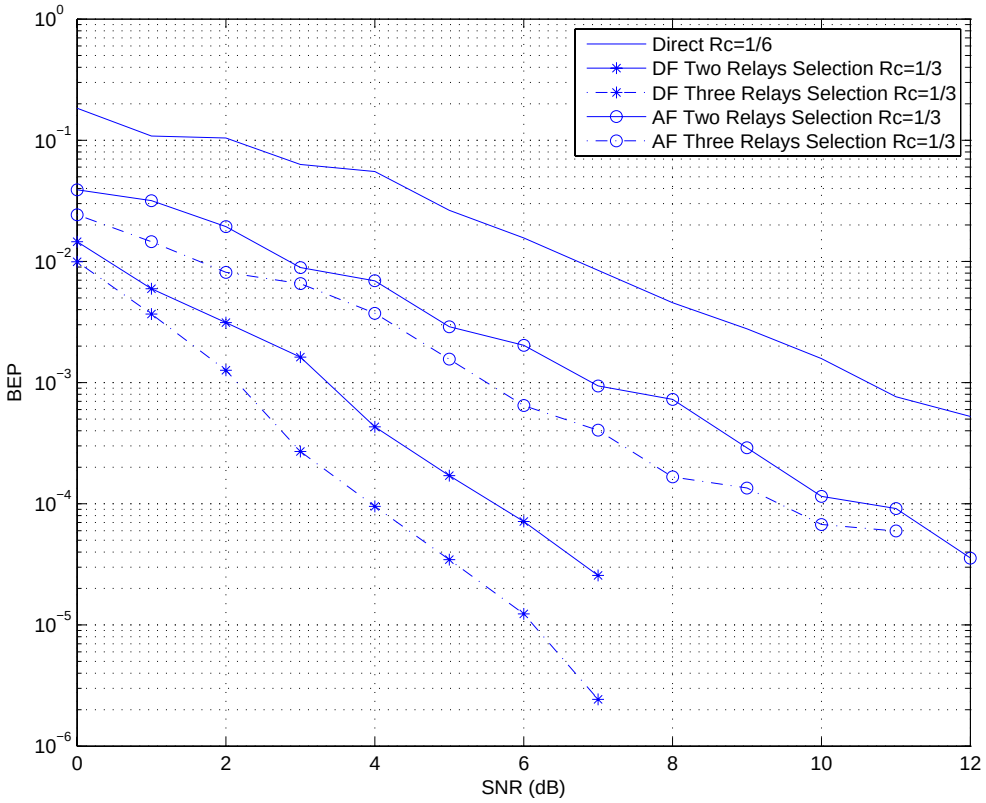

Figure 4.21: Performance of convolutionally coded OFDM multi-hop network using selection relaying and DF and AF forwarding over exponential channel 1 with $N_c = 64$.

done between the nodes in order to select the best channel which could reduce the overall throughput. Figure 4.22 shows the performance of a convolutionally coded OFDM multi-hop network using selection relaying and DF and AF forwarding over exponential channel 2 with $N_c = 64$. By using a more frequency-selective channel, we introduce more frequency diversity gain to the system. This can be seen from the SNR gain and the change of the slope of the curves. Also, DF performs much better than AF in all the schemes. Figure 4.23 shows the performance of a convolutionally coded OFDM multi-hop network using selection relaying and DF forwarding over exponential channel 1 with $N_c = 4, 8, 16, 32, 64$, and SNR = 7 dB. The figure clearly shows the improvement given by the increase in number of subcarriers to the error performance. By increasing the number of subcarriers, we add more frequency diversity to the system, which in turn improves the system's error performance. Figure 4.24 shows the performance of a convolutionally coded OFDM multi-hop network using selection relaying and DF forwarding over exponential channel 1 with $N_c = 64$, and path loss exponent $n = 0, 2, 3$. The effect is the same as the serial case but with overall gain of about 3 dB.

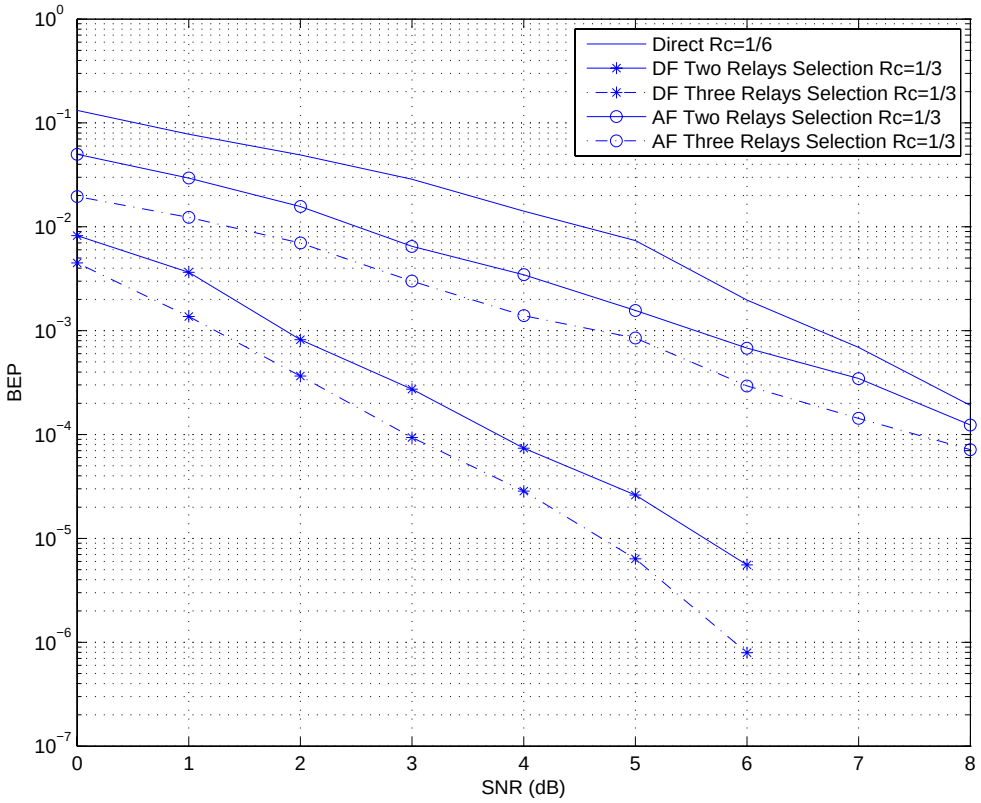

Figure 4.22: Performance of convolutionally coded OFDM multi-hop network using selection relaying and DF and AF forwarding over exponential channel 2 with $N_c = 64$.

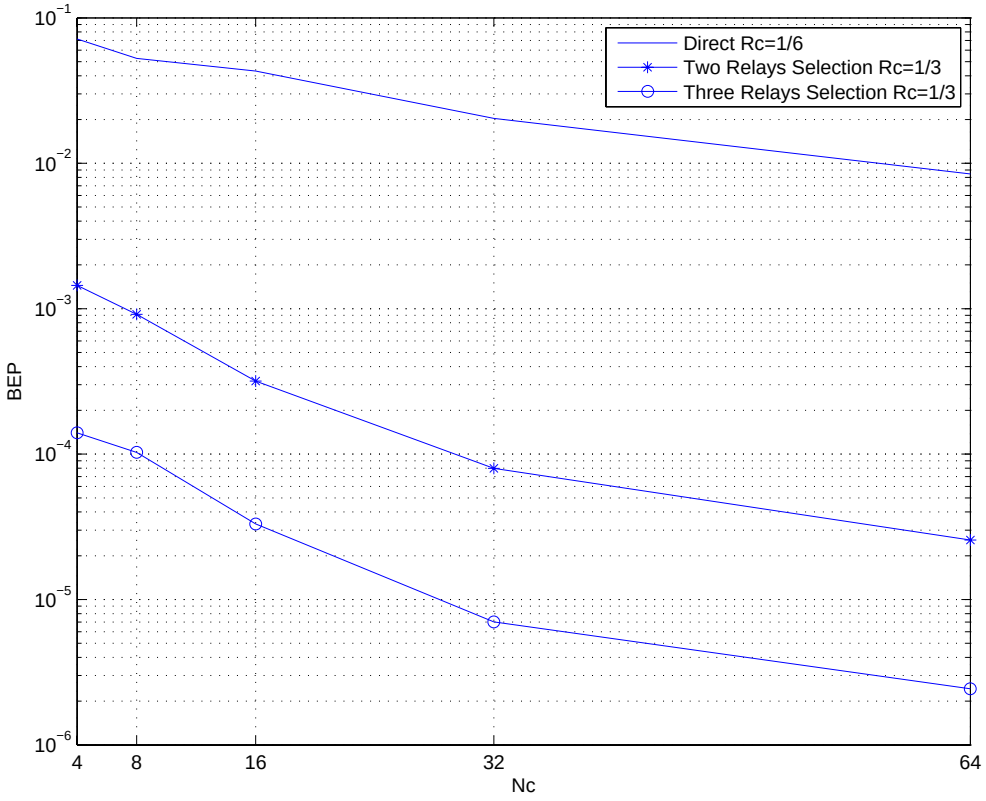

Figure 4.23: Performance of convolutionally coded OFDM multi-hop network using selection relaying and DF forwarding over exponential channel 1 with $N_c = 4, 8, 16, 32$, and 64, and SNR = 7 dB.

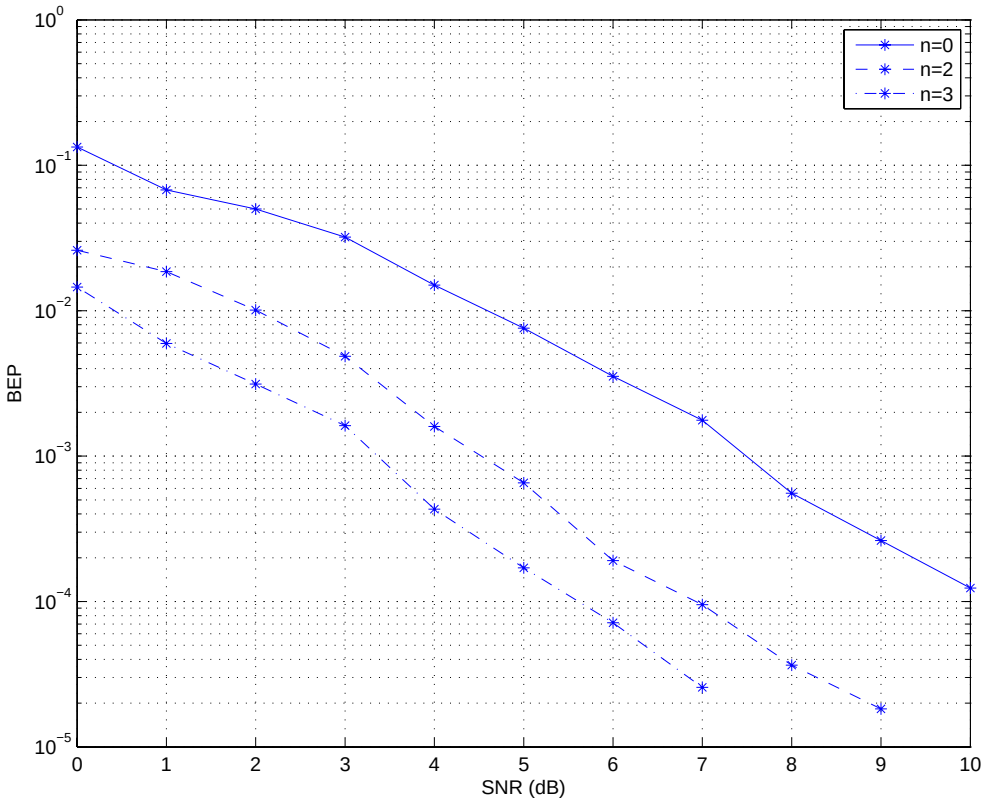

Figure 4.24: Performance of convolutionally coded OFDM multi-hop network using selection relaying and DF forwarding over exponential channel 1 with $N_c = 64$, and $n = 0, 2$, and 3.

4.5 Chapter Conclusions

In this chapter we investigated the performance of convolutionally coded multi-hop networks in OFDM wireless environments. We considered different forwarding techniques and the multi-hop topologies. Furthermore, we showed the performance of the system using serial, parallel, and selection relaying over two different wideband fading channels. Finally, we investigated the effect of the number of carriers, and path loss exponent on the error performance of the system. From the simulation results, we can conclude the following:

- Relaying can greatly improve the performance of the system.
- In serial relaying, regardless of the channel used, AF does not give much gain.
- DF introduces diversity to the system, which can be seen by the slope change of the SNR-BEP curve.
- The performances of AF and DF are very close in VCR for all of the used channels. In VRR, we can see some improvement in the performance.
- In selection relaying, DF performs much better than AF in all the channels used.
- Selection relaying performs like a serial relaying but with a good channel all the time, and so it performs better than both serial and parallel relaying.

- The diversity of the channel can be shown easily by the change of the slope between the different channel figures.

- The error performance of the system improves as the path loss exponent increases. In high path loss exponent environments, sending the data over short distances saves more power than doing the same thing in low path loss environments. So the gain given by relaying to the system gets better as the path loss exponent increases.

- Increasing the number of subcarriers N_c improves the performance in every case.

- Selection performs best. However, additional negotiation must be done between the nodes in order to select the best channel. This could reduce the overall throughput.

Chapter 5

Conclusions and Future Research

In this concluding chapter, we summarize the content of the thesis and we discuss possible future research directions.

5.1 Summary of Contributions

In Chapter 2, we investigated the error performance of both uncoded and convolutionally coded multi-hop networks over a narrowband channel using different modulation schemes over Rayleigh fading channels. The bit error probability (BEP) of both the uncoded and coded systems when using AF relaying was derived for both the serial and parallel schemes. Results show that relaying significantly improves the overall error performance of the system, especially in parallel relaying.

In Chapter 3, we investigated the performance of multi-hop networks employing

CDMA transmission in a multiple-user environment. The standard Gaussian approximation with diversity was used to derive the probability of error of the system when using serial, parallel and two schemes of selection relaying using the DF technique. Additionally, we investigated the effect of different system parameters on the error performance of the system, such as the spreading gain, the number of active users, and the path loss exponent. Results show that, as the number of users increases, the improvement coming from the relaying decreases. However, relaying still gives significant improvement, especially in parallel relaying.

Finally, in Chapter 4, we investigated the effect of relaying on the error performance of convolutionally coded multi-hop networks in the OFDM wireless environment. We showed the error performance of the system using serial, parallel, and selection relaying over two different wideband fading channels. Additionally, we investigated the effect of the number of carriers and the path loss exponent on the network performance.

5.2 Future Research

The analysis in Chapter 2 was done for serial and parallel relaying using AF technique. A good topic for future research will be to analyze the performance for selection relaying.

In Chapter 3 we investigated the performance for DF technique only, but we could

in the future investigate the system when using AF technique. The AF technique consumes less energy than DF, which is a sensitive issue in multi-hop network design. Also other methods for calculating the BEP of CDMA systems may be used, such as the improved Gaussian approximation (IGA) and the Fourier series based scheme (FS) [27]. The IGA and FS give more accurate results for the BEP of CDMA systems but with greater complexity of analysis.

In Chapter 4, we investigated the performance by simulation only. A good next step would be to derive the BEP performance of the systems used in Chapter 4 by analysis for both DF and AF.

Bibliography

[1] T. Rappaport, *Wireless Communications: Principles and Applications*. Singapore: Pearson Education, Inc., 2nd ed., 2002.

[2] A. Sheikh, *Wireless Communications: Theory and Techniques*. USA: Kluwer, 1st ed., 2004.

[3] J. Proakis, *Digital Communications*. New York, USA: McGraw-Hill, 4th ed., 2000.

[4] B. Sklar, "Rayleigh fading cannel in mobile digital communication systems part ii: Mitigation," *IEEE Communications Magazine*, vol. 35, pp. 102–109, July 1997.

[5] K. Pahlavan and P. Kishnamurthy, *Principles of Wireless Networks - A Unified Approach*. Prentice Hall Inc,, 1st ed., 2002.

[6] A. Nosratinia, T. Hunter, and A. Hedayat, "Cooperative Communication in Wireless Networks," *IEEE Communications Magazine*, vol. 42, pp. 74–80, Oc-

tober 2004.

[7] T. Hunter and A. Nosratinia, "Diversity through Coded Cooperation," *IEEE Transactions on Wireless Communication*, vol. 5, pp. 283 – 289, February 2006.

[8] A. Sendonaris, E. Erkip, and B. Auzhang, "User cooperation diversity - part i: System description," *IEEE Transactions on Wireless Communication*, vol. 51, pp. 1927–1938, November 2003.

[9] A. Sendonaris, E. Erkip, and B. Auzhang, "User cooperation diversity - part ii: Implementation aspects and performance analysis," *IEEE Transactions on Wireless Communication*, vol. 51, pp. 1939–1948, November 2003.

[10] K.-S. Hwang, Y.-C. Ko, and M.-S. Alouini, "A study of multi-hop cooperative diversity system," *Asia-Pacific Conference on Communications*, pp. 1–5, August 2006.

[11] S. Lin and D. Costello, *Error Control Coding: Fundamentals and Applications*. New Jersy, USA: Prentice-Hall Inc., 2nd ed., 2004.

[12] R. Chang and R. Gibby, "A theoretical study of performance of an orthogonal multiplexing data dransmission scheme," *IEEE Transactions on Communications*, vol. 16, pp. 529–540, August 1968.

[13] M. Engels, *Wireless OFDM Systems How to make them work*. Boston, USA: Kluwer Academic Pub, 1st ed., 2002.

[14] T.Wada, N. Nakagawall, H. Okadaj, A. Jamdipours, K. Ohuchit, and M. Saito, "Performance Improvement of Turbo Coded Multi-route Multi-hop Networks using Parity Check Codes," *Workshop on High Performance Switching and Routing*, May 2005.

[15] J. Laneman and G. Wornell, "Energy efficient antenna sharing and relaying for wireless networks," *IEEE Wireless Communications and Networking Conference (WCNC)*, vol. 1, pp. 7–12, October 2000.

[16] M. Hasna and M. Alouini, "Performance Analysis of Two-Hop Relayed Transmissions over Rayleigh Fading Channels," *IEEE Vehicular Technelogy Conference (VTC)*, vol. 4, pp. 1992–1996, September 2002.

[17] G. Kramer, M. Gastpar, and P. Gupta, "Cooperative strategies and capacity theorems for relay networks," *IEEE Transactions on Information Theory*, vol. 51, p. 30373063, September 2005.

[18] M. Katayama, K. Mizuno, M. Nakayama, and M. Shimizu, "A multi-protocol wireless multi-hop network employing a new efficient hybrid routing scheme," *The 57th IEEE Semiannual Vehicular Technology Conference*, vol. 3, p. 20132017, April 2003.

[19] M. Dianati, X. Shen, and K. Naik, "Per-user throughput of opportunistic scheduling scheme over broadcast fading channels," *IEEE International Con-*

ference on Communications, vol. 11, pp. 5234–5239, June 2006.

[20] M. Hasna, "Average ber of Multihop Communication Systems Over Fading Channels," *IEEE International Conference on Electronics, Circuits and Systems (ICECS)*, vol. 2, pp. 723–726, December 2003.

[21] M. Hasna and M. Alouini, "A Performance Study of Dual-Hop Transmissions With Fixed Gain Relays," *IEEE Transactions on Wireless Communications*, vol. 3, pp. 1963–1968, November 2004.

[22] L. Yang, M.Hasna, and M. Alouini, "Average Outage Duration of Multihop Communication Systems With Regenerative Relays," *IEEE Transactions on Wireless Communications*, vol. 4, pp. 1366–1371, July 2005.

[23] E. Malkamäki and H. Leib, "Evaluating the performance of convolutional codes over block fading channels," *IEEE Transactions on Information Theory*, vol. 45, pp. 1643–1646, July 1999.

[24] T. Hunter and A. Nosratinia, "Performance analysis of coded cooperation diversity," *IEEE International Conference on Communications*, vol. 4, pp. 2688 – 2692, May 2003.

[25] S. Zummo, "Performance Analysis of Coded Cooperation Diversity in Wireless Networks," *IEEE International Conference on Communication (ICC)*, vol. 10, pp. 4560–4565, June 2006.

[26] G. Balakrishnan, M. Yang, Y. Jiang, and Y. Kim, "Performance Analysis of Error Control Codes for Wireless Sensor Networks," *IEEE International Conference on Information Technology (ITNG)*, vol. 4, pp. 876–879, April 2007.

[27] M. Sunay and P. McLane, "Calculating error probabilities for ds cdma systems: When not to use the gaussian approximation," *Global Telecommunications Conference*, vol. 3, pp. 1744–1749, November 1996.

[28] L. Zhao, J. Mark, and Y. Yoon, "Performance of coding-spreading tradeoff in ds-cdma systems using rcpt and rcpc codes," *IEEE TRANSACTIONS ON COMMUNICATIONS*, vol. 52, pp. 882–886, JUNE 2004.

[29] R. Hoshyar, S. Jamali, and A. Bahai, "Turbo coding performance in ofdm packet transmission," *The 51st IEEE Vehicular Technology Conference Proceedings*, vol. 2, pp. 805 – 810, May 2000.

[30] L. Dai, B. Gui, and L. Cimini, "Selective relaying in ofdm multihop cooperative networks," *IEEE Wireless Communications and Networking Conference*, pp. 963–968, March 2007.

[31] J. Craig, "A new, simple and exact result for calculating the probability of error for two-dimensional signal constellations," *Military Communications Conference*, vol. 2, pp. 571 – 575, November 1991.

[32] M. Simon and M. Alouini, *Digital Communications over Fading Channels*. New York, USA: John Wiley and Sons, 1st ed., 2000.

[33] A. Viterbi and J. Omura, *Principles of Digital Communication and Coding*. New York, USA: McGraw Hill, 1st ed., 1979.

[34] G. Kaplan and S. Shamai, "Error probabilities for the blockfading gaussian channel," *Arch. Elek. Ubertragung*, vol. 49, p. 192205, July 1995.

[35] L. Ozarow, S. Shamai, and A. D. Wyner, "Information theoretic considerations for cellular mobile radio," *IEEE Transactions on Vehicular Technology*, vol. 43, p. 359378, May 1994.

[36] J. Holtzman, "A simple, accurate method to calculate spread spectrum multiple access error probabilities," *IEEE Transactions on Communications*, vol. 40, pp. 461–464, March 1992.

[37] H. Stark and J. Woods, *Probability, Random Variables, and Estimation Theory for Engineers*. Prentice Hall, 1986.

[38] J. N. Laneman, D. N. C. Tse, and G. W. Wornell, "Cooperative diversity in wireless networks:efficient protocols and outage behavior," *IEEE Transactions on Information Theory*, vol. 50, pp. 3062 – 3080, December 2004.

VITA

Mohammad M. Abdellatif

- Born on 9th March 1983 in College Station, Texas, United States of America.
- February, 2006-February, 2009 M.Sc. in Telecommunication Engineering at King Fahd University of Petroleum and Minerals, Dhahran, KSA.
    - Full Fee Waiver.
    - Held Research Assistantship during the period of study.
    - GPA 3.688/4.00.
- 1999-2004 B.Sc. in Electronics Engineering at Assiut University, Assiut, Egypt
    - Grade: Very Good (79.84 %.).